QGP Physics − from Fixed Target to LHC

6. Space-time evolution of the QGP

Prof. Dr. Johanna Stachel, Prof. Dr. Klaus Reygers

Physikalisches Institut, Universität Heidelberg

SS 2015

Space-time Evolution of A+A Collisions

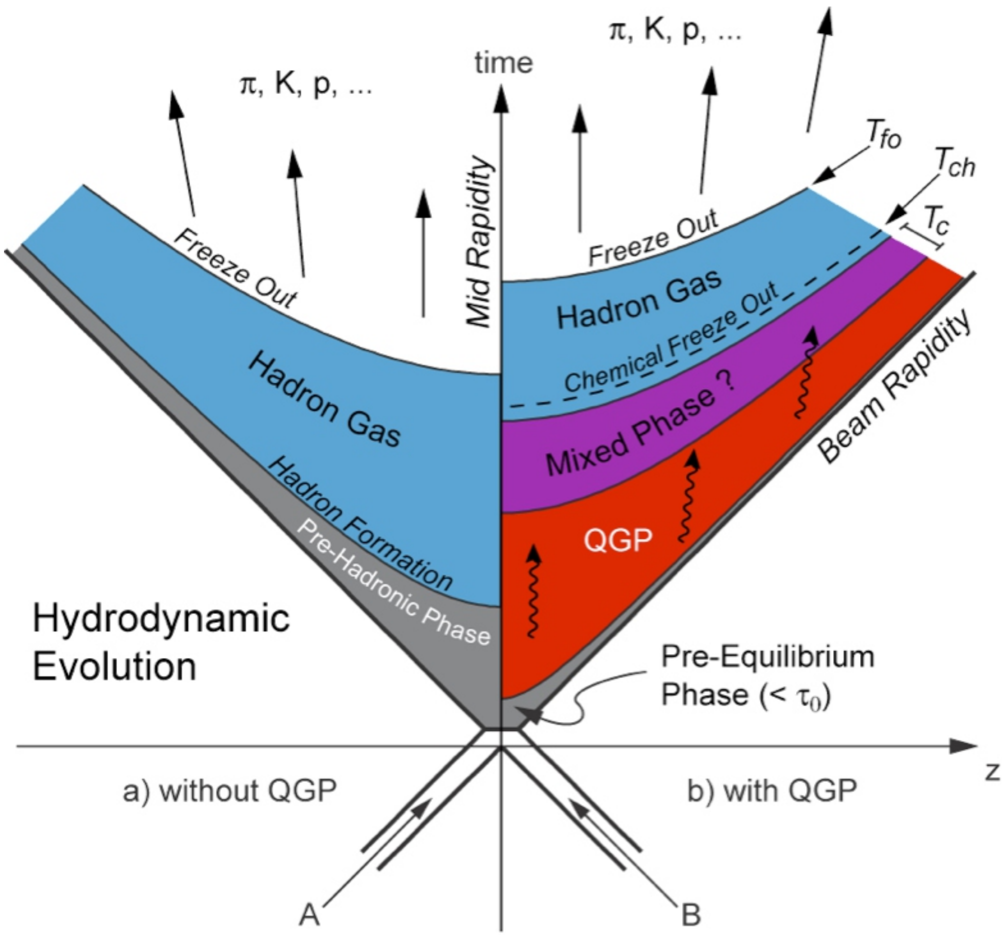

Evolution described by relativistic hydrodynamic models, which need initial conditions as input.

Simplest case: Symmetric collisions (no elliptic flow), ideal gas equation of state (bag model), only longitudinal expansion (1D, Bjorken)

Types of Collective Flow

Radial flow

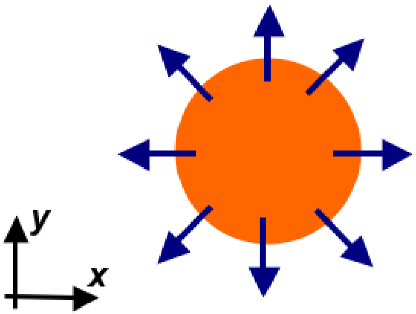

- The only type of collective flow in A+A collisions with impact parameter $b = 0$
- Affects the shape of particle spectra at low p_T

Elliptic flow

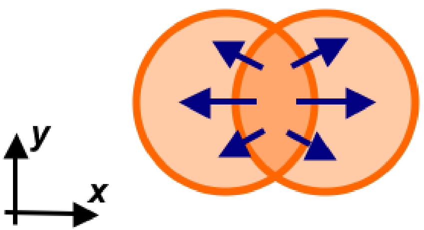

- Caused by anisotropy of the overlap zone ($b \neq 0$)
- Requires early thermalization of the medium

Directed flow

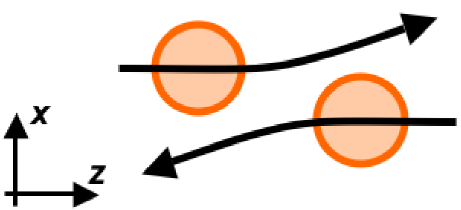

- Is produced in the pre-equilibrium phase of the collision
- Gets smaller with increasing $\sqrt{s_{NN}}$

6.1 Longitudinal Expansion

Landau Initial Conditions for the Hydrodynamic Evolution

L. D. Landau, Izv. Akad. Nauk. SSSR 17 (1953) 52
P. Carruthers and M. Duong-Van, PRD8 (1973) 859

Lev Landau

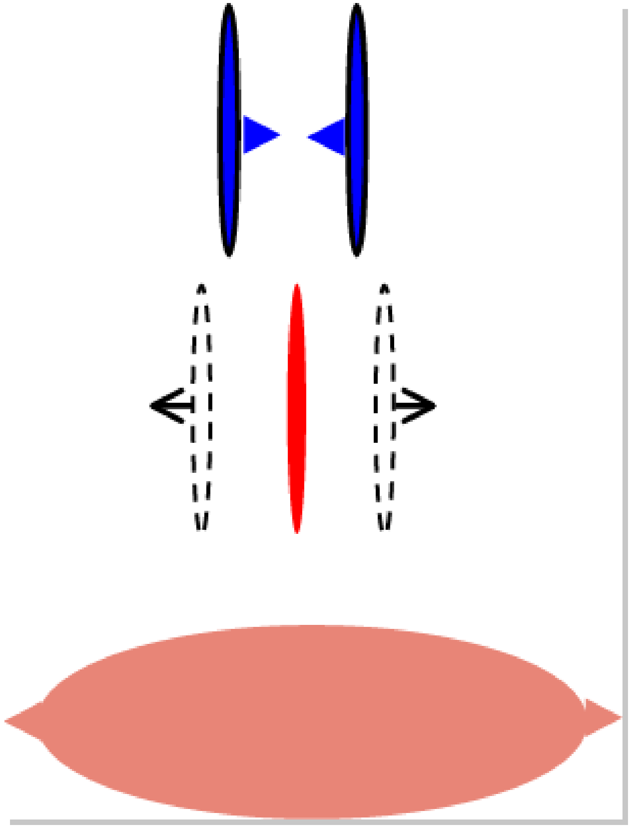

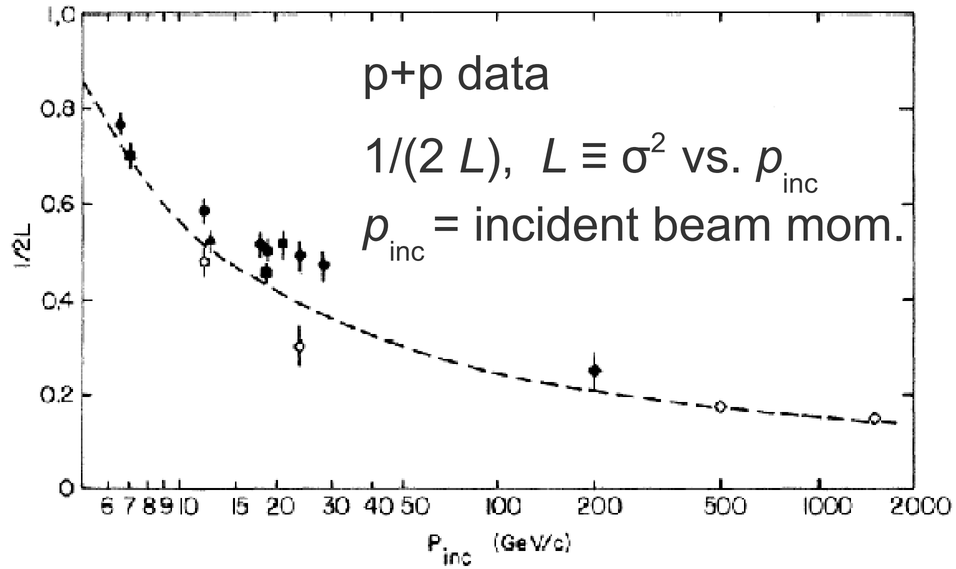

Prediction: d*N*/d*y* is Gaussian with a width given by $\sigma^2 = \ln\left(\frac{\sqrt{s}}{2m_p}\right)$

Rapidity Distributions in A+A

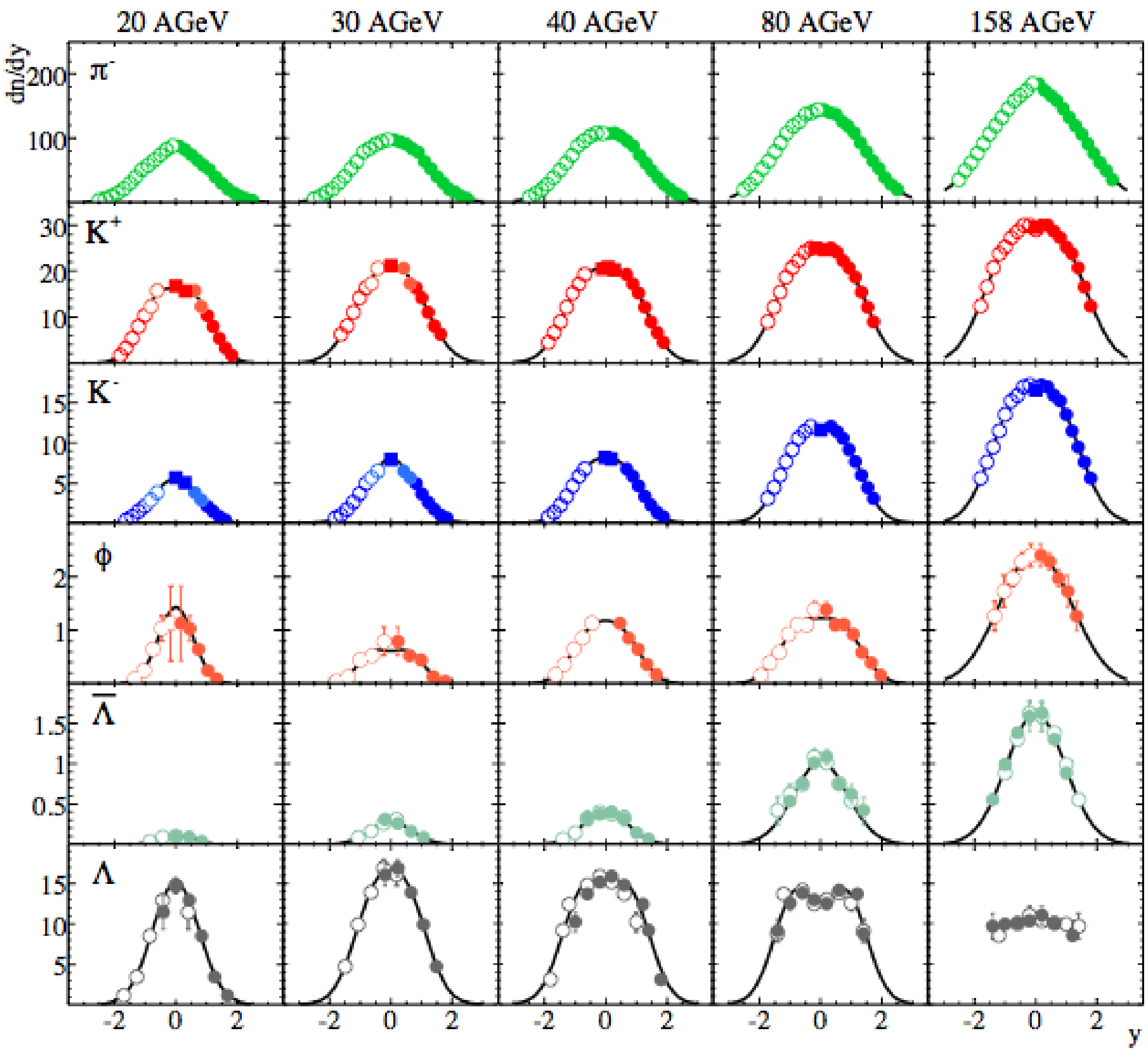

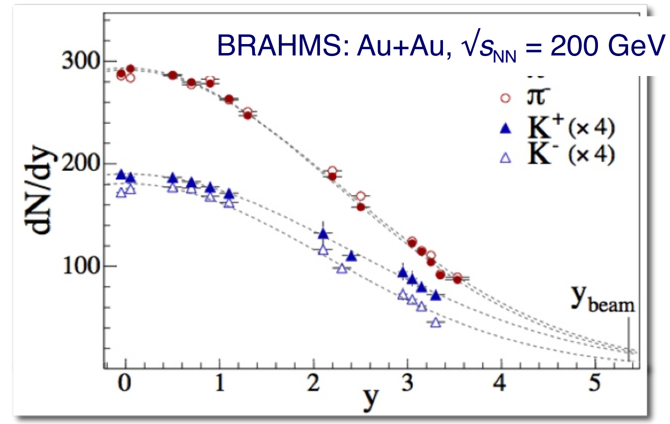

Landau … works reasonably well for heavy ions, too

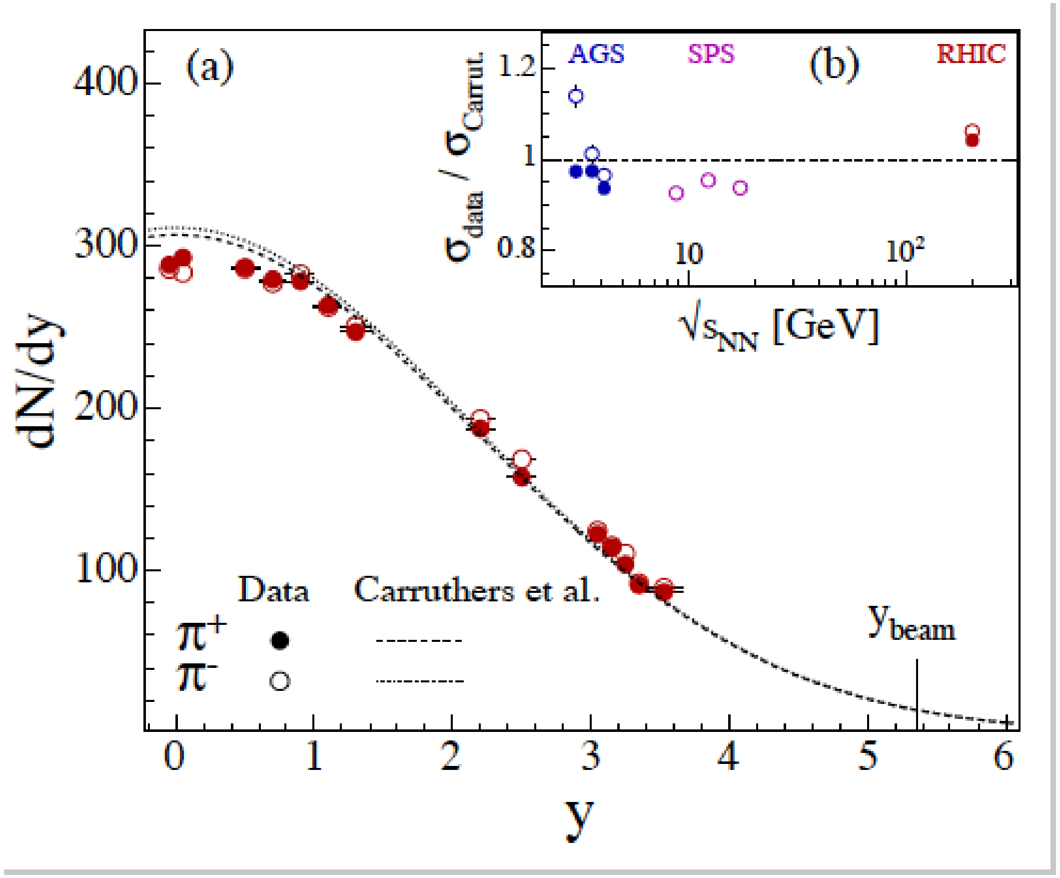

BRAHMS: PRL94, 162301 (2005)

Reminder (from Chapter 4): Space-Time Evolution in a the Bjorken Model

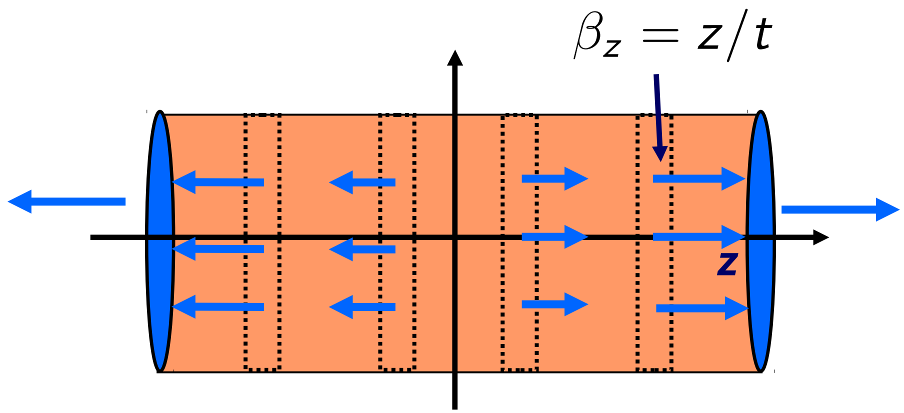

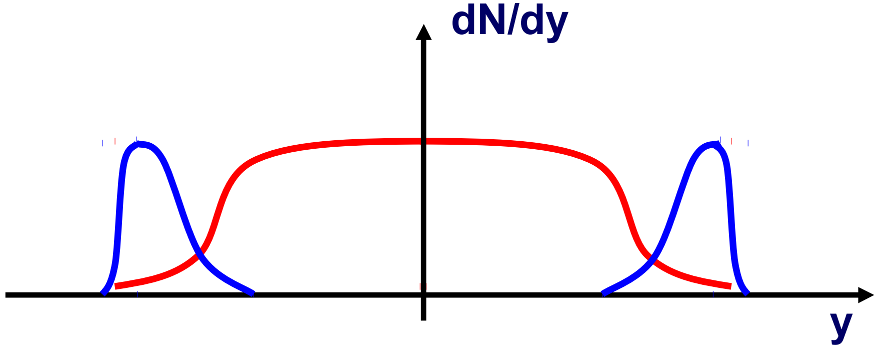

Velocity of the local system at position z at time t:

$$\beta_z = z/t$$

Proper time τ in this system:

$$\begin{aligned}\tau &= t/\gamma = t\sqrt{1-\beta^2} \\ &= \sqrt{t^2 - z^2}\end{aligned}$$

In the Bjorken model all thermodynamic quantities only depend on τ, e.g., the particle density:

$$n(t, z) = n(\tau)$$

This leads to a constant rapidity density of the produced particles (at least at central rapidities):

$$\frac{dN_{ch}}{dy} = \text{const.}$$

1D Bjorken Model (I)

$$\beta_z = z/t$$

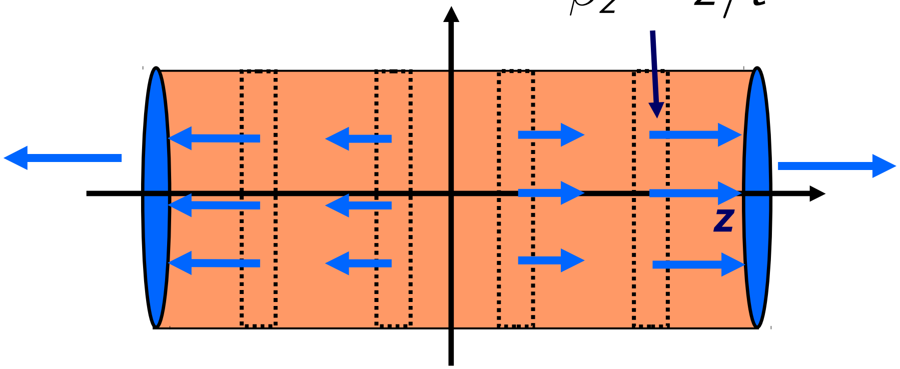

The Bjorken model is a 1d hydrodynamic model (expansion only in *z* direction). The initial conditions correspond to the one which one would get from free streaming particles starting at (t, z) = (0, 0).

$$\tau = t/\gamma = t\sqrt{1-\beta_z^2} = \sqrt{t^2 - z^2}$$

preserved in the hydro evolution, i.e., $u^\mu(\tau) = \frac{x^\mu}{\tau}$

Initial conditions in the Bjorken model:

$$\varepsilon(\tau_0) = \varepsilon_0, \quad u^\mu = \frac{1}{\tau_0}(t, 0, 0, z) = \frac{x^\mu}{\tau_0}$$

Initial energy density

In this case the equations of ideal hydrodynamics simplify to

$$\frac{\mathrm{d}\varepsilon}{\mathrm{d}\tau} + \frac{\varepsilon + p}{\tau} = 0$$

$\varepsilon = E/V$:	energy density
p :	pressure
$s = S/V$:	entropy density

1D Bjorken Model (II)

For an ideal gas of quarks and gluons, i.e., for

$$\varepsilon = 3p, \quad \varepsilon \propto T^4$$

This leads to

$$\varepsilon(\tau) = \varepsilon_0 \left(\frac{\tau}{\tau_0}\right)^{-4/3}, \quad T(\tau) = T_0 \left(\frac{\tau}{\tau_0}\right)^{-1/3}$$

The temperature drops to the critical temperature at the proper time

$$\tau_c = \tau_0 \left(\frac{T_0}{T_c}\right)^3$$

And thus the lifetime of the QGP in the Bjorken model is

$$\Delta\tau_{\mathrm{QGP}} = \tau_c - \tau_0 = \tau_0 \left[\left(\frac{T_0}{T_c}\right)^3 - 1\right]$$

1D Bjorken Model (III)

Entropy conservation in ideal hydrodynamics leads in the case of the Bjorken model (independent of the equation of state) to

$$s(\tau) = \frac{s_0 \tau_0}{\tau}$$

which follows in case of an ideal QGP directly from

$$s = \frac{\varepsilon + p}{T} = \frac{4}{3}\frac{\varepsilon}{T} = \frac{4}{3}\frac{\varepsilon_0}{T_0}\frac{\tau_0}{\tau}$$

If we consider a QGP/pion gas phase transition we have a first oder phase transition and a mixed phase with temperature T_c. The entropy in the mixed phase is given by

$$s(\tau) = s_\pi(T_c)\xi(\tau) + s_{\mathrm{QGP}}(T_c)(1 - \xi(\tau)) = \frac{s_0 \tau_0}{\tau}$$

$\xi(\tau)$: fraction of fireball in pion gas phase

This equation determines the time dependence of $\xi(\tau)$ and the time τ_h at which the mixed phase vanishes:

$$\xi(\tau) = \frac{1 - \tau_c/\tau}{1 - g_\pi / g_{\mathrm{QGP}}} \quad \rightsquigarrow \quad \tau_h = \tau_c \frac{g_{\mathrm{QGP}}}{g_\pi}$$

Inserting the number of degrees of freedom we obtain

$$N_f = 2\,(3) \quad \rightsquigarrow \quad g_{\mathrm{QGP}} = 37\,(47.5) \quad \rightsquigarrow \quad \tau_h = 12.3\,(15.8)\tau_c$$

QGP Lifetime in the 1D Bjorken Model with a transition from an ideal QGP to an ideal pion gas

Initial temperature from initial energy density:

$$\varepsilon_0 = g_{\mathrm{QGP}} \frac{\pi^2}{30} T^4 \quad \rightarrow \quad T_0 = \left(\frac{30}{\pi^2} \frac{\varepsilon_0}{g_{\mathrm{QGP}}} \right)^{1/4}$$

Getting the proper units (example):

$$\varepsilon_0 = 11\,\mathrm{GeV/fm}^3 \underset{\uparrow}{=} 11 \cdot 0.197^3\,\mathrm{GeV}^4 \quad \text{for } \tau_0 = 1\mathrm{fm}/c$$

$$1 = \hbar c = 0.197\,\mathrm{GeV} \cdot \mathrm{fm}$$

Energy density × τ	$\Delta\tau_{\mathrm{QGP}}$	$\Delta\tau_{\mathrm{mixed}}$
$\varepsilon_0\,\tau = 3$ GeV/fm^2	1.4 fm/c	28 fm/c
$\varepsilon_0\,\tau = 5$ GeV/fm^2	2.6 fm/c	40 fm/c
$\varepsilon_0\,\tau = 14$ GeV/fm^2	6.7 fm/c	87 fm/c

parameters: $N_f = 2$, $T_c = 155$ MeV, $\tau_0 = 1$ fm/c

[Mathematica notebook]

1D Bjorken Model: Energy Density and Temperature as a Function of Proper Time

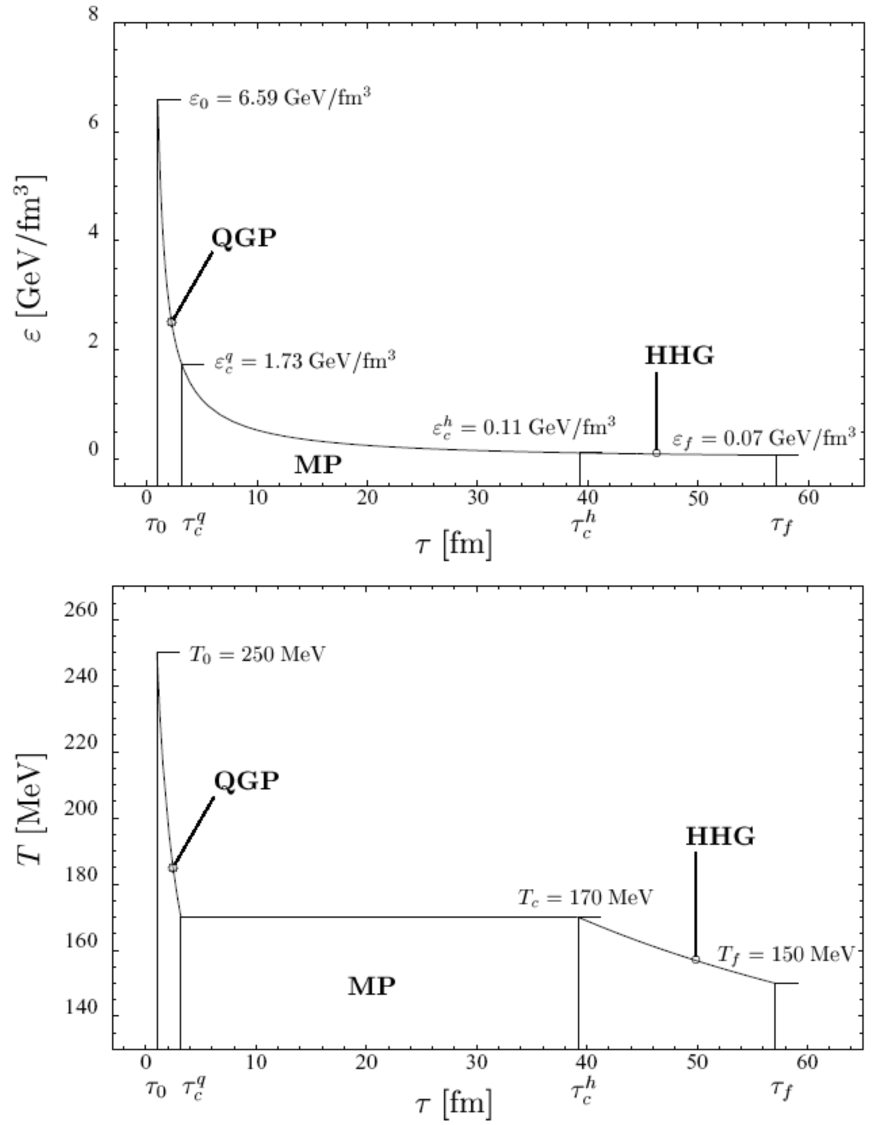

Energy Density and Time Scales in the Bjorken Picture

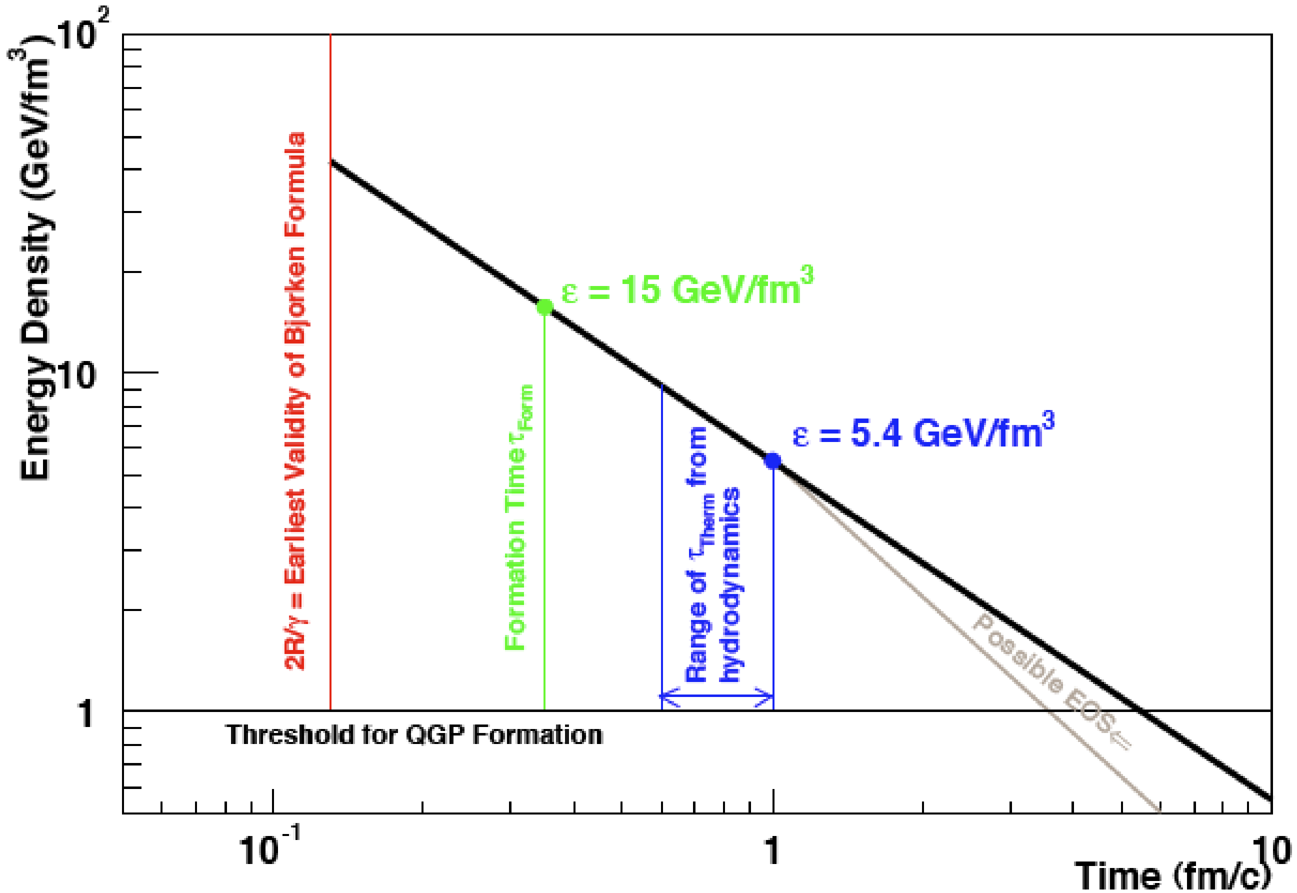

τ_0 = 1 fm/*c* is generally considered as a conservative estimate for the use in the Bjorken formula. Other estimates yields shorter times (e.g. τ_0 = 0.35 fm/*c*) resulting in initial energy densities at RHIC of up to 15 GeV/fm^3

6.2 p_T Spectra and Radial Flow

m_T Spectra from a Stationary Thermal Source

Stationary thermal source:

$$E\frac{d^3n}{d^3p} = \frac{1}{m_T}\cdot\frac{dn}{dm_T dy d\phi} = \frac{gV}{(2\pi)^3} E e^{-(E-\mu)/T}$$

$V = \text{volume}$

$g = \text{spin/isospin-degeneracy factor}$

$\mu = b\mu_b + s\mu_s = \text{chemical potential from baryon and strangeness quantum numbers}$

The corresponding transverse mass spectrum can be obtained by integrating over rapidity:

$$\frac{1}{m_T}\frac{dn}{dm_t} = \frac{V}{2\pi^2} m_T K_1\left(\frac{m_T}{T}\right) \xrightarrow{m_T \gg T} V' \sqrt{m_T} e^{-m_T/T}$$

$K_1 = \text{Modified Bessel functions of 2nd kind}$

Schnedermann, Sollfrank, Heinz, Phys.Rev.C48:2462-2475,1993

Relation between Temperature and Slope

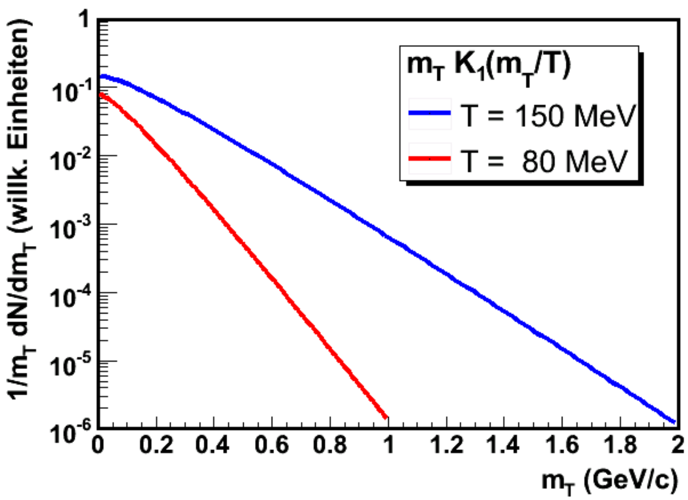

Slope of the m_T (or p_T) spectrum reflects the temperature of the fireball

- However, other effects like collective flow and resonance decays affect the slope as well and make the extraction of the temperature more difficult

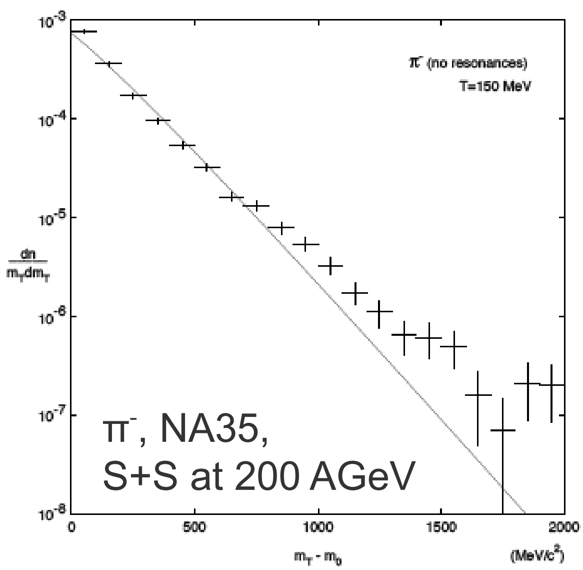

- m_T spectra are indeed approximately exponential with an almost uniform slope $1/T$
- However, clear deviation are visible:
  A stationary thermal source clearly is an oversimplification

Schnedermann, Sollfrank, Heinz,
Phys.Rev.C48:2462-2475,1993

Rapidity Distribution for a Stationary Fireball

$$\frac{dn_{th}}{dy} = \frac{V}{(2\pi)^2} T^3 \left(\frac{m^2}{T^2} + \frac{m}{T} \frac{2}{\cosh y} + \frac{2}{\cosh^2 y} \right) \exp\left(-\frac{m}{T} \cosh y \right)$$

Reduces for light particles to: $$\frac{dn}{dy} \propto \frac{1}{\cosh^2(y - y_0)}$$

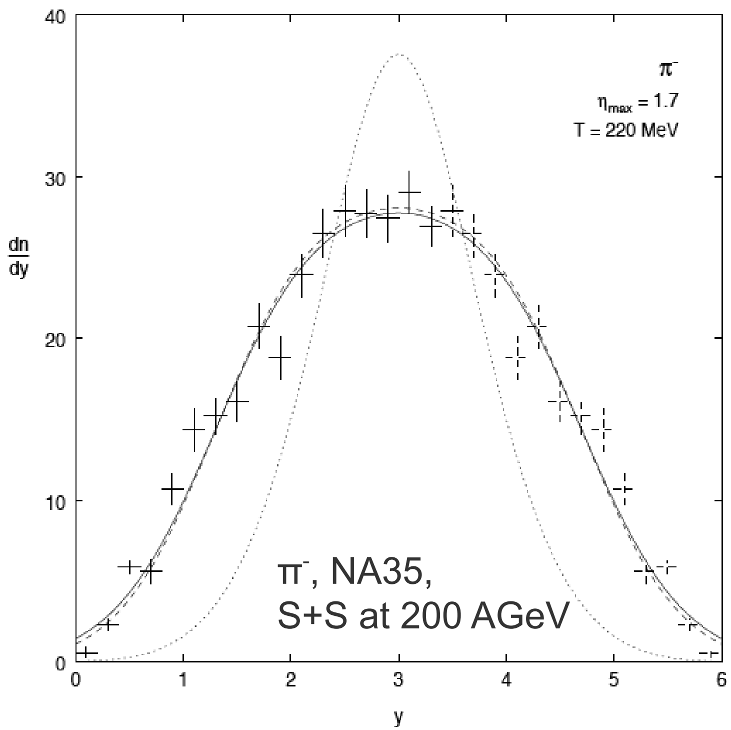

- Full width at half height for stationary fireball in sharp contrast to the experimental value

$$\Gamma_{\text{th}}^{\text{fwhm}} \approx 1.76 \quad \Gamma_{\text{exp.}}^{\text{fwhm}} \approx 3.3 \pm 0.1$$

- Superposition of fireballs with different rapidities (following the Bjorken picture) can describe the data

$$\frac{dn}{dy}(y) = \int_{\eta_{\text{min}}}^{\eta_{\text{max}}} d\eta \frac{dn_{th}}{dy}(y - \eta)$$

Effect of Resonance Decays on Transverse Spectra

Apart from directly emitted pions there are also pions which originate from the decay for resonances, e.g.,

$$\rho^0 \to \pi^+\pi^-, \quad \omega \to \pi^+\pi^-\pi^0, \quad \Delta \to N\pi^-$$

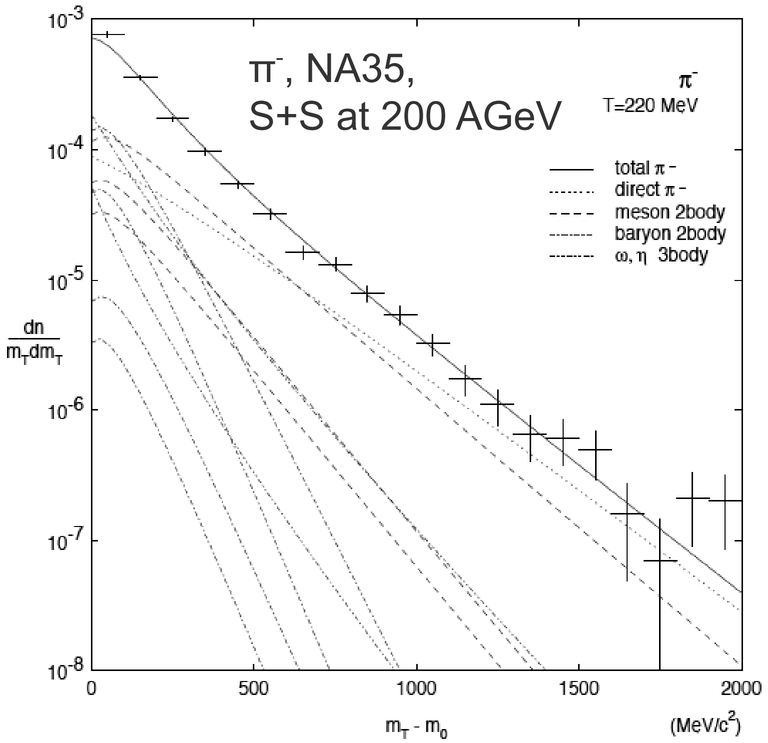

The kinematics of the resonance decays result in very steeply dropping daughter pion spectra and raise considerably the total pion yield at low m_T

Including resonanc decays, it is possible to the describe the spectrum of pions over the whole range in m_T , with the temperature T corresponding to the slope at high m_T

Radial Flow

Schnedermann, Sollfrank, Heinz, Phys.Rev.C48:2462-2475,1993

- Arguments for the existence of radial flow
  - At $T \approx 200$ MeV the mean free path of pions in hadronic matter is much less than 1 fm. On the other hand, the size of the fireball is several fm. Consequently, the pions cannot leave the interaction zone at $T \approx 200$ MeV without further collisions, the reaction region cannot decouple thermally and should by continuing expansion force the pions to cool down further.
  - It is inconsistent to assume that a thermalized system expands collectively in longitudinal direction without generating also transverse flow from the high pressures in the hydrodynamic system
  - Experimental argument: Transverse flow flattens, in the region $p_T < m$, the transverse mass spectra of the heavier particles more than for the lighter particles, in agreement with data (next slide)

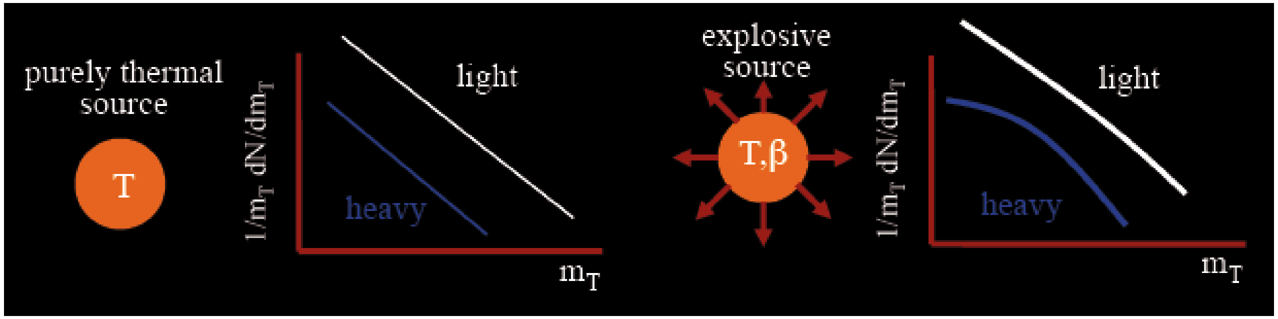

Heavier particles profit more from collective flow than the light ones:

$$\langle E \rangle \approx \langle E_{\mathrm{th}} \rangle + \frac{m_0}{2} v_{\mathrm{collective}}^2$$

Identified Particle Spectra in Pb-Pb and pp at the LHC

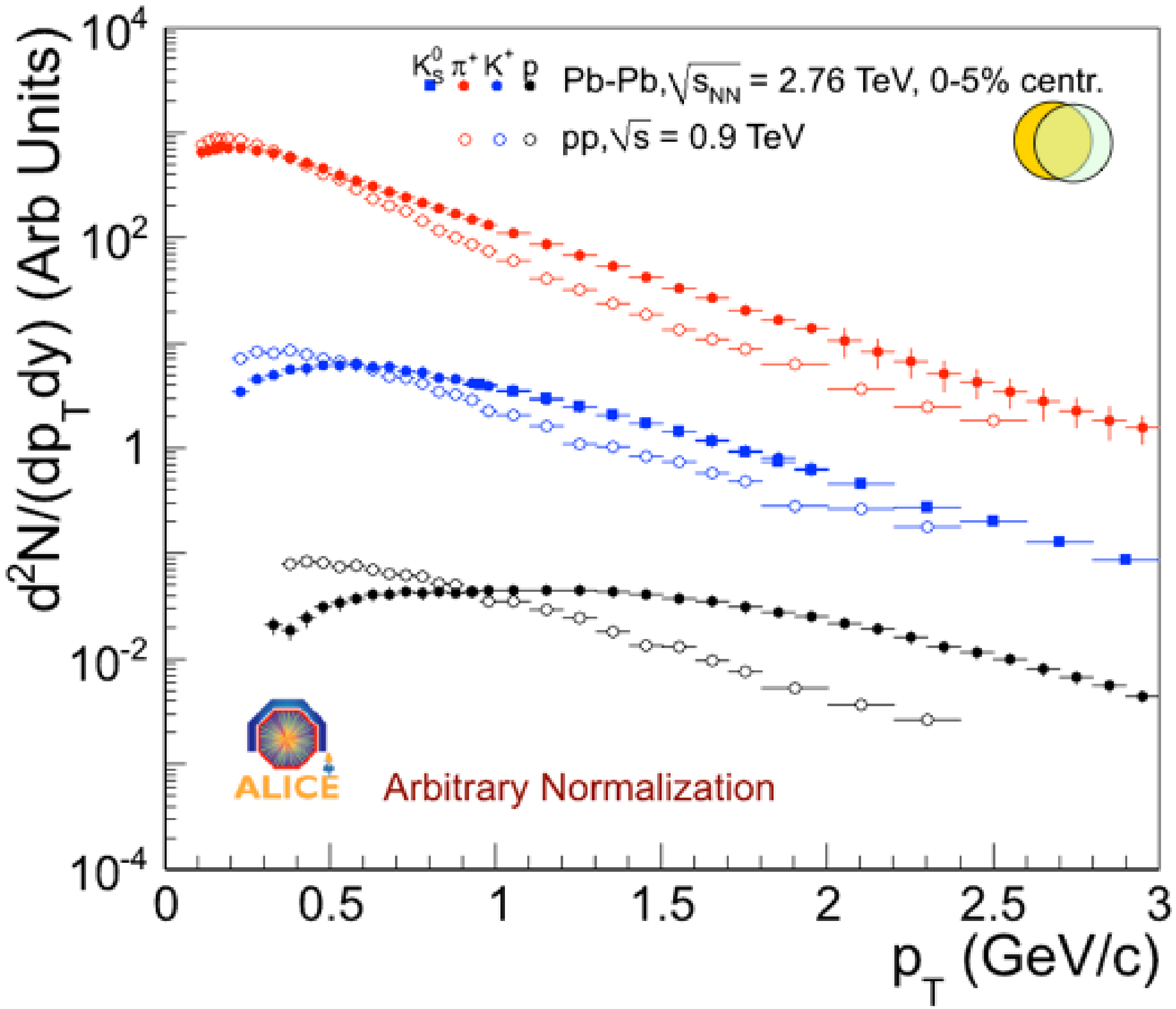

Change of shape of p_T spectra from pp to Pb-Pb as expected from radial flow

The Blast-wave Model: A Simple Model to Describe the Effect of Radial Flow on Particle Spectra

Transverse velocity profile: $\beta_T(r) = \beta_s \left(\frac{r}{R}\right)^n$

Superposition of thermal sources with different radial velocities:

$$\frac{1}{m_T}\frac{dn}{dm_T} \propto \int_0^R r\,dr\,m_T I_0\left(\frac{p_T \sinh\rho}{T}\right) K_1\left(\frac{m_T\cosh\rho}{T}\right)$$

$$\rho := \mathrm{arctanh}(\beta_T) \quad \text{"transverse rapidity"}$$

$$I_0,\ K_1:\ \text{modified Bessel functions}$$

Schnedermann, Sollfrank, Heinz,
Phys.Rev.C48:2462-2475,1993

Freeze-out at a 3d hyper-surface,
typically instantaneous in radius *r*, e.g.:

$$t_\mathrm{f}(r,z) = \sqrt{\tau_f^2 + z^2}$$

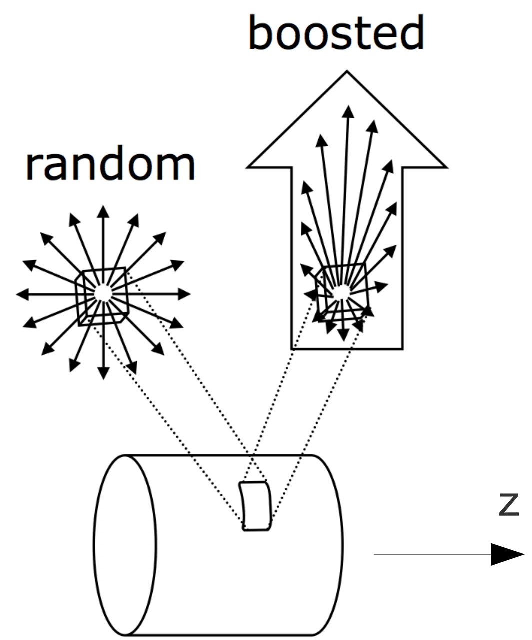

Example: Radial Flow Velocity Profile from Blast-wave Fit to 2.76 TeV Pb-Pb Spectra (0-5%)

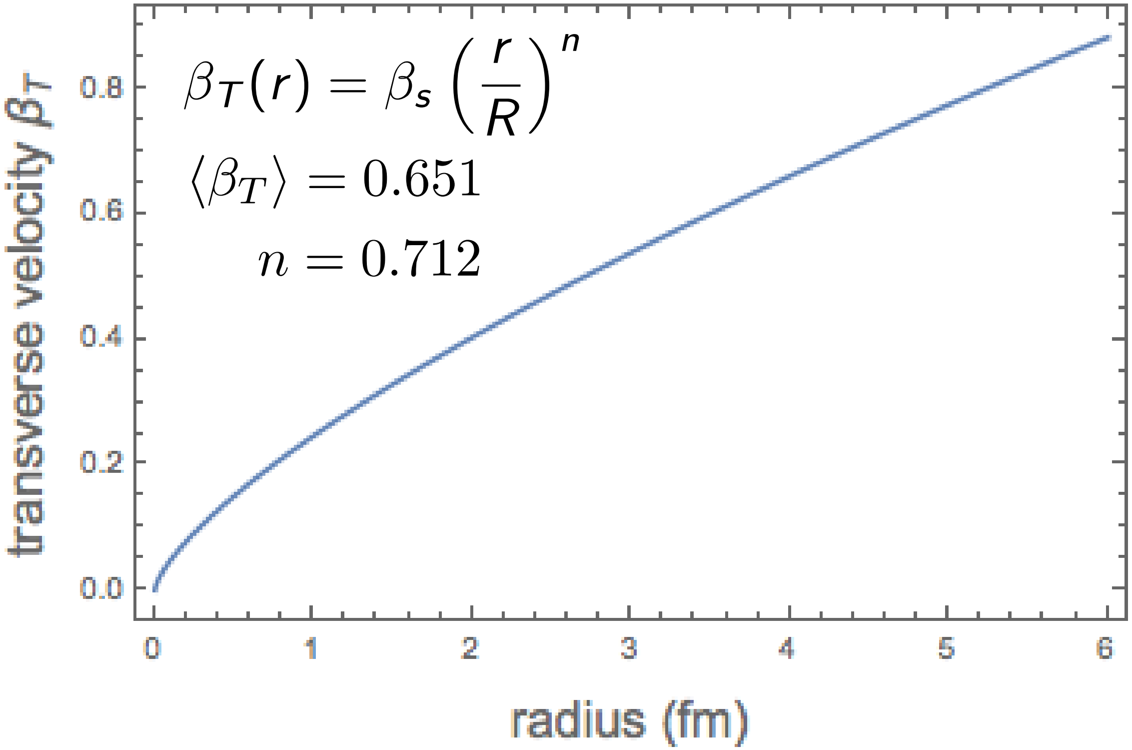

Parameters:
arXiv:1303.0737

$$\langle\beta_T\rangle = \frac{\int_0^R \int_0^{2\pi} r dr d\varphi \beta_T(r)}{\int_0^R \int_0^{2\pi} r dr d\varphi} = \frac{2}{n+2}\beta_s$$

$$\langle\beta_T\rangle = 0.651, n = 0.712 \quad \rightarrow \quad \beta_s = 0.88$$

Example: Pion and Proton p_T Spectra from the Blast-wave model

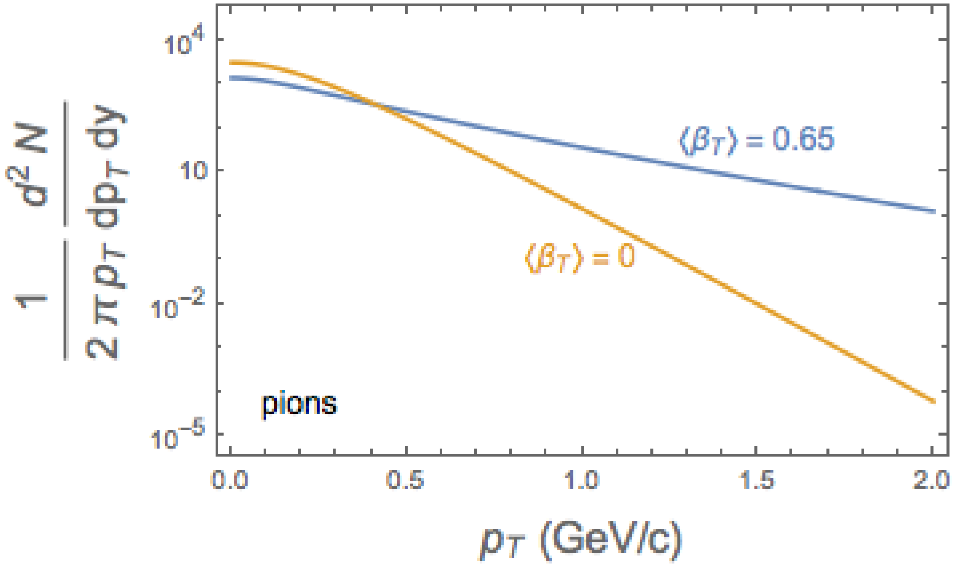

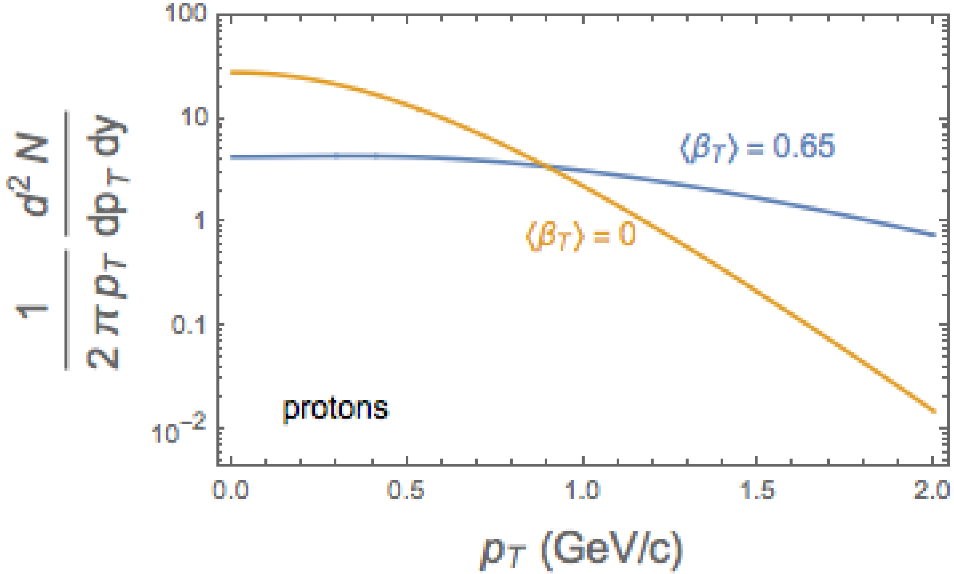

[Mathematica notebook]

Parameters for 0-5% most central Pb-Pb collisions at 2.76 TeV, arXiv:1303.0737

Larger p_T kick for particle with higher mass:

$$p = \beta_{\mathrm{source}} \gamma_{\mathrm{source}} m + \text{"thermal"}$$

Local Slope of m_T Spectra with Radial Flow

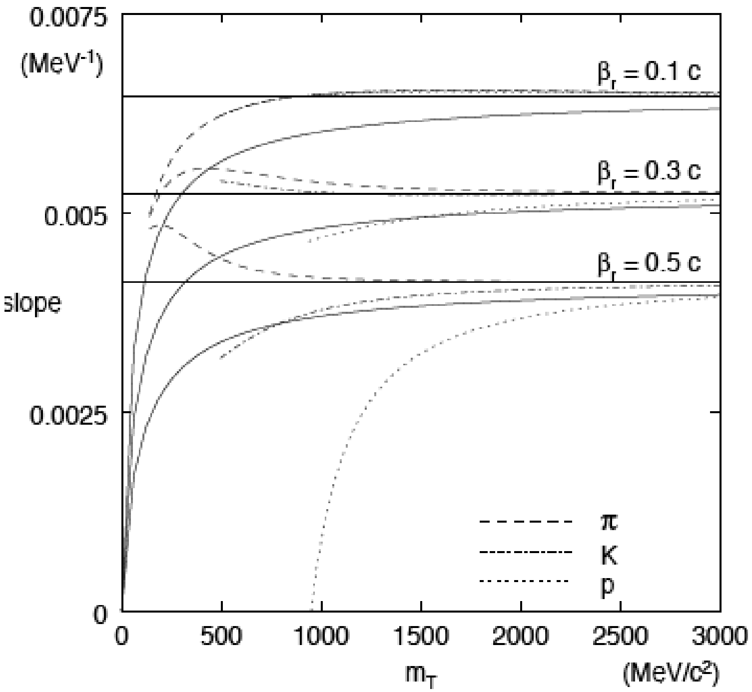

m_T slopes with transverse flow for pions for fixed transverse expansion velocity β_r

$$\lim_{m_t \to \infty} \frac{d}{dm_T} \ln\left(\frac{1}{m_T}\frac{dn}{dm_T}\right) = -\frac{1}{T}\sqrt{\frac{1-\beta_r}{1+\beta_r}}$$

The apparent temperature, i.e., the inverse slope at high m_T, is larger than the original temperature by a blue shift factor:

$$T_{\mathrm{eff}} = T\sqrt{\frac{1+\beta_r}{1-\beta_r}}$$

Blast-Wave Fits at CERN SPS Energy (NA49)

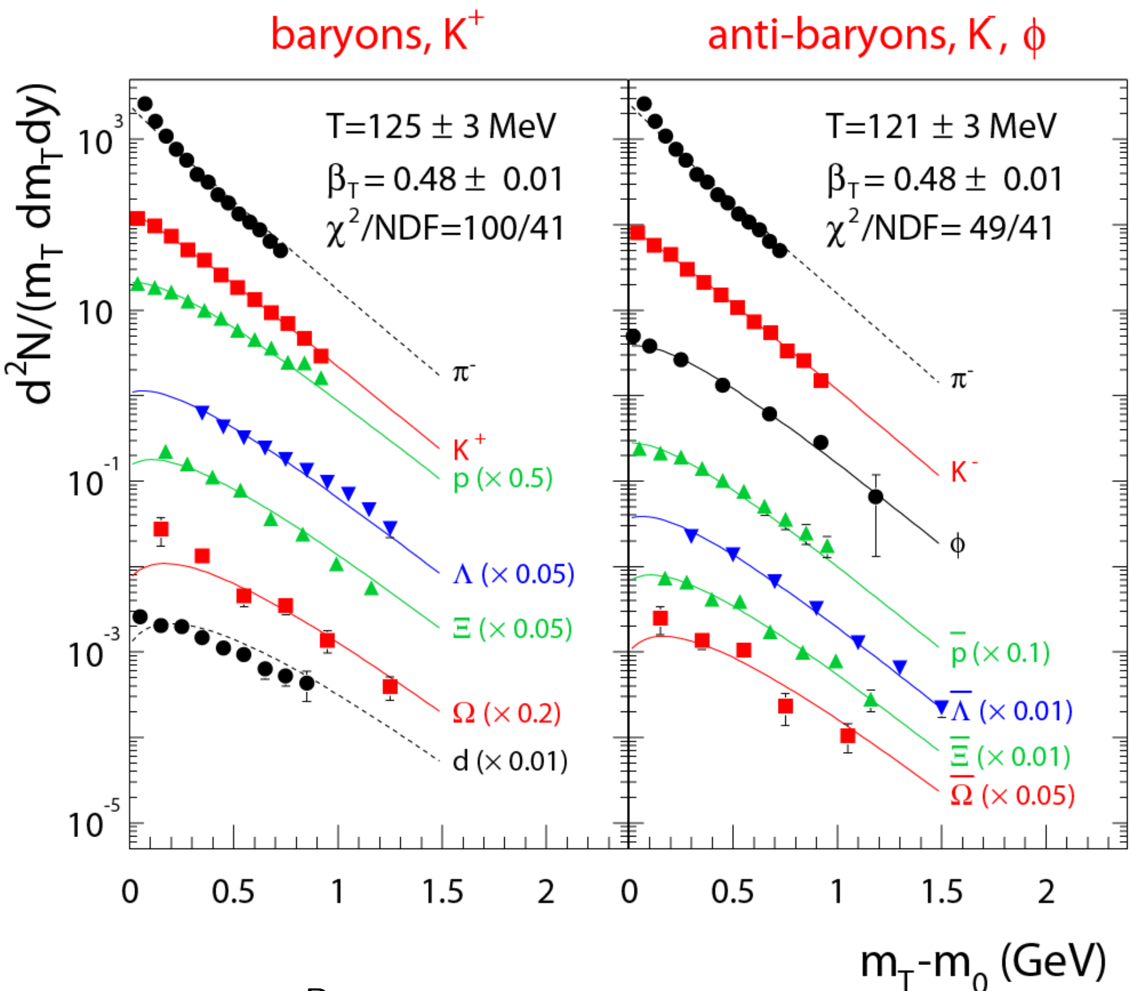

$$\frac{1}{m_T}\frac{dn}{dm_T} \propto \int_0^R r\,dr\,m_T\,I_0\left(\frac{p_T \sinh\rho}{T}\right) K_1\left(\frac{m_T \cosh\rho}{T}\right)$$

Blast-Wave Fits at RHIC Energies (STAR)

STAR, Phys.Rev.C83:034910,2011

Simultaneous fit to all particle species for given centr. class:

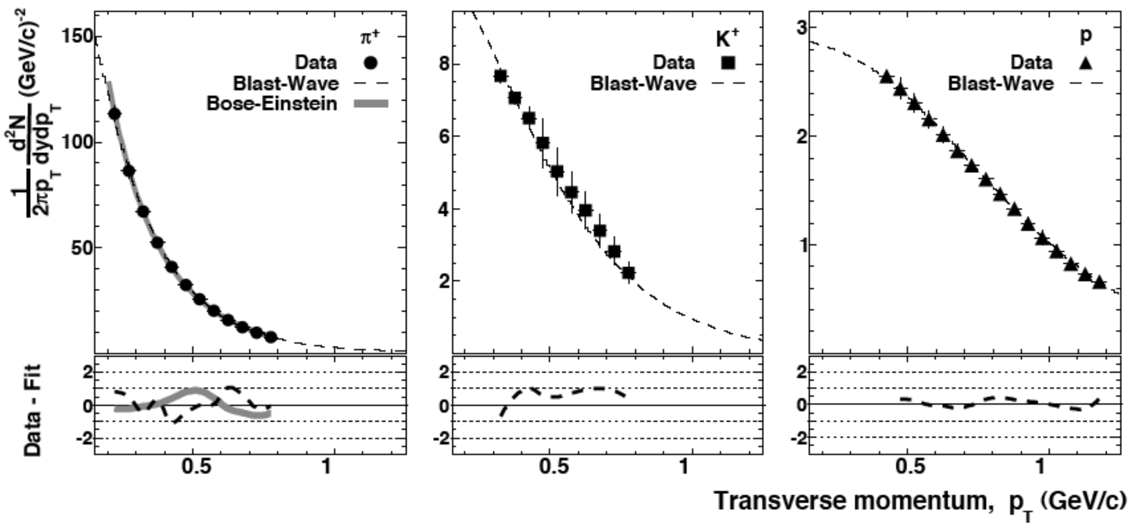

Cu+Cu at 200 GeV, 10% most central

Central A+A collisions at RHIC energies described with
T = 100 – 120 MeV,
$\langle\beta\rangle$ = 0.45 – 0.6 c

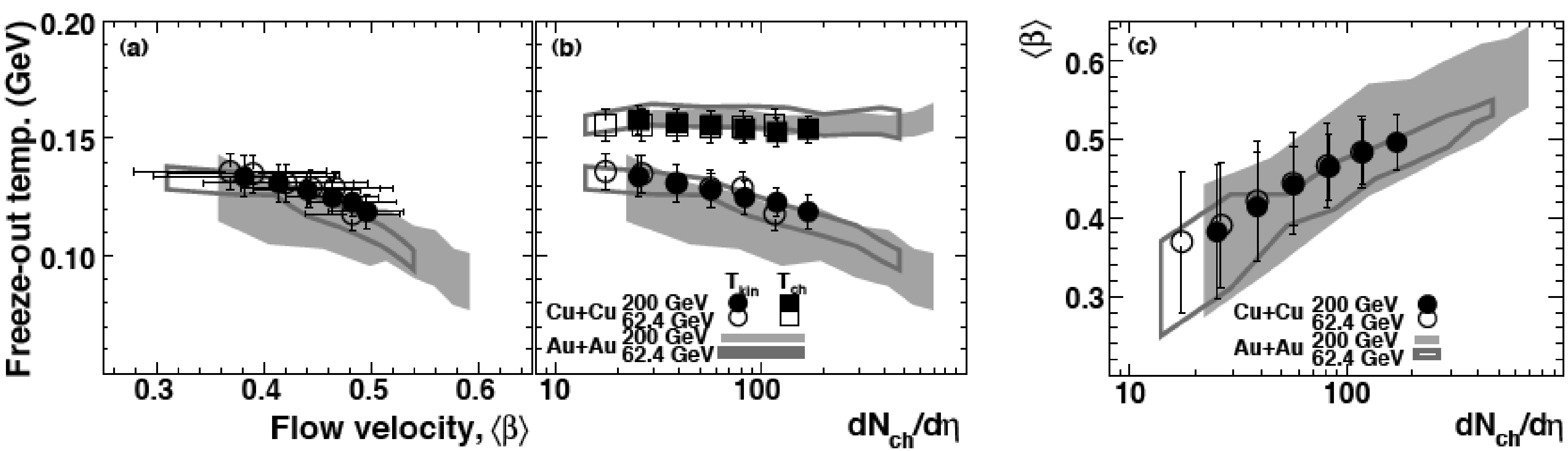

π, K, p Spectra and Blast-wave Fits at the LHC (1/2)

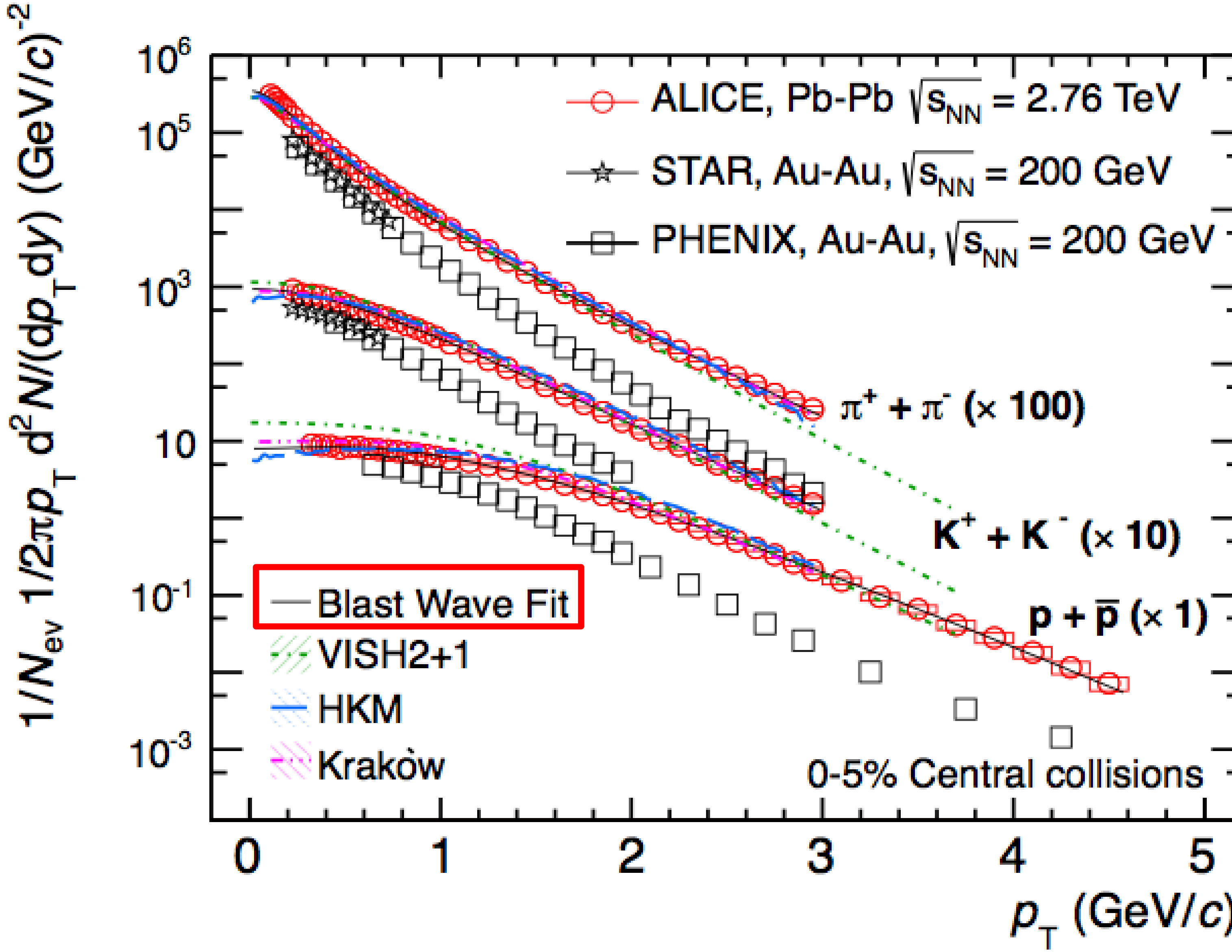

π, K, p Spectra and Blast-wave Fits at the LHC (2/2)

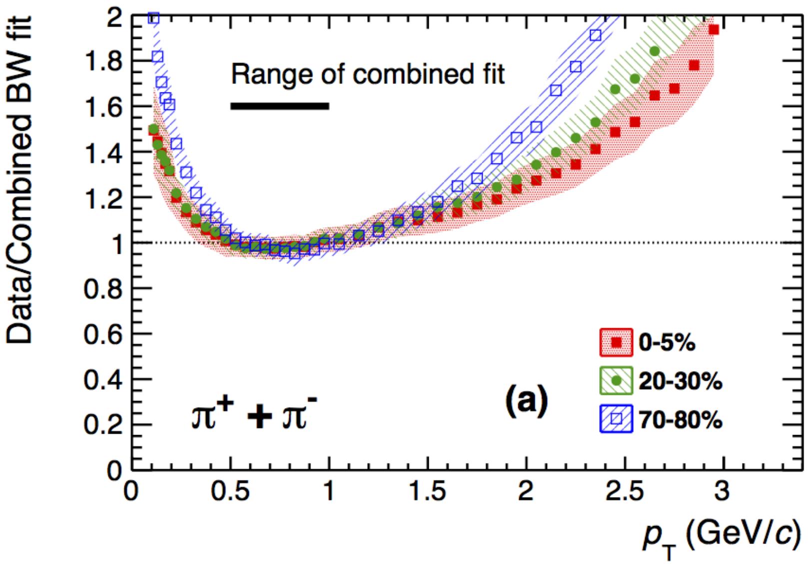

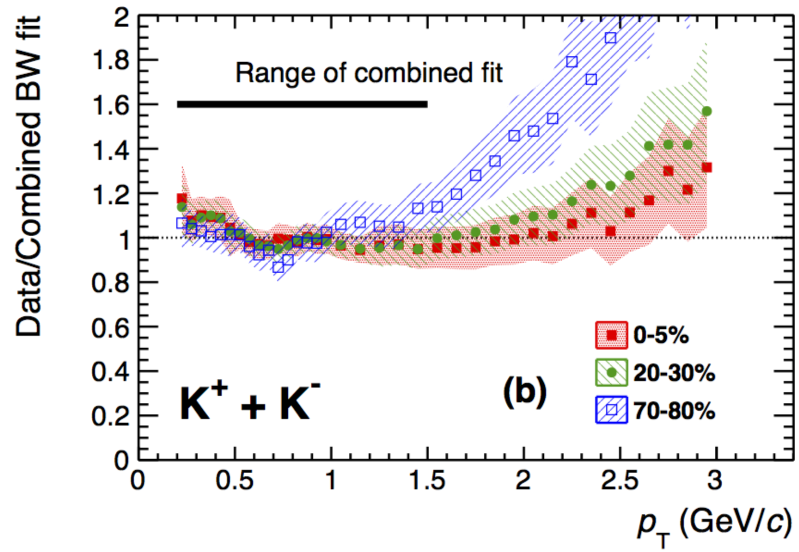

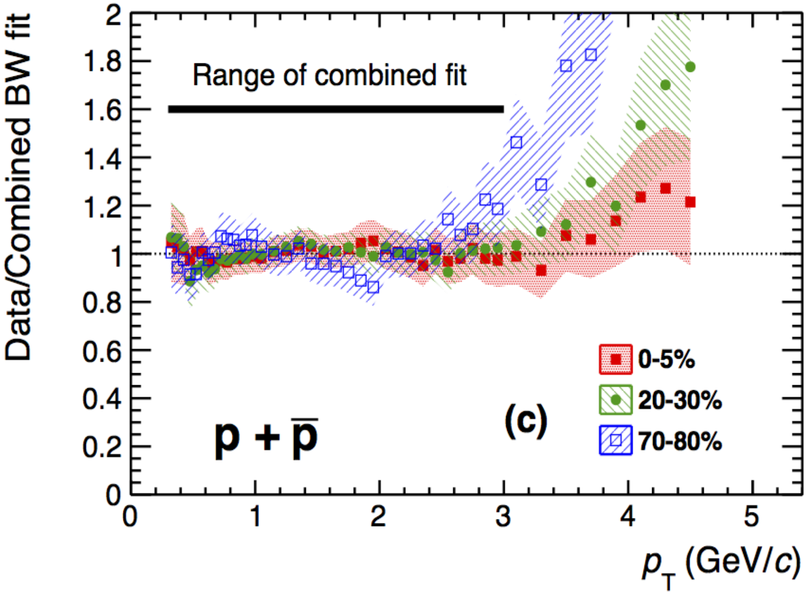

Due to contributions from resonance decay at low p_T and hard scattering contributions at high p_T, the p_T range for the blast-wave fit needs to be chosen carefully.

T und <β> for Different Centralities at RHIC and the LHC

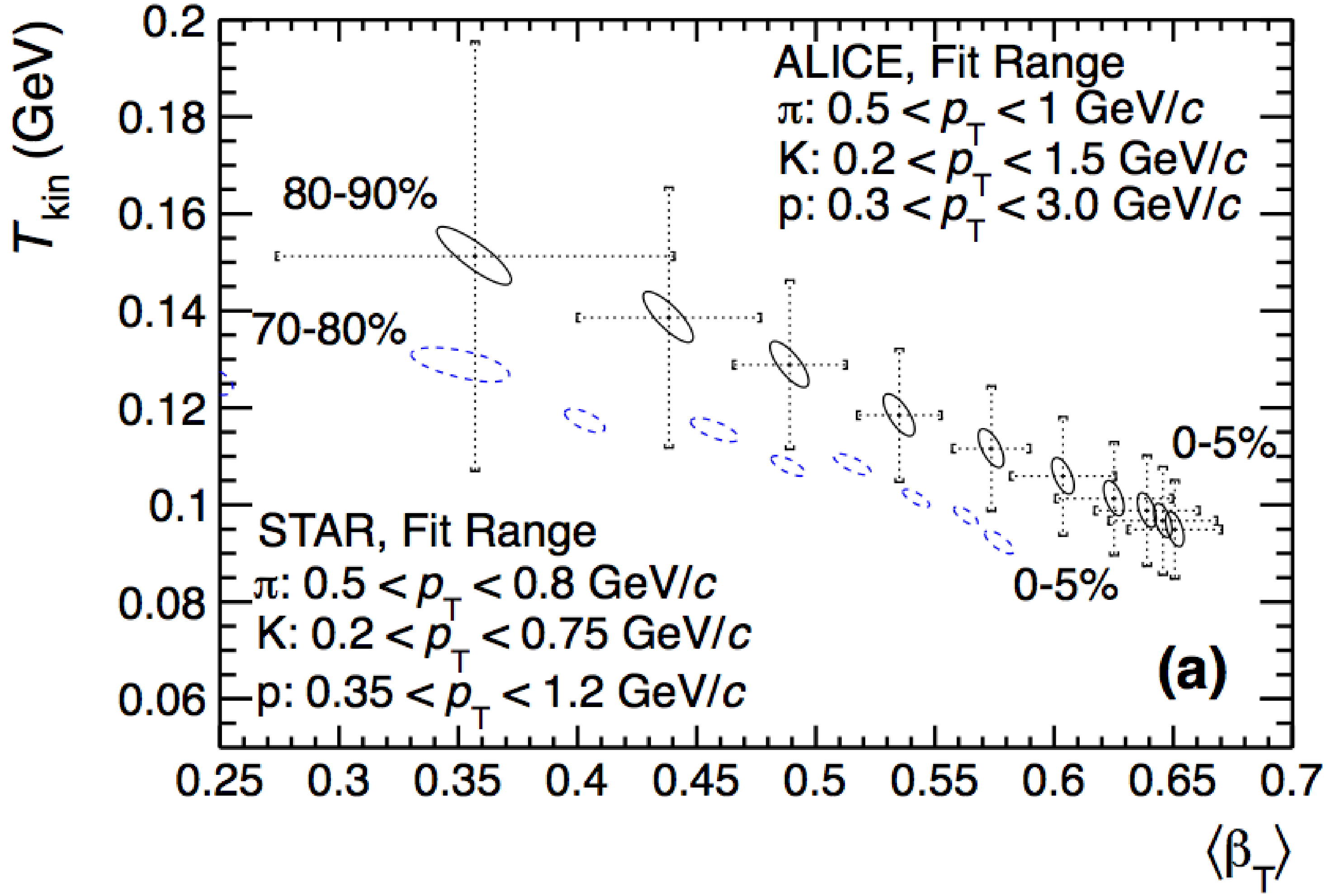

10% larger flow velocities in the most central collisions at the LHC than at RHIC

Radial Flow Velocities as a Function of $\sqrt{s}_{NN}$

Phenix white paper, Nucl.Phys.A757:184-283, 2005 (→ link)

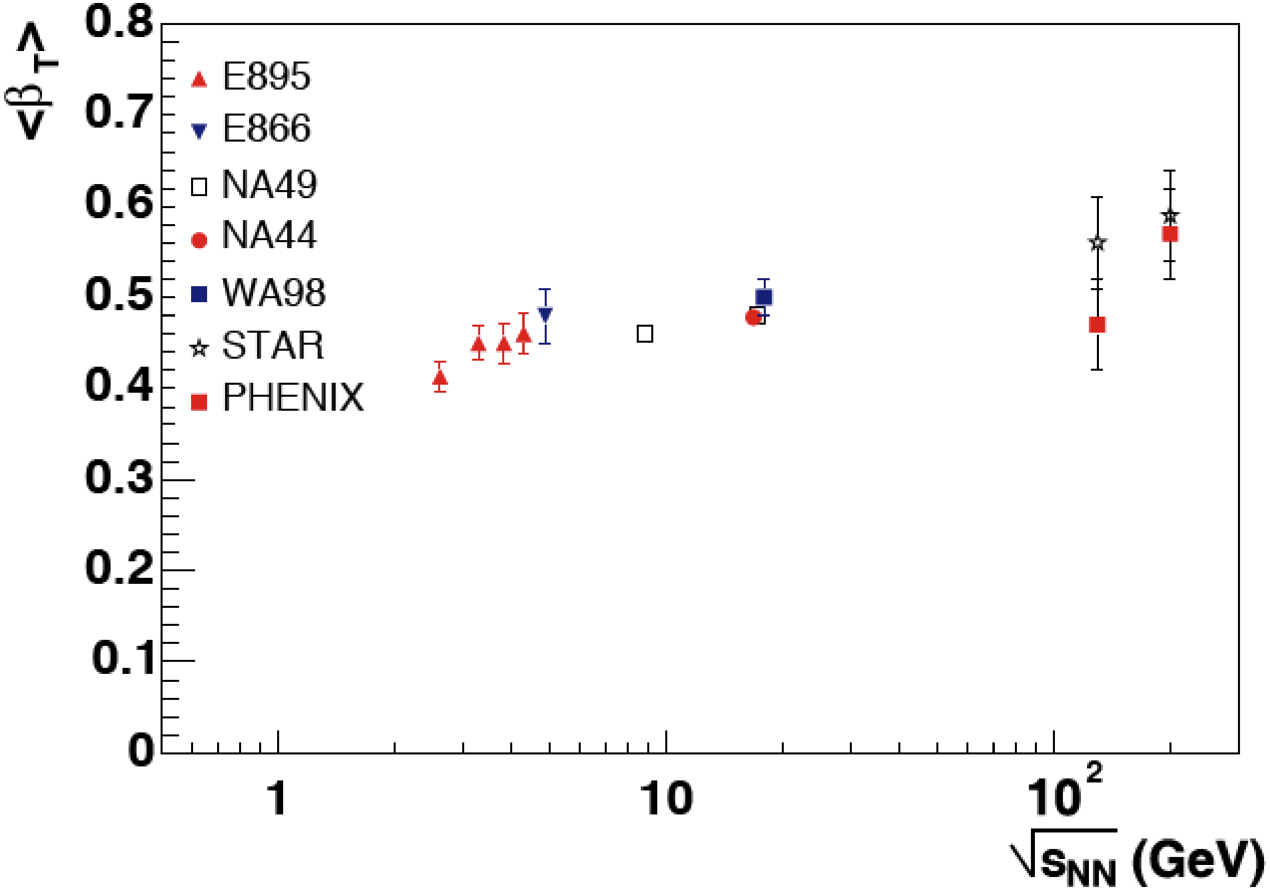

Radial flow velocity in A+A depends only weakly or not at all on CMS energy

Particle Spectra from Hydrodynamics (I)

Initial conditions for hydro calc.:

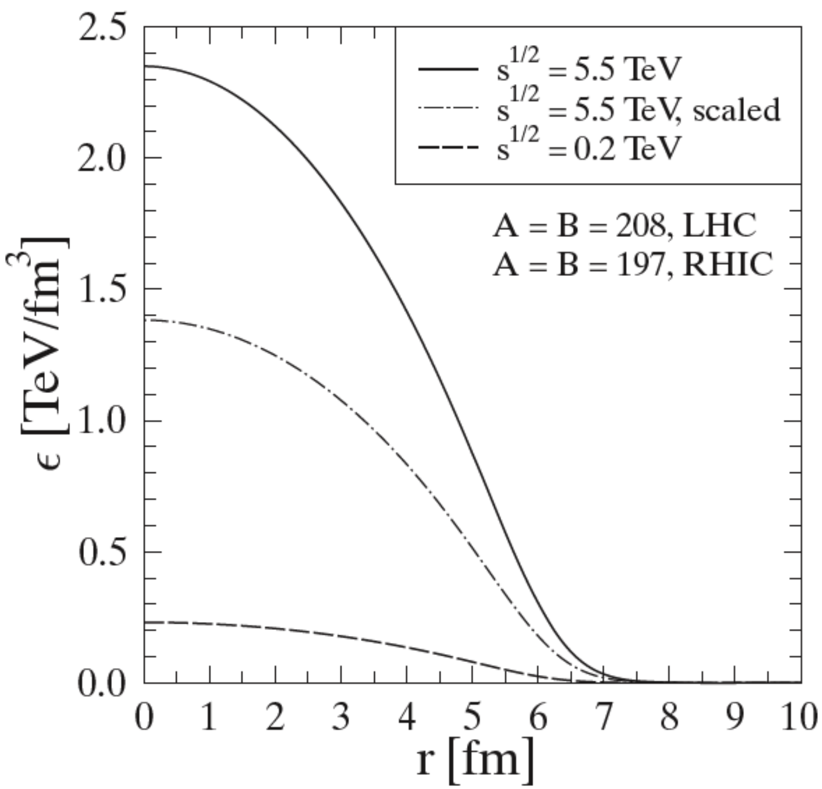

- Fireball evolution treated as an expansion of an (almost) ideal liquid
- Ideal fluid ("perfect liquid")
  - Local thermal equilibrium, mean free path $\lambda = 0$
  - Zero viscosity
- State of the art: viscous hydro (shear viscosity / entropy density > 0)
- Hydro description of the fireball evolution requires early thermalization
- Equation of state (EOS) is needed (e.g., form lattice QCD)
- Input: Initial conditions, e.g., from Glauber calculation:

$$\varepsilon(r) \propto \frac{dN_{\text{part}}}{dr} \ (\text{or} \propto \frac{dN_{\text{coll}}}{dr})$$

Particle Spectra from Hydrodynamics (II)

Transverse expansion of the fireball in a hydro model
(temperature profile):

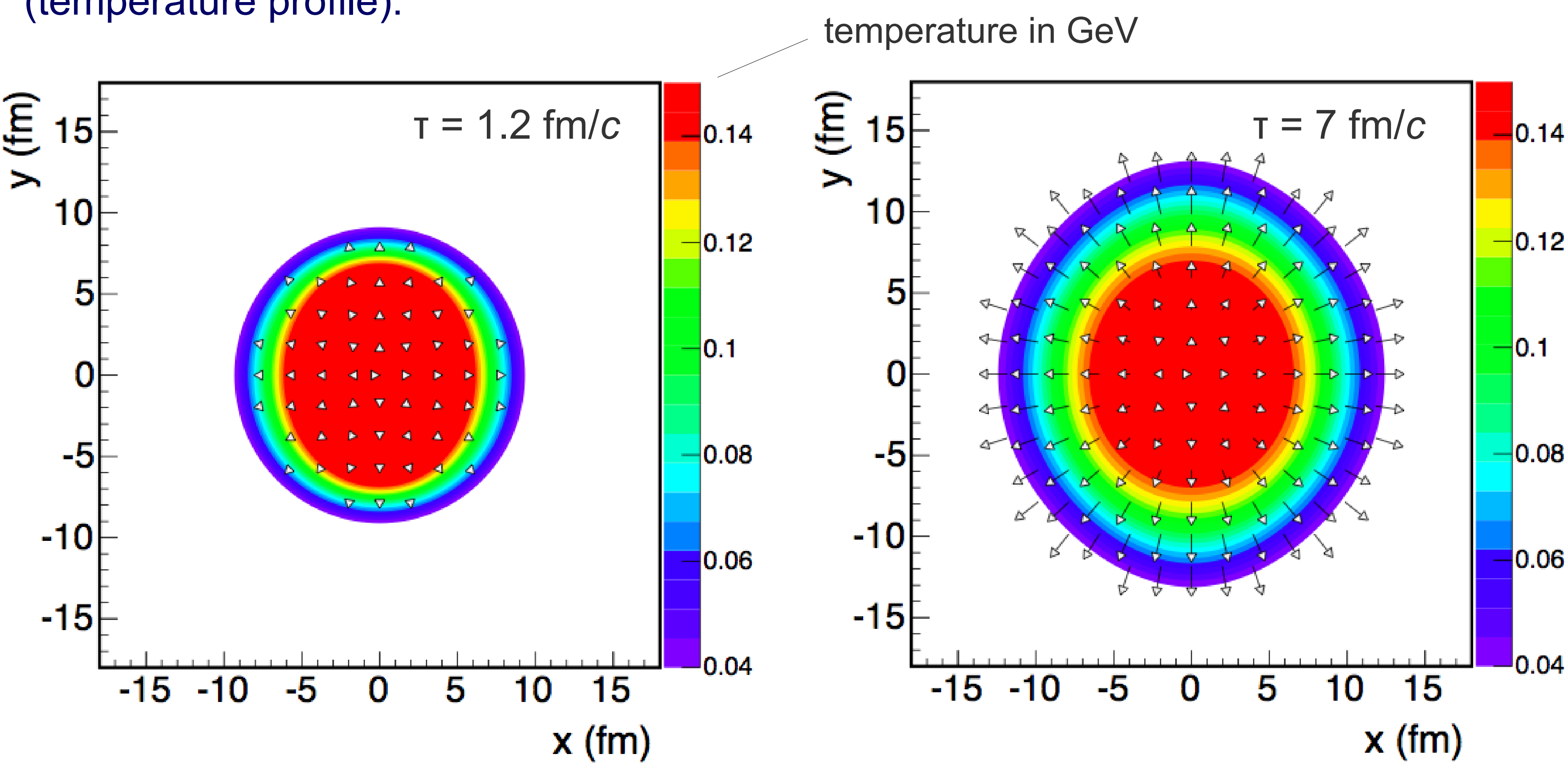

Particle Spectra in Ideal Hydrodynamics (II): Temperature Contours and Flow lines

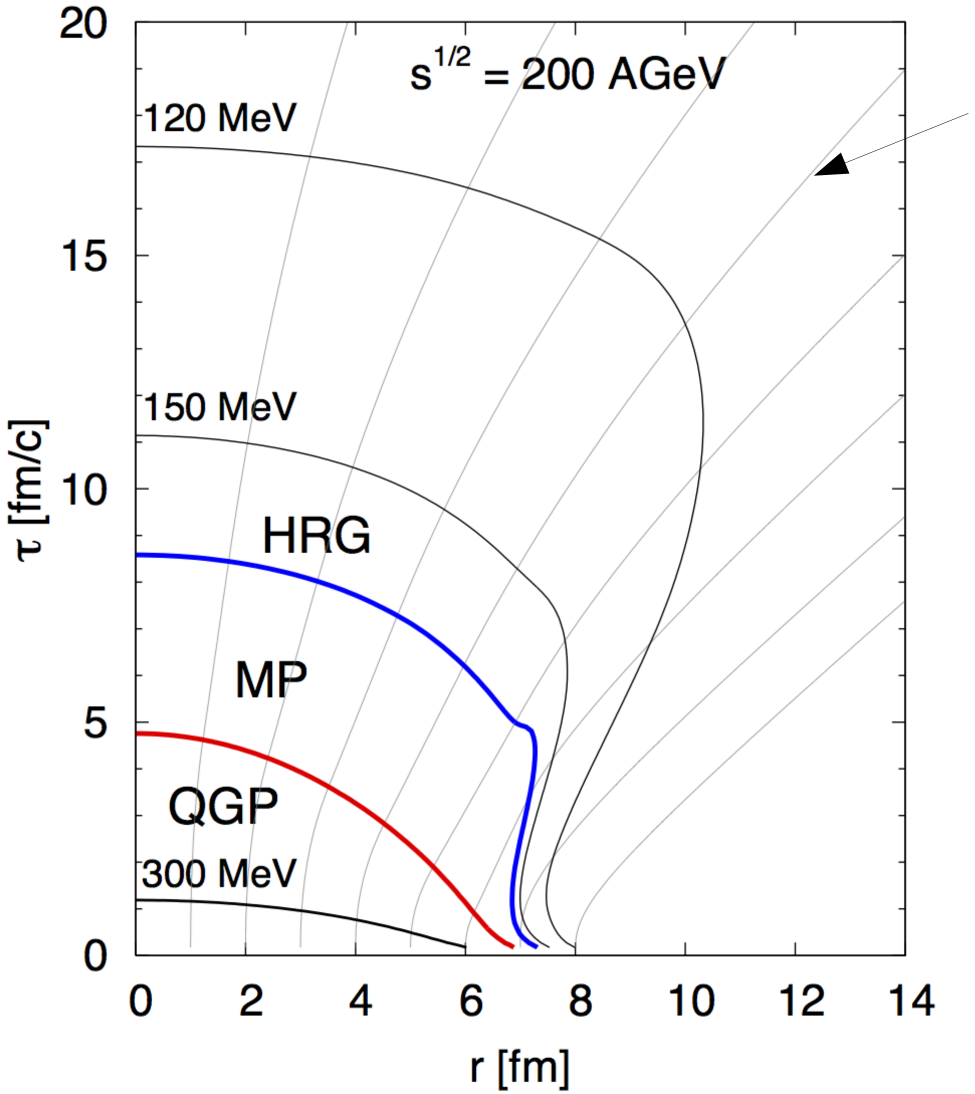

Flow lines indicate how the fluid elements move

Particle Spectra in Ideal Hydrodynamics (IV): Hydro Models Describe π, K, p Spectra at the LHC

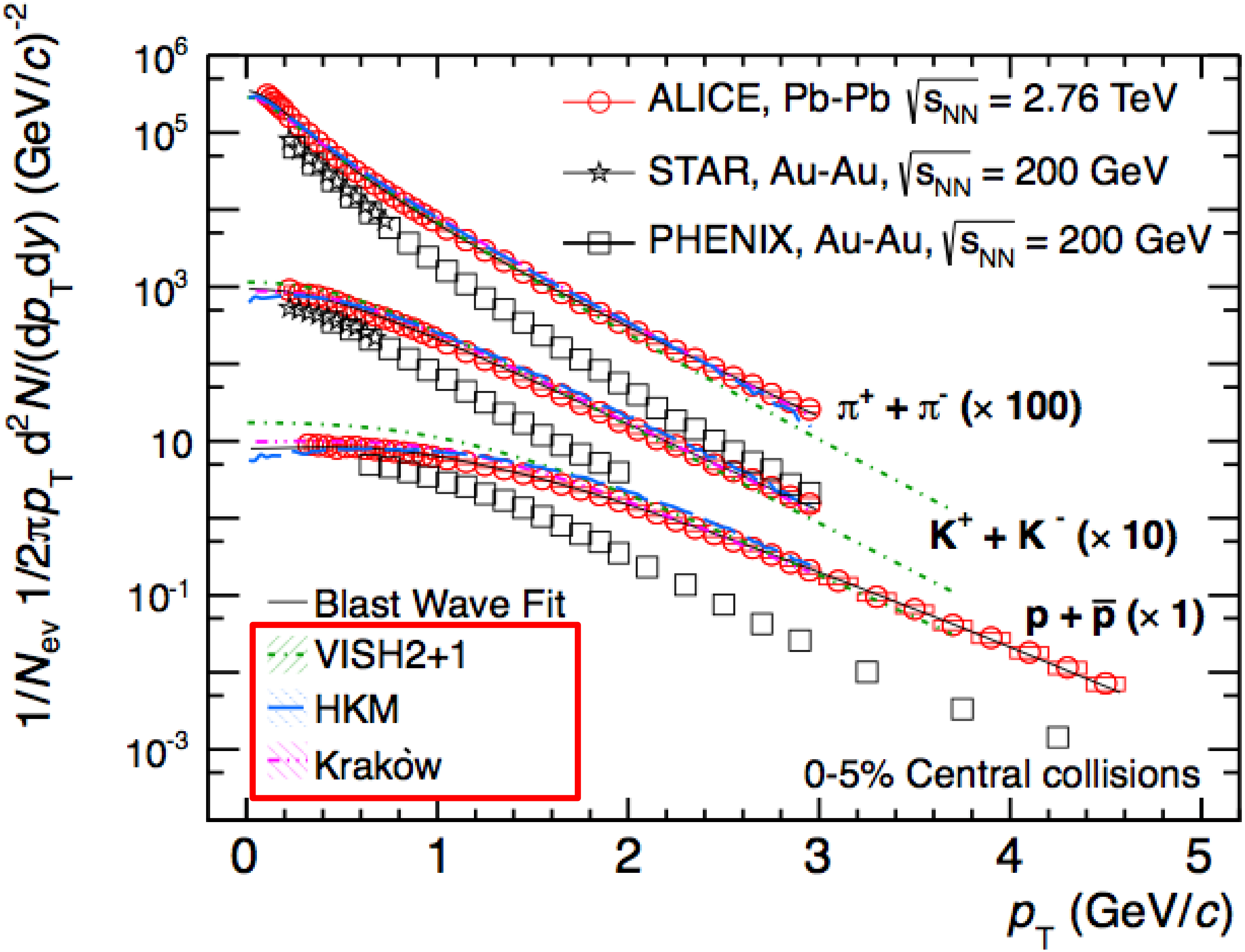

Particle Spectra in Ideal Hydrodynamics (V): Validity of the Hydro Description: Up to p_T= 2 - 3 GeV/*c*

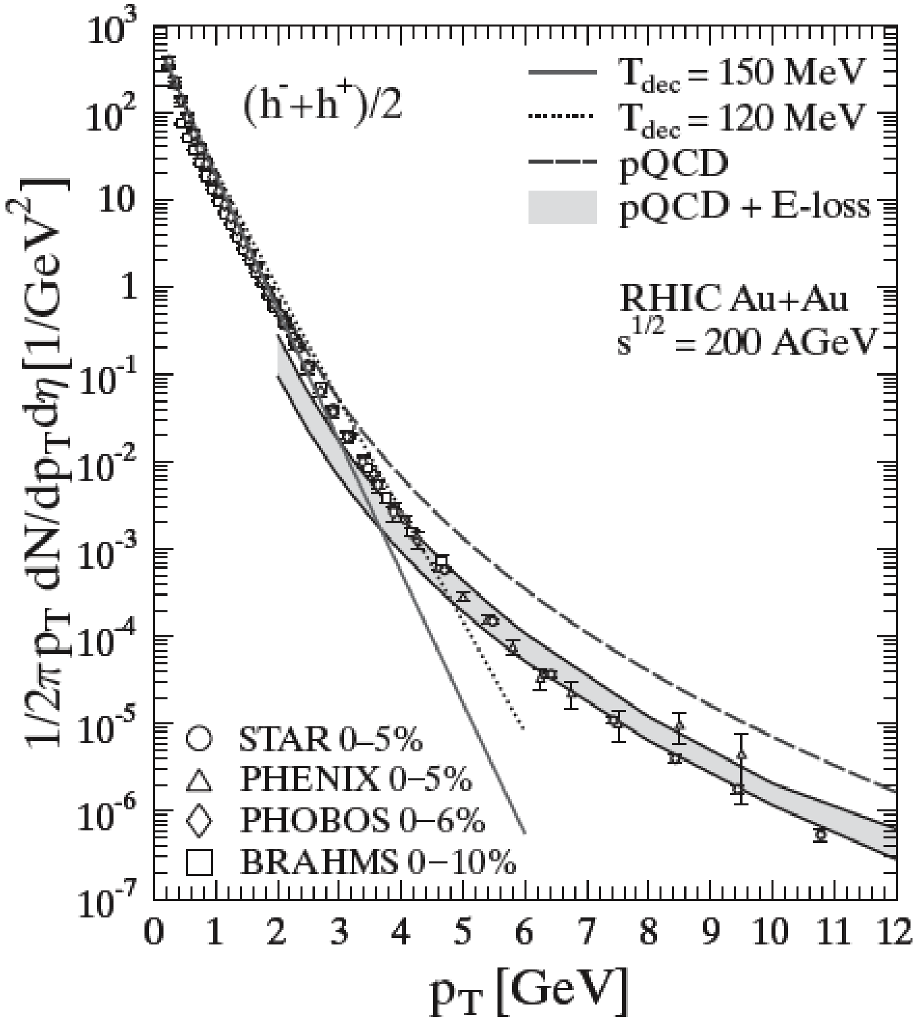

At large p_T the hydro description yields exponential spectra

However, around p_T = 2 – 3 GeV/c the measured spectra start to follow a power law shape

6.3 Directed and Elliptic Flow

The Reaction Plane

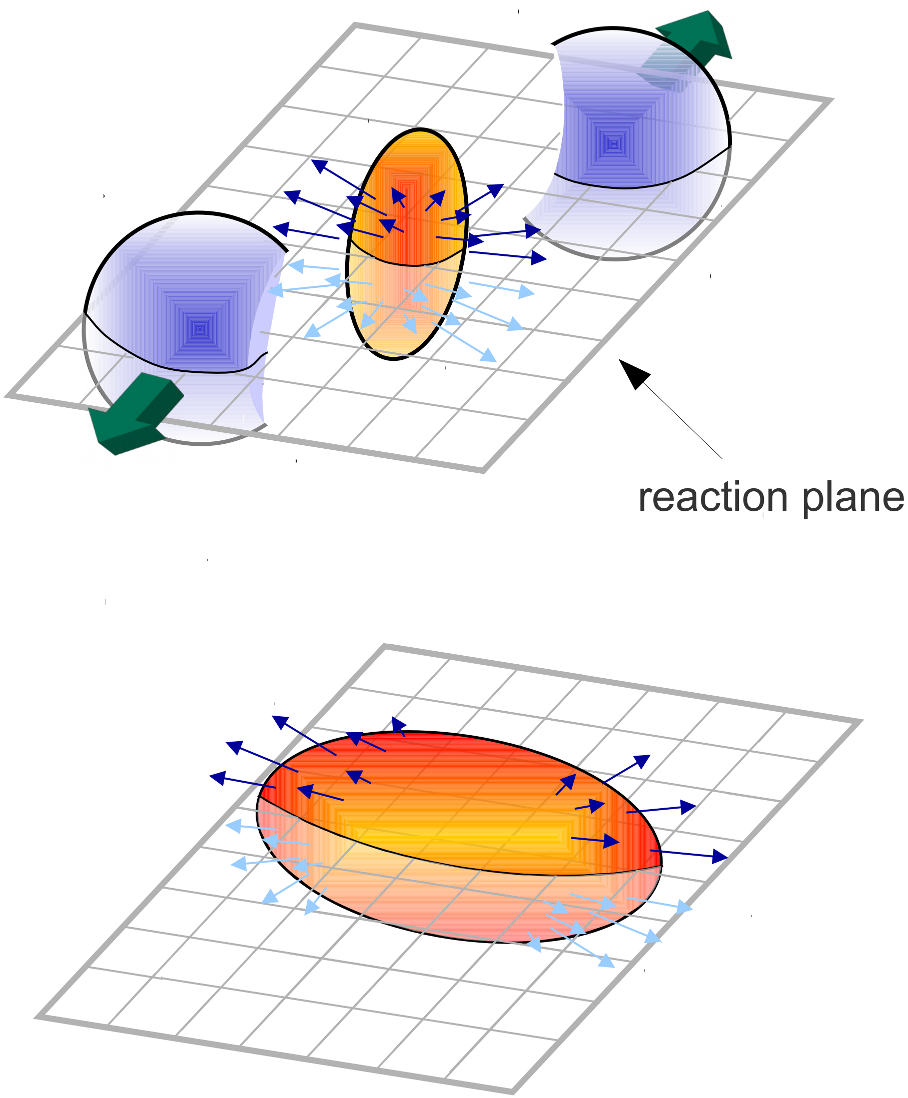

The impact parameter vector ***b*** and the beam axis span the reaction plane

Experimentally, the reaction plane can be measured (with some finite resolution) on an event-by-event basis

One can then study particle production as a function of the emission angle w.r.t. the reaction plane

Fourier Decomposition

anisotropy in coordinate space $\rightarrow$ anisotropy in momentum space

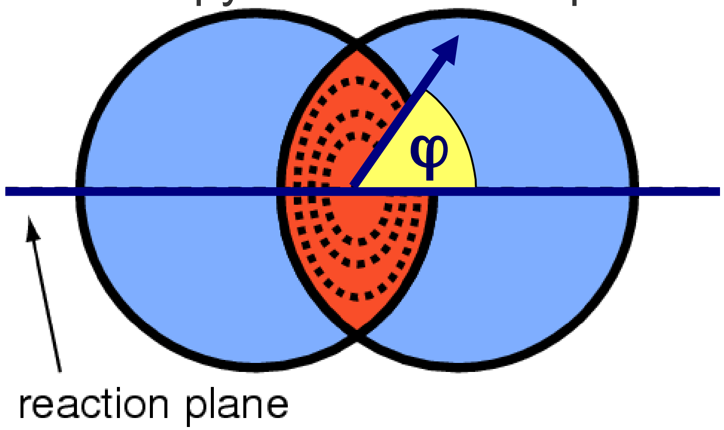

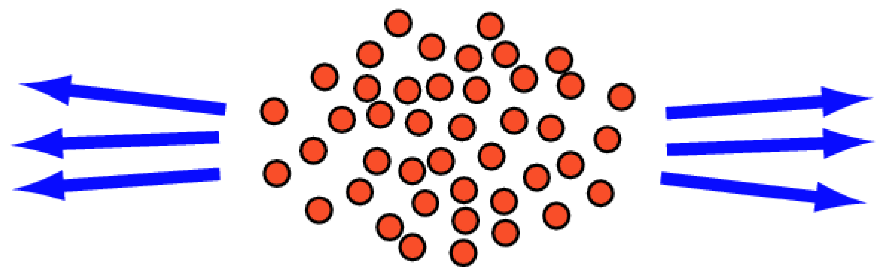

$$E\frac{d^3N}{d^3\mathbf{p}} = \frac{1}{2\pi}\frac{d^2N}{p_t\,dp_t\,dy}\left(1+2\sum_{n=1}^{\infty} v_n \cos[n(\varphi-\Psi_{RP})]\right)$$

The sine terms in the Fourier expansion vanish because of the reflection symmetry with respect to the reaction plane.

Fourier coefficients: $v_n(p_T, y) = \langle \cos[n(\varphi - \Psi_{RP})]\rangle$

v_1 : Strength of the directed flow (small at midrapidity)

v_2 : Strength of the elliptic flow

Visualization of v_n

$$f(\varphi) = 1 + 2 v_n \cos(n\varphi)$$

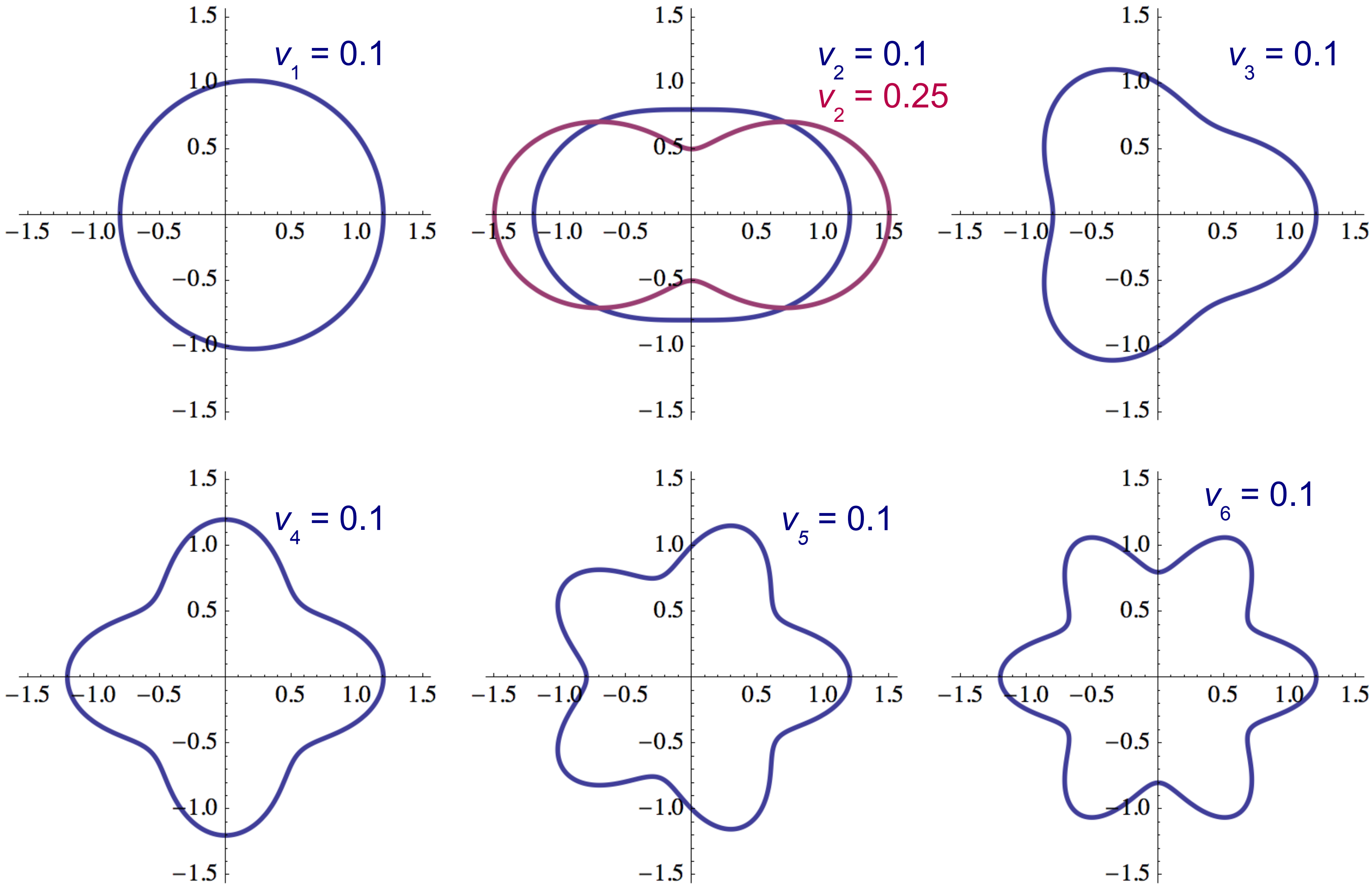

Odd Harmonics

When studying flow w.r.t. to the reaction plane one expects the odd harmonics to be zero due to symmetry reasons:

$$E\frac{\mathrm{d}^3N}{\mathrm{d}^3\mathbf{p}} = \frac{1}{2\pi}\frac{\mathrm{d}^2N}{p_\mathrm{t}\mathrm{d}p_\mathrm{t}\mathrm{d}y}\left(1+2\sum_{n,\,\mathrm{even}} v_n\cos[n(\varphi-\Psi_\mathrm{RP})]\right)$$

$$\approx \frac{1}{2\pi}\frac{\mathrm{d}^2N}{p_\mathrm{t}\mathrm{d}p_\mathrm{t}\mathrm{d}y}\left(1+2v_2\cos[2(\varphi-\Psi_\mathrm{RP})]+2v_4\cos[4(\varphi-\Psi_\mathrm{RP})]\right)$$

Triangular flow component

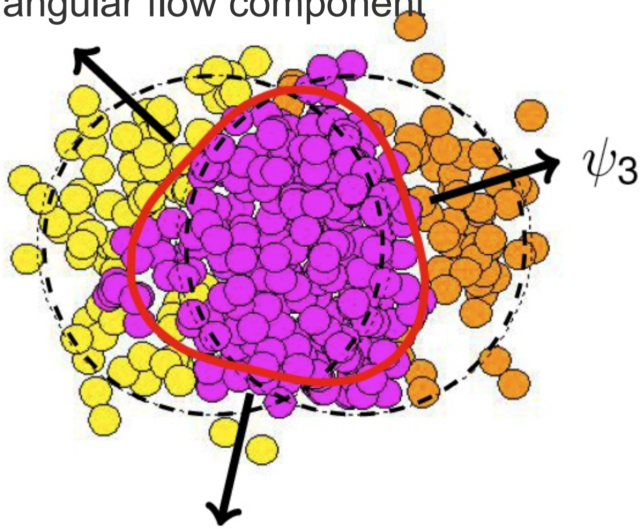

Recently, it was realized that fluctuations of the overlap zone may lead to flow patterns that need to be described by odd harmonics, e.g., triangular flow (v_3). However, the triangular flow appears to be uncorrelated to the reaction plane:

$$\frac{\mathrm{d}N}{\mathrm{d}\varphi} \propto 1+2\sum_{n=1} v_n\cos[n(\varphi-\Psi_n)]$$

Directed Flow (I)

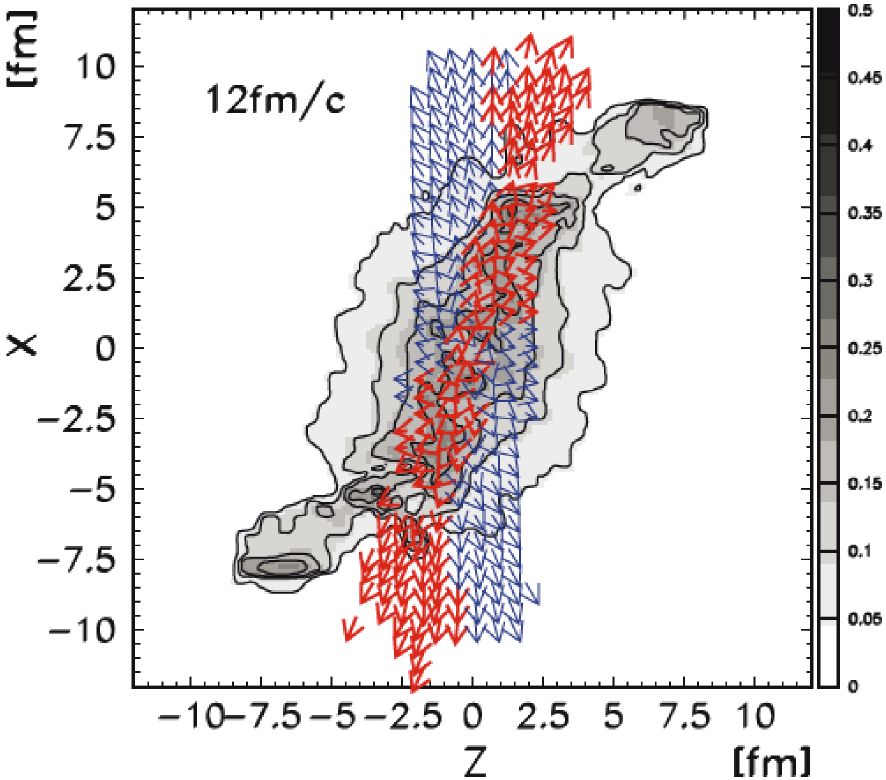

Net-baryon density at t = 12 fm/c in the reaction plane with velocity arrows for mid-rapidity (|y| < 0.5) fluid elements

arXiv:0809.2949

Where the colliding nuclei start to overlap, dense matter is created which deflects the remaining incoming nuclear matter.

The deflection of the remnants of the incoming nucleus at positive rapidity is in the +x direction leading to $p_x > 0$, and the remnants of the nucleus at negative rapidity are deflected in the direction thus having a $p_x < 0$

The deflection happens during the passing time of the colliding heavy-ions. Thus, the system is probed at early times.

Directed Flow (II)

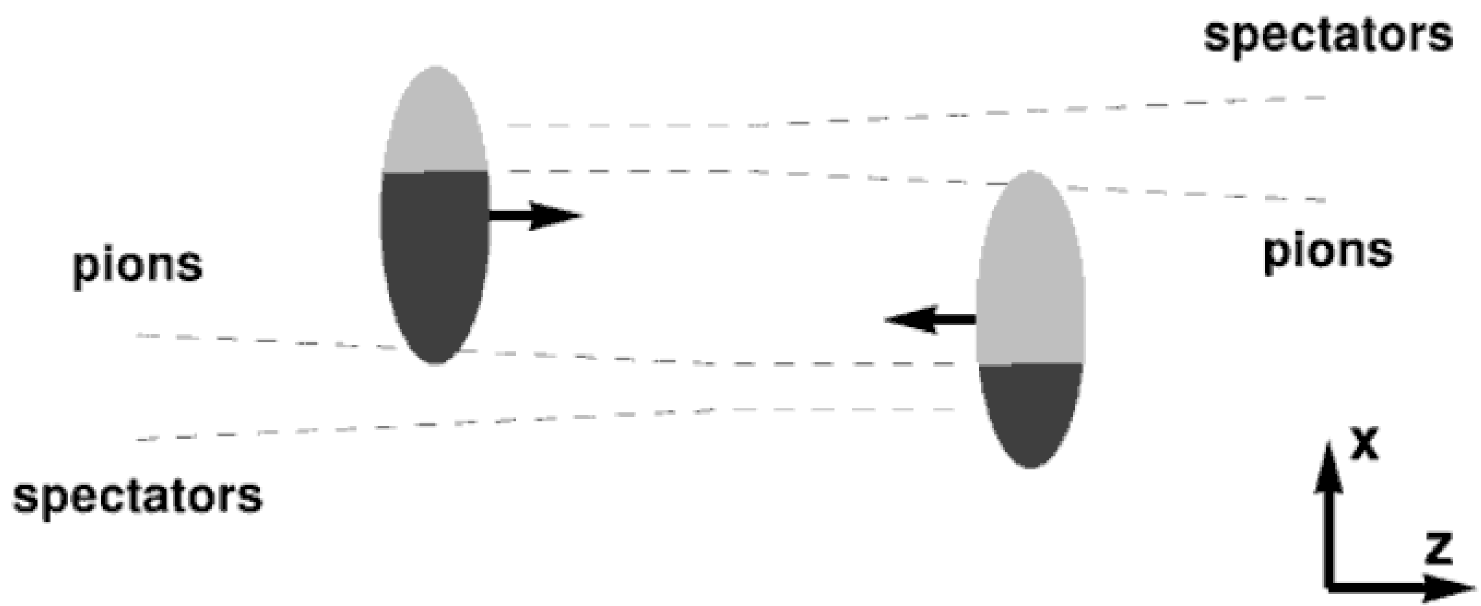

Fig. 2.9 Schematic view of the directed flow observed at relativistic energies. For positive and large rapidities ($y \sim y_P$) the spectators are deflected towards positive values of x. For positive and small rapidities ($y \geq 0$) the produced particles have negative v_1, hence they are deflected towards negative values of x.

The directed flow for spectator nucleons and pions has a different sign.This suggests a different origin of v_1 for protons and pions.

Directed Flow (III)

STAR, Phys.Rev.Lett.101:252301,2008

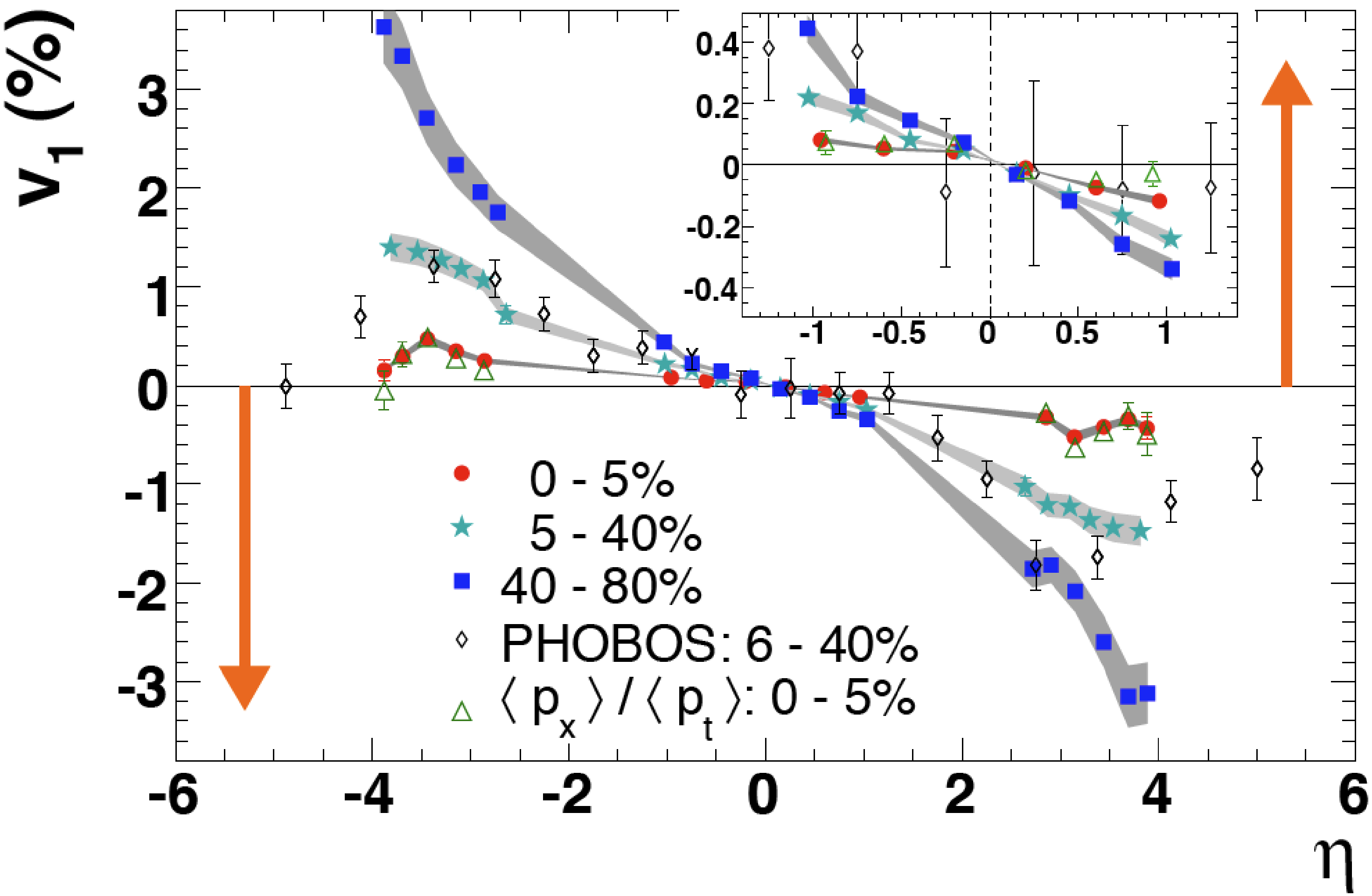

Directed flow of charged hadrons. The orange arrows indicate the sign of the directed flow (and the rapidity) of spectator neutrons.

Basic Elements of Relativistic Hydrodynamics (I)

Energy-momentum tensor $T^{\mu\nu}$:

The conserved currents associated with the energy and momentum can be written as a tensor $T^{\mu\nu}$. $T^{\mu\nu}$ is the four-momentum component in the μ (= 0, 1, 2, 3) direction per three-dimensional surface area perpendicular to the ν direction.

$$\Delta \mathbf{p} = (\Delta E, \Delta p_x, \Delta p_y, \Delta p_z) \qquad \Delta \mathbf{x} = (\Delta t, \Delta x, \Delta y, \Delta z)$$

$$\mu = \nu = 0: \quad T_R^{00} = \frac{\Delta E}{\Delta x \Delta y \Delta z} = \frac{\Delta E}{\Delta V} = \varepsilon$$

$$\mu = \nu = 1: \quad T_R^{11} = \frac{\Delta p_x}{\Delta t \Delta y \Delta z}$$

force in x direction acting on an surface $\Delta y\, \Delta z$ perpendicular to the force → pressure

$$T^{\mu\nu} = \begin{pmatrix} \text{energy density} & \text{energy flux density} \\ \text{momentum density} & \text{momentum flux density} \end{pmatrix} \equiv \begin{pmatrix} \varepsilon & \vec{j}_\varepsilon \\ \vec{g} & \Pi \end{pmatrix}$$

Energy-momentum tensor in the fluid rest frame:

$$T_R^{\mu\nu} = \begin{pmatrix} \varepsilon & 0 & 0 & 0 \\ 0 & P & 0 & 0 \\ 0 & 0 & P & 0 \\ 0 & 0 & 0 & P \end{pmatrix}$$

Isotropy in the fluid rest frame implies that the energy flux T_{0j} and the momentum density T_{j0} vanish and that $\Pi^{ij} = P\,\delta^{ij}$

See also Ollitrault, arXiv:0708.2433 (→ link)

Basic Elements of Relativistic Hydrodynamics (II)

Energy-momentum tensor (in case of local thermalization) after Lorentz transformation to the lab frame:

$T_{\mu\nu}$ is symmetric. This is a non-trivial consequence of relativity.

$$T^{\mu\nu} = (\varepsilon + P)\, u^\mu u^\nu - P\, g^{\mu\nu}$$

metric tensor diag(1,-1,-1,-1)

Energy density and pressure in the co-moving system

4-velocity: $u^\mu = \mathrm{d}x^\mu/\mathrm{d}\tau = \gamma(1, \vec{v})$

Energy and momentum conservation:

$$\partial_\mu T^{\mu\nu} = 0, \quad \nu = 0, \ldots, 3$$

$$\partial_\mu = \left(\frac{\partial}{\partial t}, \vec{\nabla}\right)$$

in components:

$$\begin{cases} \dfrac{\partial}{\partial t}\varepsilon + \vec{\nabla}\vec{j}_\varepsilon = 0 & \text{(energy conservation)} \\ \dfrac{\partial}{\partial t} g_i + \nabla_j \Pi_{ij} = 0 & \text{(momentum conservation)} \end{cases}$$

Conserved quantities, e.g., baryon number:

continuity equation

$$j_B^\mu(x) = n_B(x)\, u^\mu(x), \qquad \partial_\mu j_B^\mu(x) = 0 \quad \Leftrightarrow \quad \frac{\partial}{\partial t} N_\mathrm{B} + \vec{\nabla}(N_\mathrm{B}\vec{v}) = 0$$

$$N_\mathrm{B} = \gamma n_\mathrm{B}$$

Hydrodynamic Models

Ingredients of hydrodynamic models

- Equation of motion and baryon number conservation:

  $$\partial_\mu T^{\mu\nu} = 0, \quad \partial_\mu j^\mu_{\mathrm{B}}(x) = 0$$

  5 equations for 6 unknowns:

  $$(u_x, u_y, u_z, \varepsilon, P, n_{\mathrm{B}})$$

- Equation of state: $P(\varepsilon, n_{\mathrm{B}})$ (needed to close the system)
- Initial conditions, e.g., from Glauber calculation
- Freeze-out condition

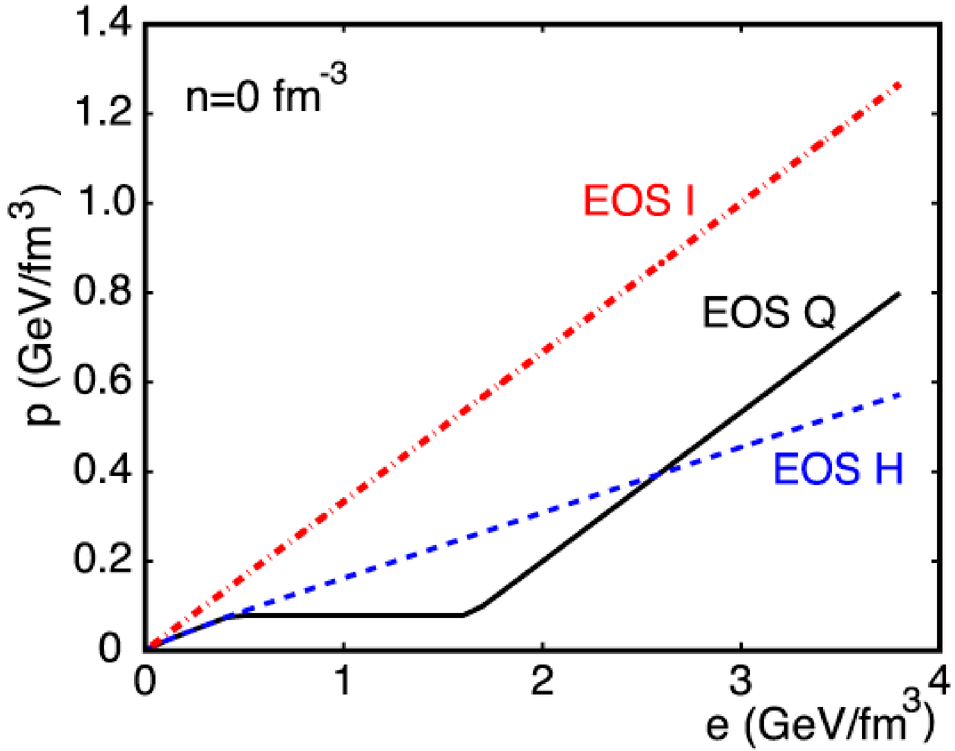

EOS I: ultra-relativistc gas $P = \varepsilon/3$

EOS H: resonance gas, $P \approx 0.15\ \varepsilon$

EOS Q: phase transition, QGP ↔ resonance gas

Freeze-Out: Cooper-Frye Formula

$$E\frac{dN}{d^3p} = \int_\Sigma f(x,p,t)p\cdot d\sigma(x)$$
$$= \frac{d}{(2\pi)^3}\int_\Sigma \frac{p\cdot d\sigma(x)}{\exp\left[(p\cdot u(x)-\mu(x))/T(x)\right]\pm 1}$$

$f p\, d\sigma = f p^\mu d\sigma_\mu$: local flux of particle *i* with momentum *p* through the freeze-out hyper-surface Σ. The freeze-out hyper-surface can, e.g., defined by the condition $T = T_c$.

$d\sigma_\mu$: normal vector to the freeze-out hyper surface

Cooper, Frye, Phys. Rev. D10 (1974) 186

Space-time Evolution of the Fireball in a Hydro Model

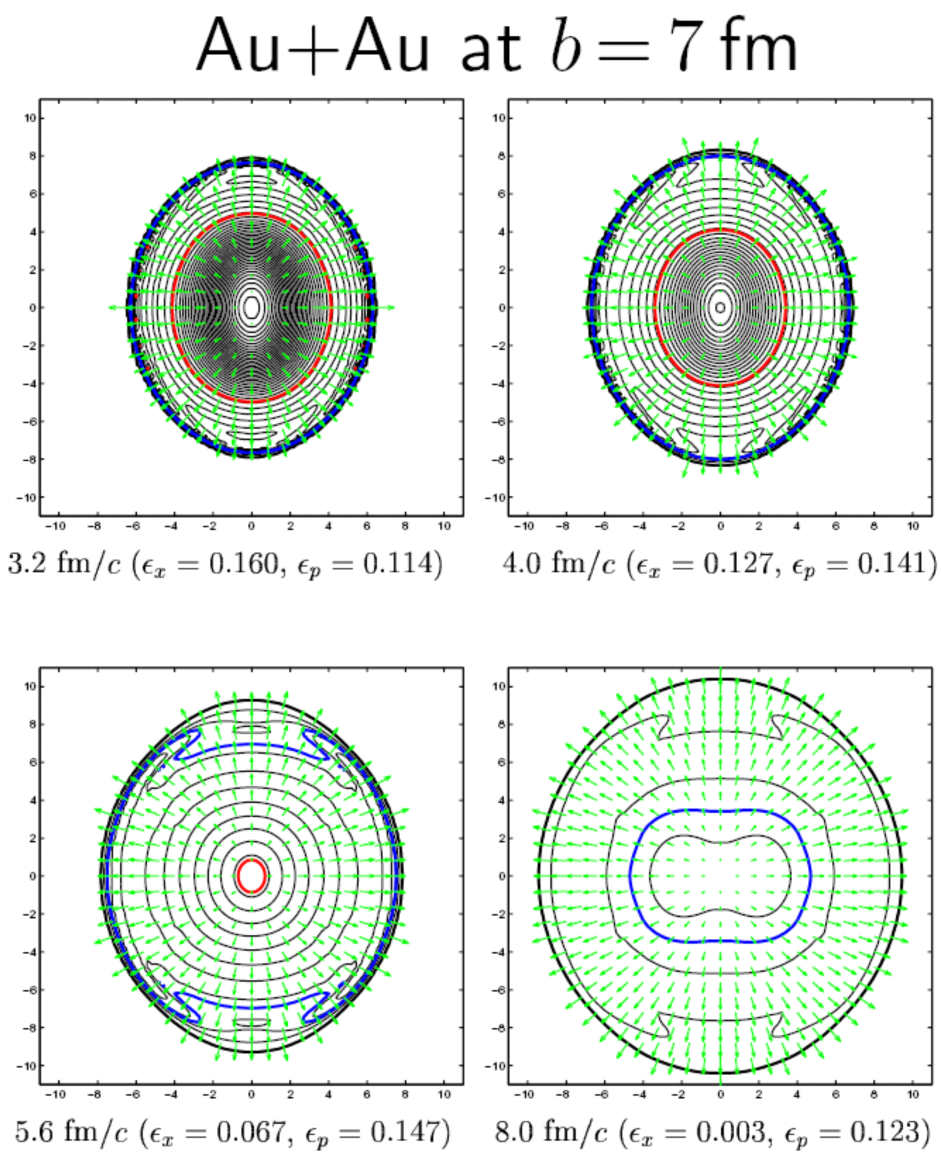

Elliptic flow is “self-quenching”:
The cause of elliptic flow, the initial spacial anisotropy, decreases as the momentum anisotropy increases

Time Dependence of the Momentum Anisotropy

Ulrich Heinz, Peter Kolb, arXiv:nucl-th/0305084

Anisotropy in coordinate space

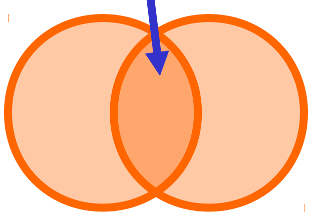

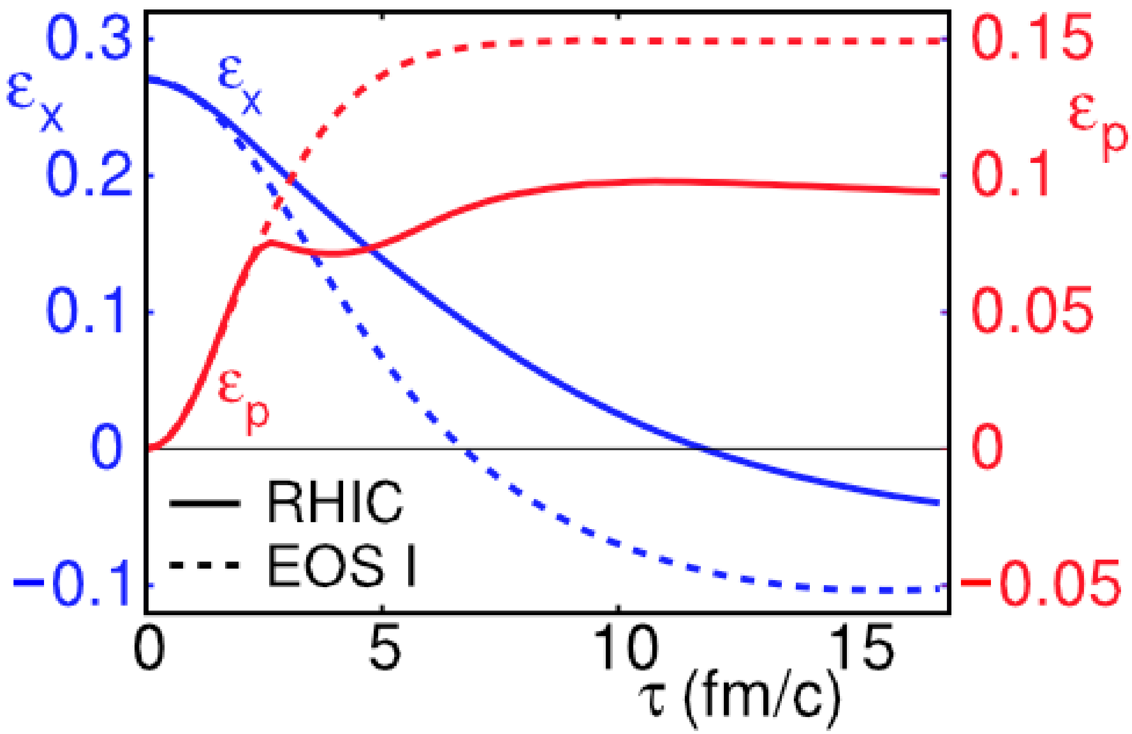

Anisotropy in momentum space

In hydrodynamic models the momentum anisotropy develops in the early (QGP) phase of the collision. Thermalization times of less then 1 fm/*c* are needed to describe the data.

Impact parameter Dependence of v_2/ε_x

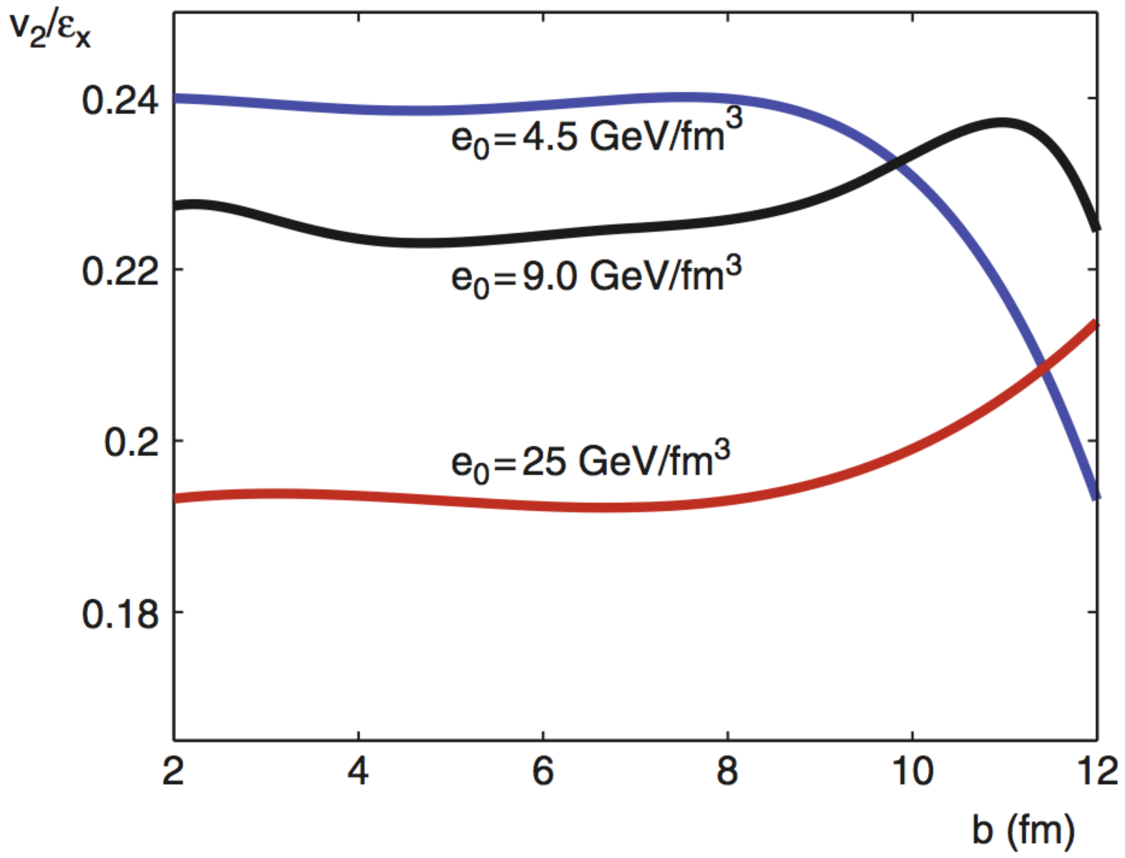

Ideal hydrodynamics predicts $v_2 \approx 0.2\ \varepsilon_x$

Elliptic Flow of Cold Atoms

- 200 000 Li-6 atoms in an highly anisotropic trap (aspect ratio 29:1)
- Very strong interactions between atoms (Feshbach resonance)
- Once the atoms are released the one observed a flow pattern similar to elliptic flow in heavy-ion collisions

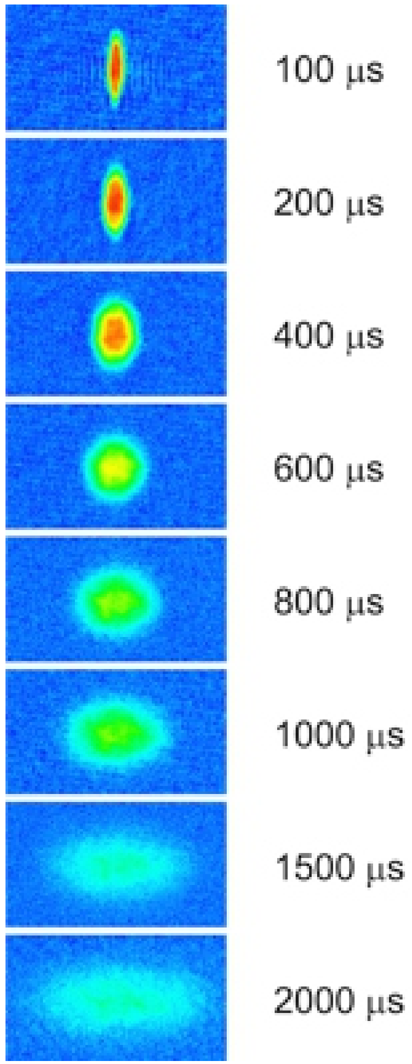

v_2 as a Function of $\sqrt{s_{NN}}$

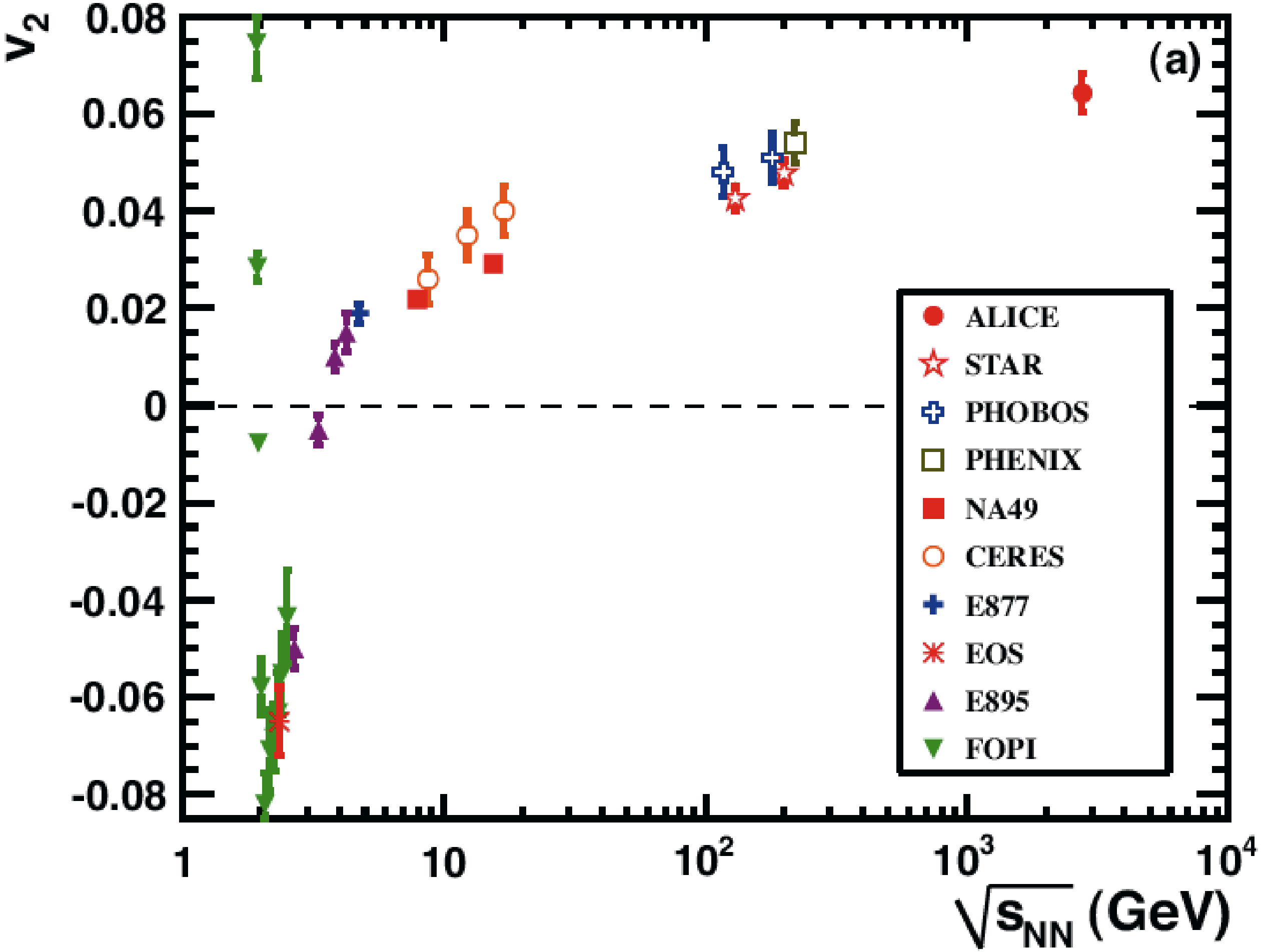

R. Snellings, arXiv:1102.3010,
P. Sorensen, arXiv:0905.0174

- $\sqrt{s_{NN}} > \sim 4$ GeV:
initial eccentricity leads to pressure gradients that cause positive v_2
- $2 < \sqrt{s_{NN}} < 4$ GeV:
velocity of the nuclei is small so that presence of spectator matter inhibits in-plane particle emission ("squeeze-out")
- $\sqrt{s_{NN}} < 2$ GeV:
rotation of the collision system leads to fragments being emitted in-plane

$v_2(p_T)$ for Different Energies: Strikingly Similar

STAR, Quark Matter 2012 (→ link)

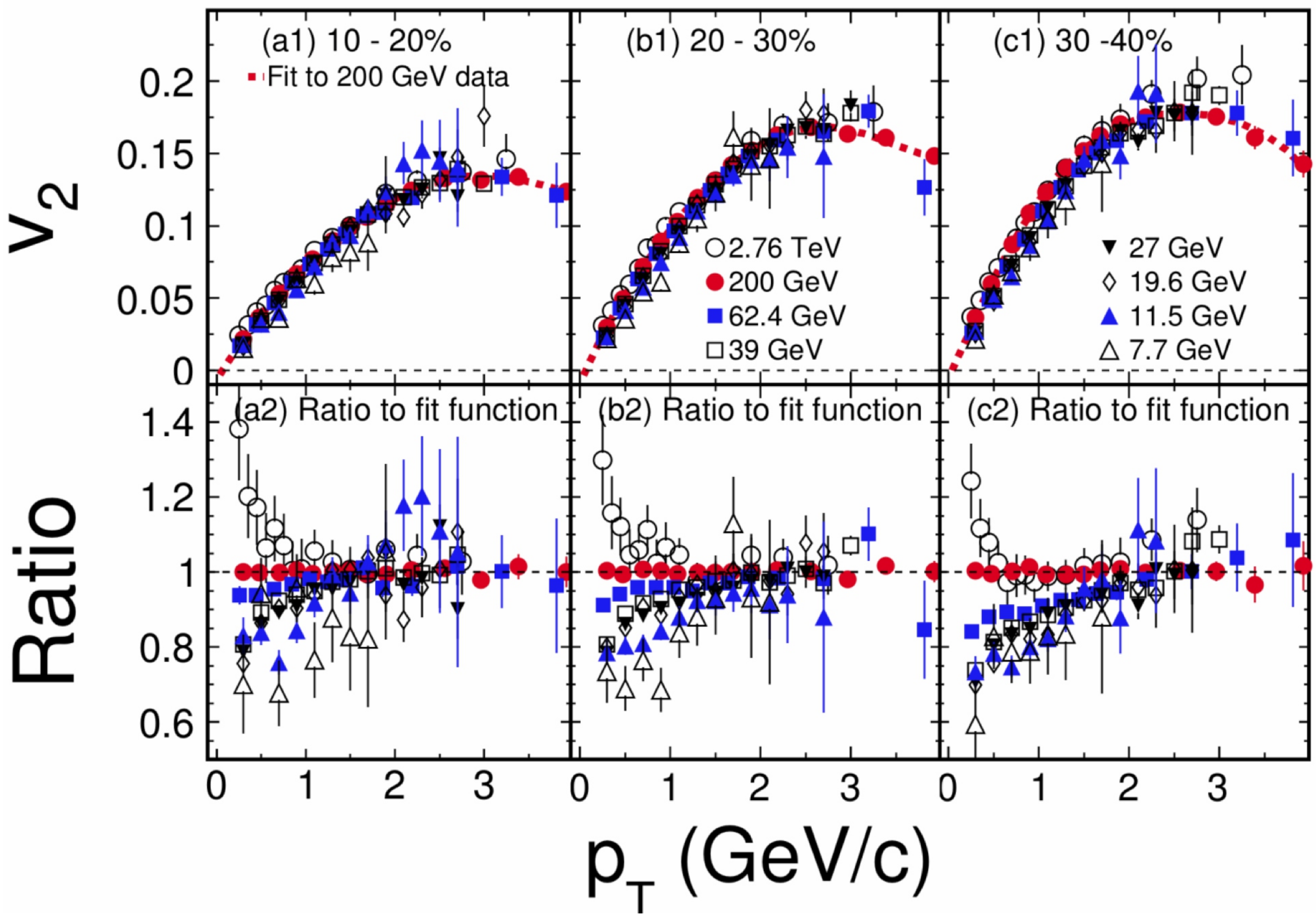

How does this affect the interpretation of v_2 as a QGP signal?

Sensitivity to the Equation-of-State

R. Snellings, arXiv:1102.3010

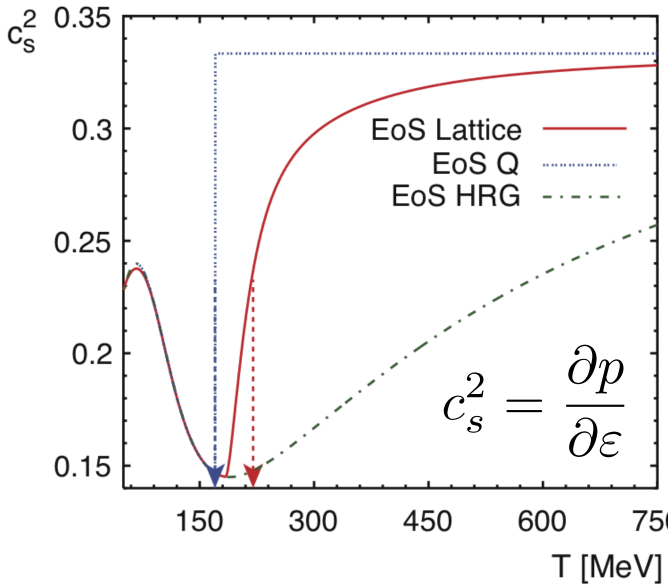

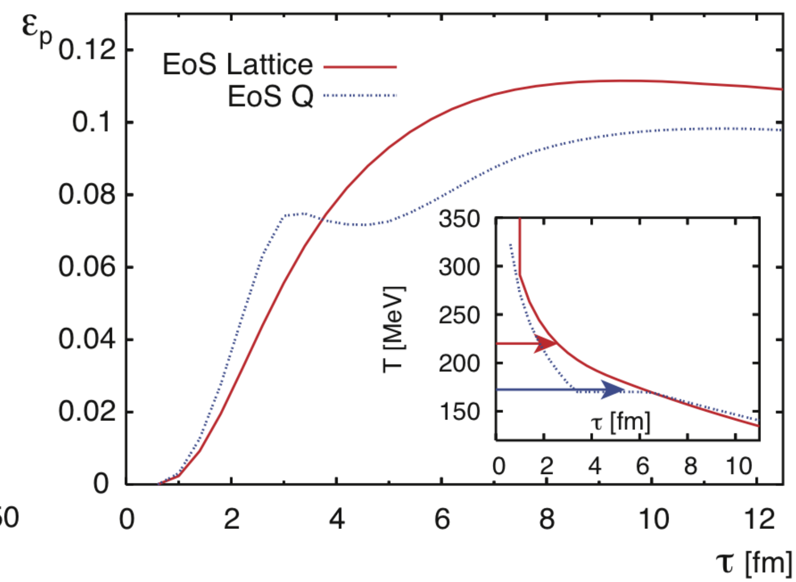

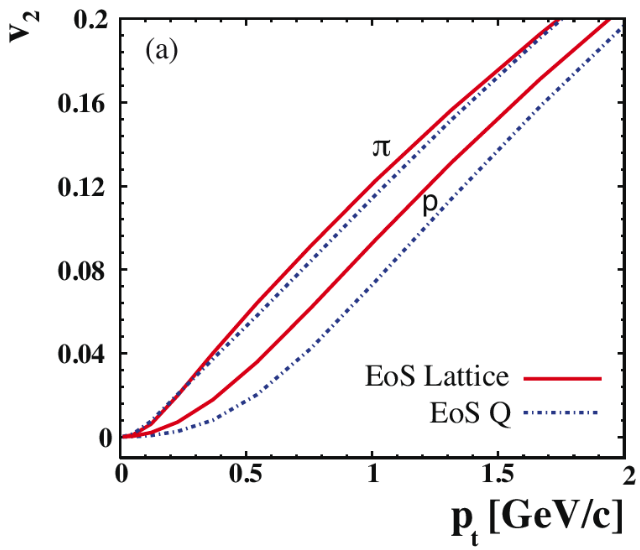

The sensitivity to the EoS corresponds to the fact that v_2 is sensitive to the sound velocity.

The measurement of v_2 for different particle species helps constrain the EoS.

Sensitivity to Initial Condition

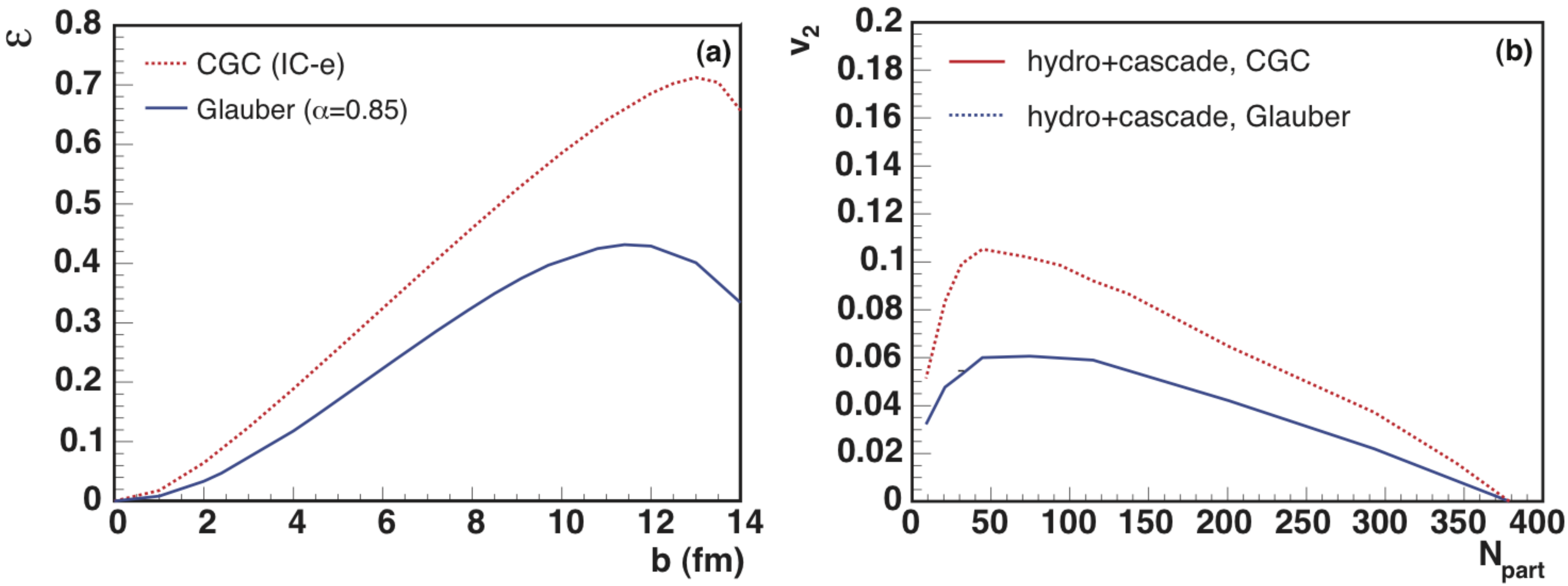

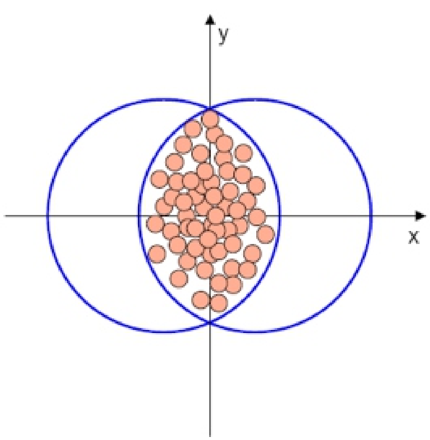

Eccentricity:

$$\varepsilon = \frac{\langle y^2 - x^2 \rangle}{\langle y^2 + x^2 \rangle}$$

In hydrodynamic models: $v_2 \propto \varepsilon$.

The initial eccentricity results from the 2D profile of produced gluons. Gluon saturation models predict larger eccentricities than Glauber calc's (in which the gluon profile follows the wounded nucleon profile, or $d^2N_{coll}/dxdy$)

Sensitivity to Viscosity

Kovtun, Son, Starinets, PRL 94 (2005) 111601

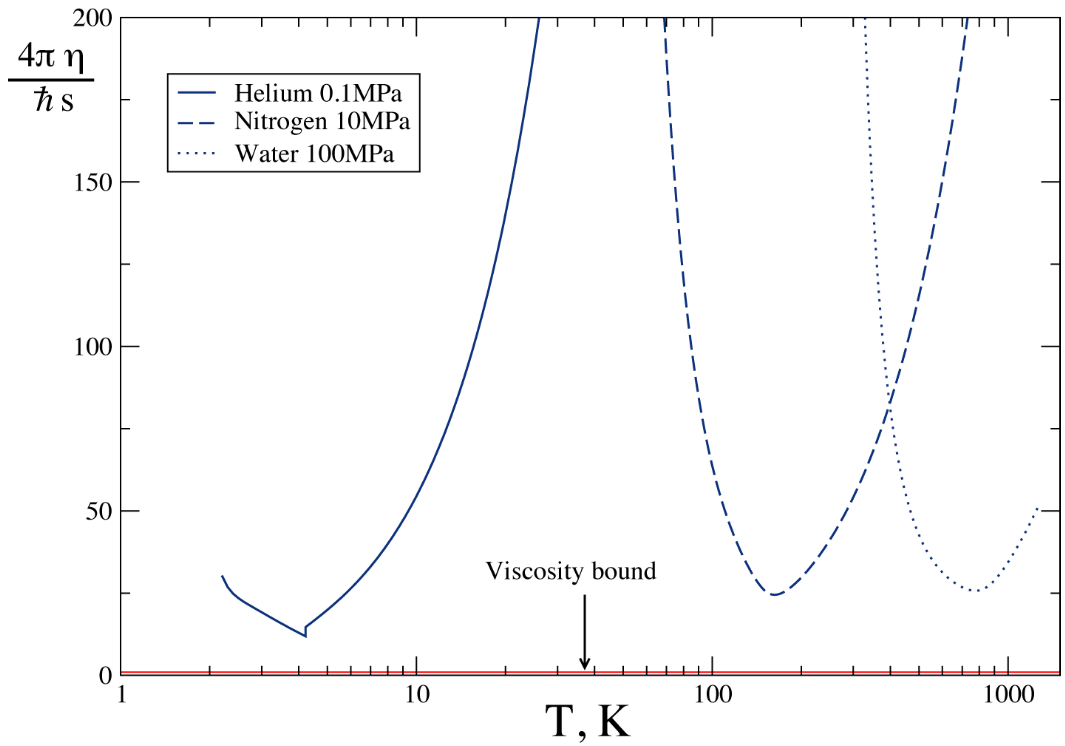

Based on a correspondence between string theory and quantum field theory ("AdS/CFT correspondence") Kovtun, Son, and Starinets argued that there is a lower limit for the viscosity of any fluid:

$$\frac{\eta}{s} = \frac{\hbar}{4\pi k_B}$$

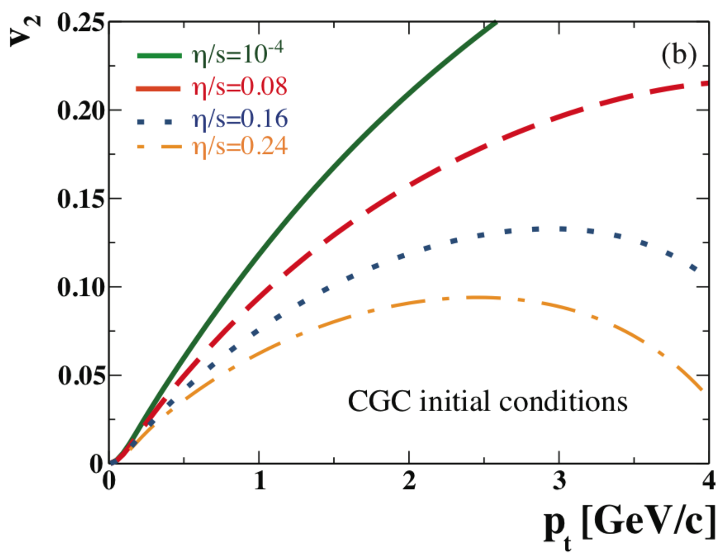

v_2 is sensitive to the viscosity of the quark-gluon plasma. The larger η/s, the smaller is the resulting v_2

Event Plane Method (I)

S. A. Voloshin, A. M. Poskanzer, R. Snellings, arXiv:0809.2949

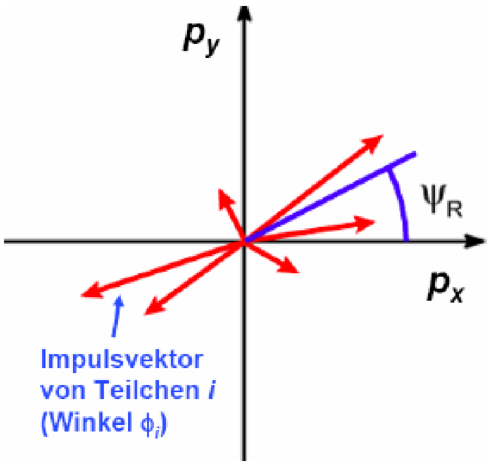

Event flow vector Q_n:

$$Q_{n,x} = \sum_i w_i \cos(n\phi_i) = Q_n \cos(n\Psi_n)$$

$$Q_{n,y} = \sum_i w_i \sin(n\phi_i) = Q_n \sin(n\Psi_n)$$

The optimal choice for w_i is to approximate $v_n(p_T; y)$. $w_i = p_{T,i}$ is often used as a good approximation.

Event plane angle:

$$\Psi_n = \frac{1}{n} \mathrm{atan2}(Q_{n,y}, Q_{n,x})$$

$\mathrm{atan2}(y,x)$ is defined such that $(r, \mathrm{atan2}(y,x))$ are the polar coordinates of the cartesian coordinates (x,y); $r := \sqrt{x^2+y^2}$. atan2 is a C/C++ function.

Event Plane Method (II)

Fourier coefficient w.r.t. the event plane (not the reaction plane):

$$v_n^{\text{observed}}(p_T, y) = \langle \cos[n(\varphi - \Psi_{\text{RP}})] \rangle$$

To remove auto-correlations one has to subtract the Q-vector of the particle of interest from the total event Q-vector, obtaining ψ_n to correlate with the particle.

Alternatively, one determines the reaction plane at forward rapidities and correlates this event plane with particles measured at mid-rapidity.

Since finite multiplicity limits the estimation of the angle of the reaction plane, the v_n have to be corrected for the event plane resolution for each harmonic:

$$v_n = \frac{v_n^{\text{observed}}}{R_n}, \qquad R_n = \langle \cos[n(\Psi_n - \Psi_{\text{RP}})] \rangle$$

To estimate the event plane resolution one can measure the reaction plane with two identical detectors A and B (symmetric around mid-rapidity)

$$R_n = \sqrt{\langle \cos[n(\Psi_n^A - \Psi_n^B)] \rangle}$$

v_2 from Two Particle Correlations

The correlation of all particles with the reaction plane implies a 2-particle correlation:

$$\begin{aligned}
\langle\langle e^{i2(\varphi_1-\varphi_2)}\rangle\rangle &= \langle\langle e^{i2(\varphi_1-\Psi_{\mathrm{RP}}-(\varphi_2-\Psi_{\mathrm{RP}}))}\rangle\rangle, \\
&= \langle\langle e^{i2(\varphi_1-\Psi_{\mathrm{RP}})}\rangle\langle e^{-i2(\varphi_2-\Psi_{\mathrm{RP}})}\rangle + \delta_2\rangle, \\
&= \langle v_2^2 + \delta_2\rangle,
\end{aligned}$$

Double brackets denote an average over all particles within an event, followed by averaging over all events. δ_2: two-particle correlations independent of the reaction plane ("non-flow")

So v_n can also be determined from 2-particle azimuthal distribution (if non-flow contributions can be neglected):

two-particle cumulant

$$v_n\{2\}^2 = \langle\cos[n(\varphi_1-\varphi_2)]\rangle =: c_n\{2\}$$

Reduction of non-flow Contributions with higher-order Cumulants

$$
\begin{aligned}
c_2\{2\} &\equiv \left\langle\left\langle e^{i2(\varphi_1-\varphi_2)}\right\rangle\right\rangle = \langle v_2^2+\delta_2\rangle \\
c_2\{4\} &\equiv \left\langle\left\langle e^{i2(\varphi_1+\varphi_2-\varphi_3-\varphi_4)}\right\rangle\right\rangle - 2\left\langle\left\langle e^{i2(\varphi_1-\varphi_2)}\right\rangle\right\rangle^2, \\
&= \langle -v_2^4+\delta_4\rangle
\end{aligned}
$$

$c_n\{4\}$ is a measure of genuine 4-particle correlations, i.e., it is insensitive to two-particle non-flow correlations. It can, however, still be influenced by higher order non-flow contributions, denoted here by δ_4.

$$
\begin{aligned}
v_n\{2\}^2 &:= c_n\{2\} \\
v_n\{4\}^4 &:= -c_n\{4\}
\end{aligned}
$$

These observables measure (assuming $\sigma << \langle v_n \rangle$):

$$
v_n\{2\} = \langle v_n\rangle + \frac{1}{2}\frac{\sigma^2}{\langle v_2\rangle}
$$

$$
v_n\{4\} = \langle v_n\rangle - \frac{1}{2}\frac{\sigma^2}{\langle v_2\rangle}
$$

arXiv:1102.3010

Non-Flow Effects

We have seen that not only flow leads to azimuthal correlations.
Examples: resonance decays, jets, …

$$v_n\{2\}^2 = \langle v_n^2 \rangle + \delta_n$$

Different methods have different sensitivities to nonflow effects.
The 4-particle cumulant method is significantly less sensitive to nonflow effects than the 2-particle cumulant method

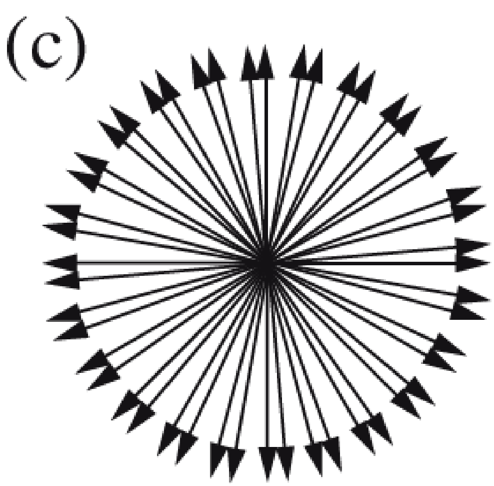

Example:
$v_2 = 0$, $v_2\{2\} > 0$

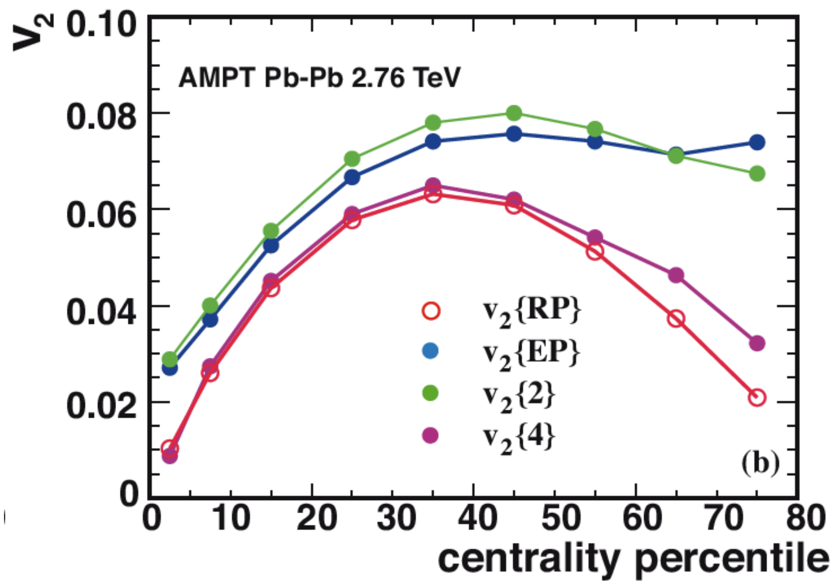

Mass Ordering (1/3)

Consider a source that emits particles according to a Boltzmann distribution:

energy of the particle in the fluid rest frame

$$\frac{d^3n}{d^3p} \propto \exp\left(-\frac{E^*}{T}\right)$$

The energy of a particle in the fluid rest frame can be written in the lab frame as

$$E^* = p^\mu u_\mu$$

Consider particle with velocity parallel to the fluid cell velocity and p_z = 0:

$$u_0 = \cosh \rho$$
$$u = \sinh \rho$$

transverse rapidity

$$E^* = p^\mu u_\mu = m_T u_0 - p_T u$$

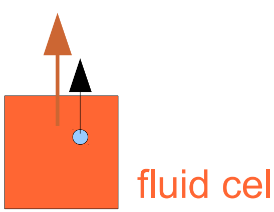

$$u^\mu = \gamma(1, \vec{\beta}), \quad u^\mu u_\mu = 1 = u_0^2 - u^2 \quad \rightarrow \quad u_0 = \sqrt{1 + u^2}$$

Mass Ordering (2/3)

Yield written with (φ dependent) 4-velocity (u_0,u) = γ(1, β):

$$\frac{d^3n}{d^3p} \propto \exp\left(\frac{-m_T u_0(\varphi) + p_T u(\varphi)}{T}\right) \qquad (*)$$

Let's assume a modulation of the radial flow velocity given by:

$$u(\varphi) = u + 2\alpha\cos(2\varphi)$$

Using $u_0 = \sqrt{u^2+1}$ and expanding to first order in α:

$$u_0(\varphi) = u_0 + 2\beta\alpha\cos(2\varphi) \quad \text{with} \quad \beta = \frac{u}{u_0}$$

Plugging this into (*) and expanding to first order in α:

$$\frac{d^3n}{d^3p} \propto \exp\left(\frac{-m_T u_0 + p_T u}{T}\right)\left[1 + 2\frac{\alpha}{T}(p_T - \beta m_T)\cos(2\varphi)\right]$$

Thus, we get a v_2 of:

average radial flow velocity of the fluid cell

$$v_2 = \frac{\alpha}{T}(p_t - \beta m_T)$$

Mass Ordering (3/3)

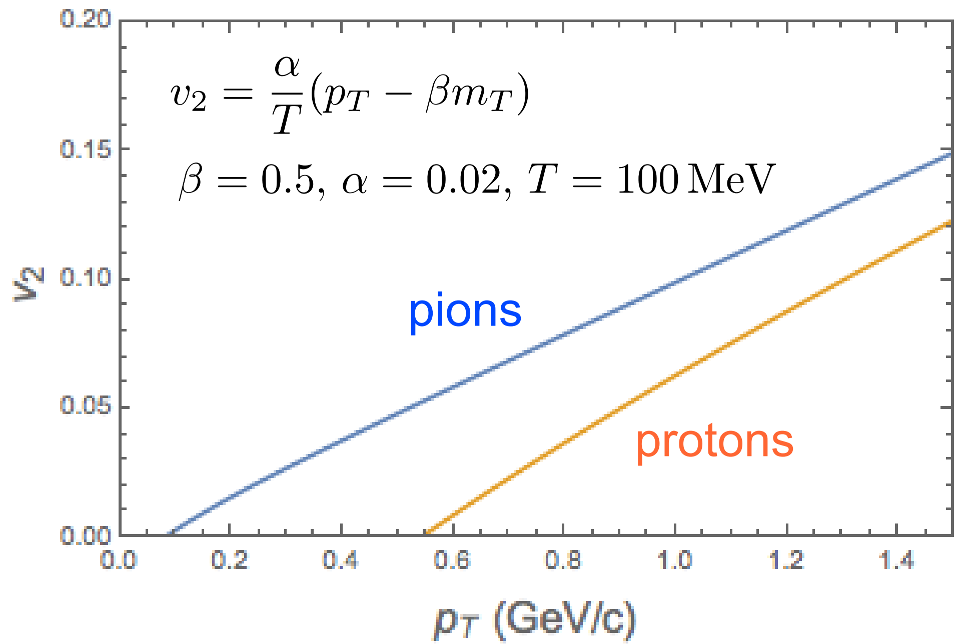

For light particle (pions) $p_T \approx m_T$ and the v_2 increases approximately linearly with p_T.

For heaver particles, m_T is larger at the same value of p_T, resulting in a smaller v_2.

Elliptic Flow at RHIC

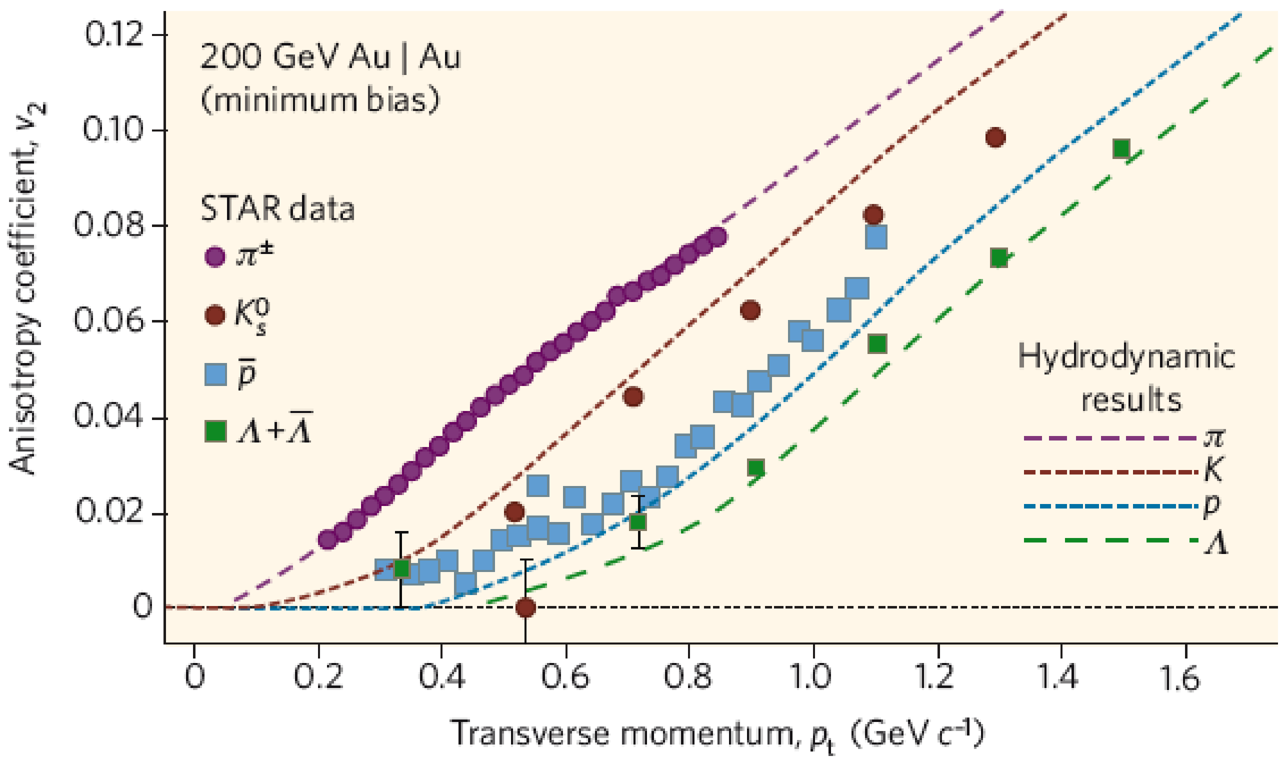

Plot from
Braun-Munzinger, Stachel,
Nature 448:302-309,2007

- Measured v_2 in good agreement with ideal hydro
- Hydro predicts mass ordering: $v_2 \sim \frac{1}{T}(p_T - \beta m_T), \quad \beta = \text{average flow velocity}$
- Indeed observed!
- "Perfect liquid" created at RHIC

Maximum v_2 from Hydro

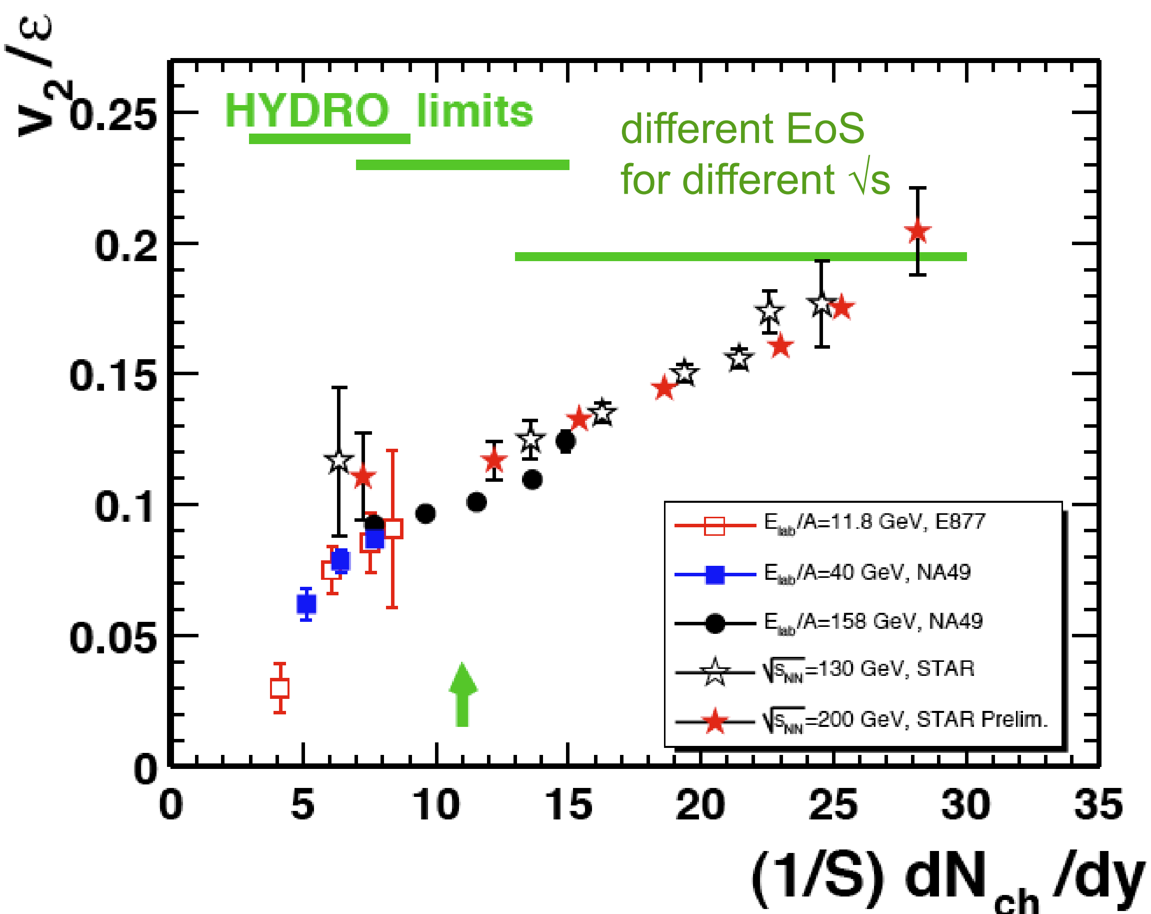

charged particle multiplicity per unit of rapidity per transverse area S of the source

Hydro limit only reached at RHIC energies

Breakdown of Ideal Hydro

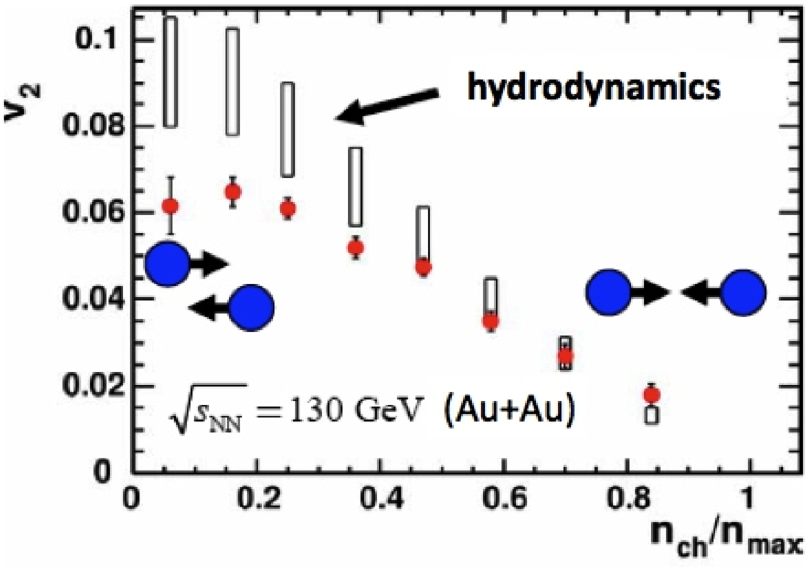

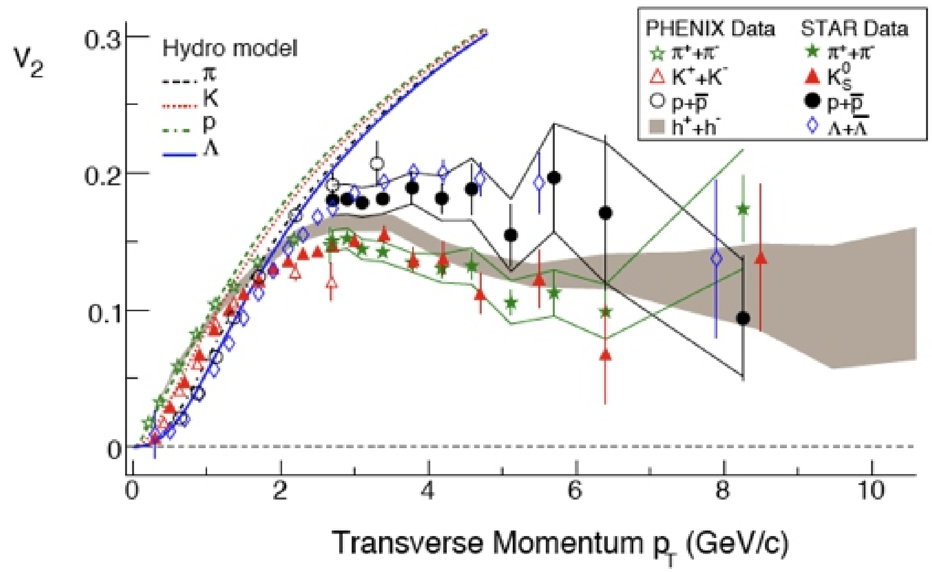

Hydro description for Au+Au at RHIC only works in central collisions and for $p_T < 1.5$ GeV/c

Viscosity of Pitch

Pitch drop experiment, started in Queensland, Australia in 1927

Date	Event	Duration		
		Years	Months	
1927	Hot pitch poured			
October 1930	Stem cut			
December 1938	1st drop fell	8.1	98	
February 1947	2nd drop fell	8.2	99	
April 1954	3rd drop fell	7.2	86	
May 1962	4th drop fell	8.1	97	
August 1970	5th drop fell	8.3	99	
April 1979	6th drop fell	8.7	104	
July 1988	7th drop fell	9.2	111	
November 2000	8th drop fell[A]	12.3	148	
April 2014	9th drop[B]	13.4	156	

https://en.wikipedia.org/wiki/Pitch_drop_experiment

QGP has larger viscosity than pitch!

It is η/s that determine the properties of a fluid, not η alone.

Competition for the Most Ideal Fluid

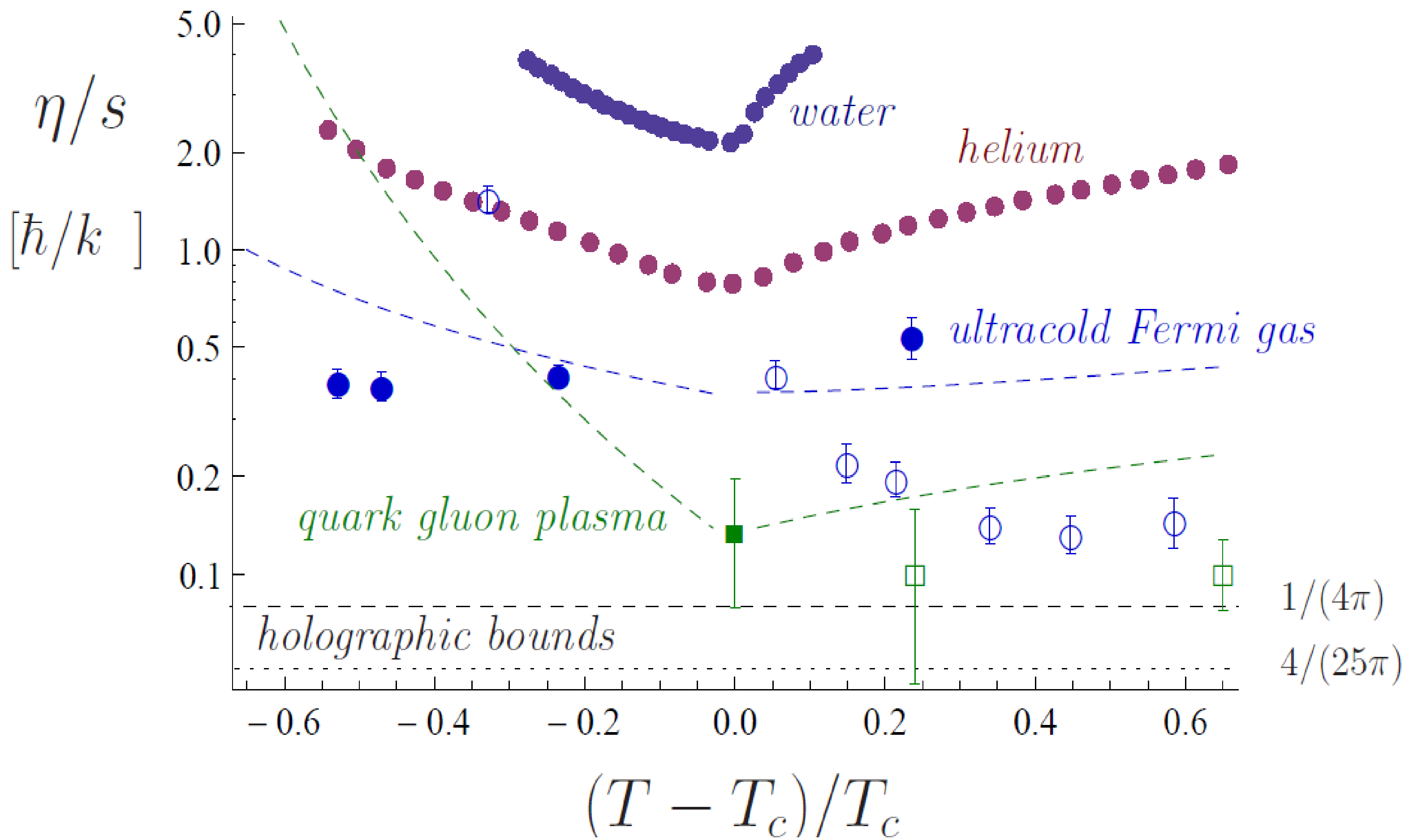

A. Adams, L.D. Carr, T. Schaefer, P. Steinberg. J.E. Thomas, arXiv:1205.5180

How Perfect is the QGP Fluid at RHIC?

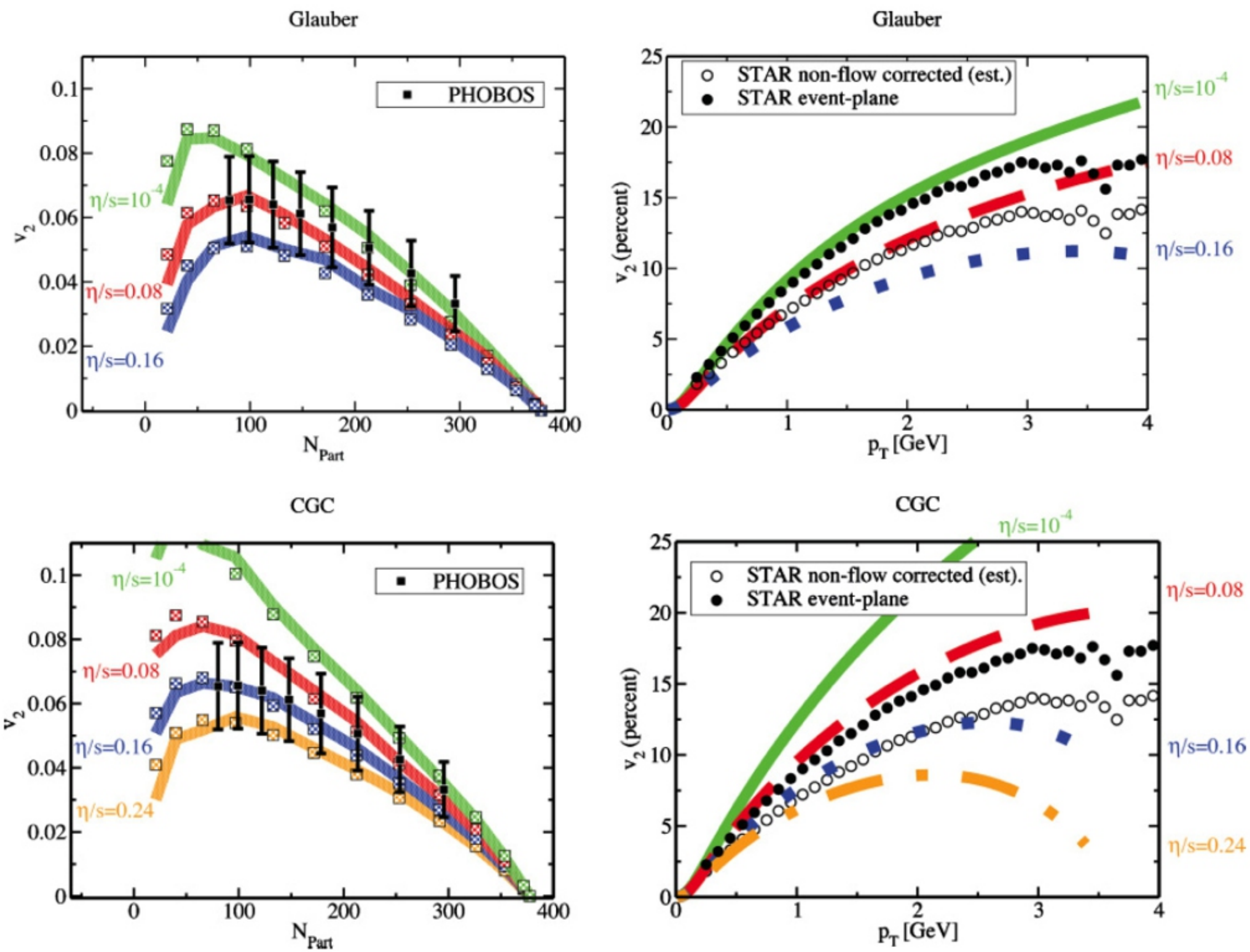

Glauber initial cond.

$$\Rightarrow \quad 0 < \eta/s < 0.1$$

CGC initial cond.

$$\Rightarrow \quad 0.08 < \eta/s < 0.2$$

Conservative estimate for the QGP (taking into account e.g. effects of EOS variations, bulk viscosity, ...):

$$\eta/s \quad < \quad 5 \times \left.\frac{\eta}{s}\right|_{KSS} \quad = \quad 5 \times \frac{1}{4\pi}$$

Luzum, Romatschke, Phys.Rev.C78:034915,2008

v_2 vs. Centrality in Pb+Pb at $\sqrt{s_{NN}}$ = 2.76 TeV from ALICE Compared to v_2 at RHIC

ALICE, Phys. Rev. Lett. 105, 252302 (2010)

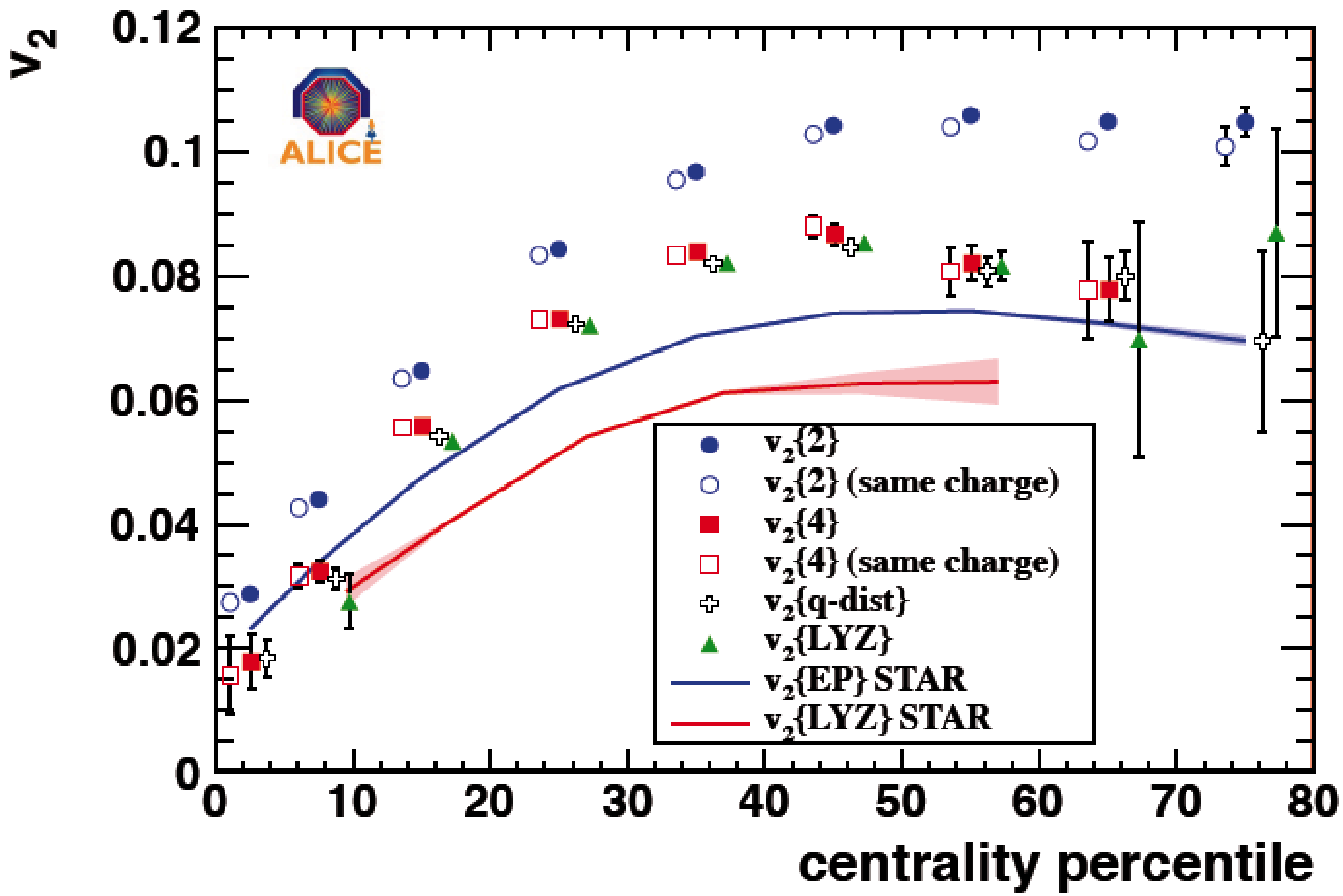

v_2 increases up to 30% (for more peripheral collisions)

$v_2(p_T)$ in Pb+Pb at $\sqrt{s_{NN}}$ = 2.76 TeV from ALICE Compared to v_2 at RHIC

ALICE, Phys. Rev. Lett. 105, 252302 (2010)

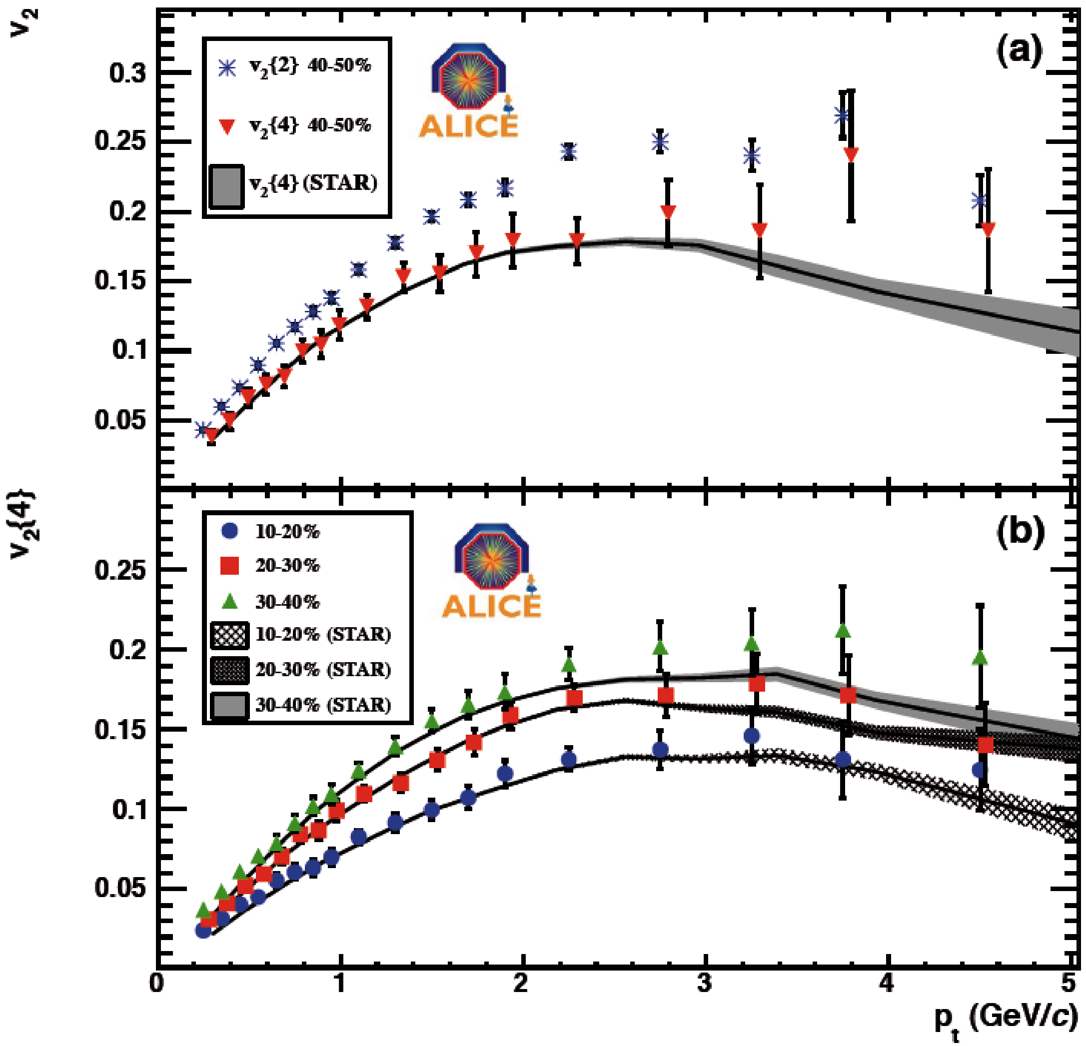

$v_2(p_T)$ at LHC and RHIC is virtually identical.

The increase of the mean p_T at the LHC can explain the increase of the p_T-integrated v_2 value.

Mass Ordering also Observed at LHC Energies

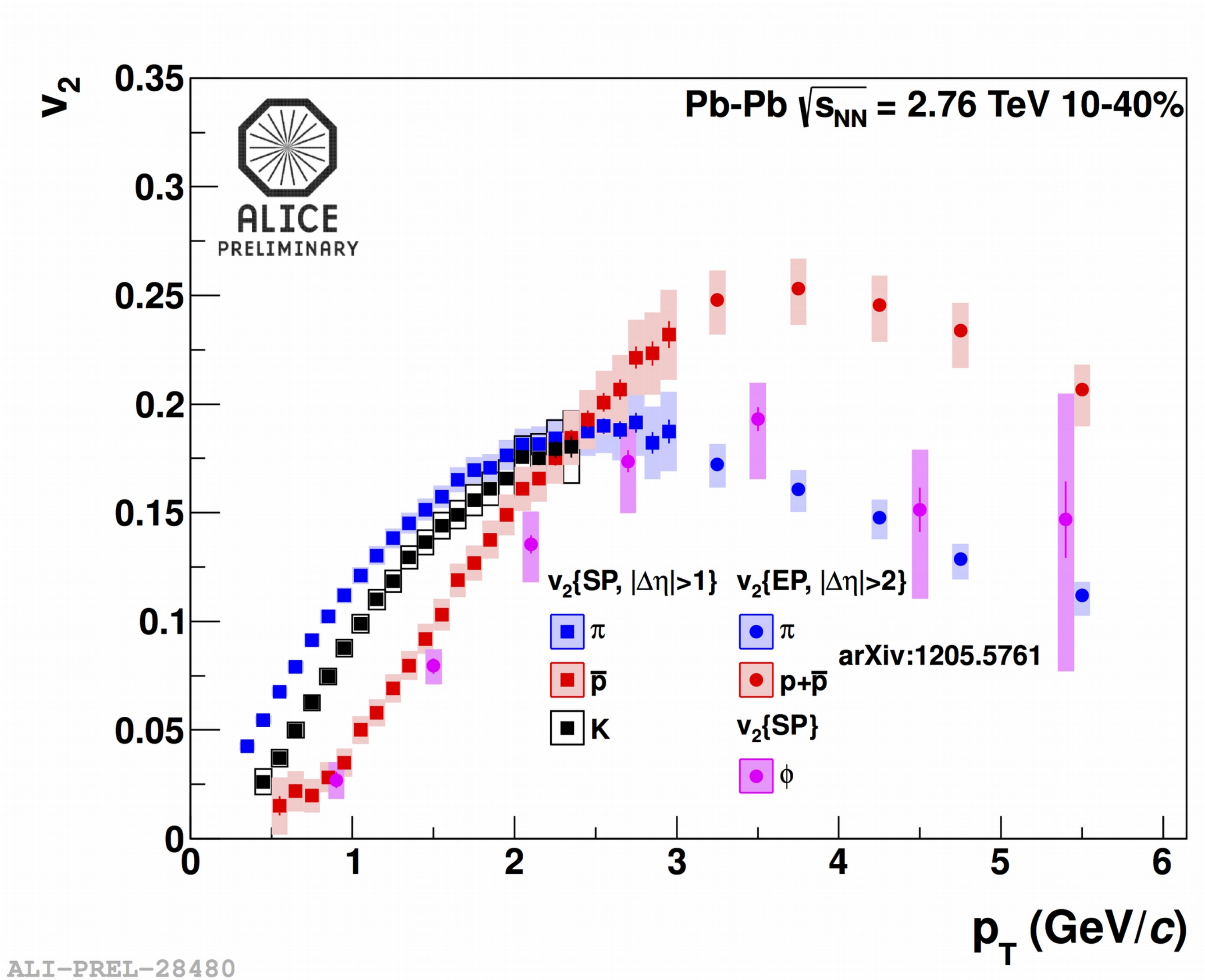

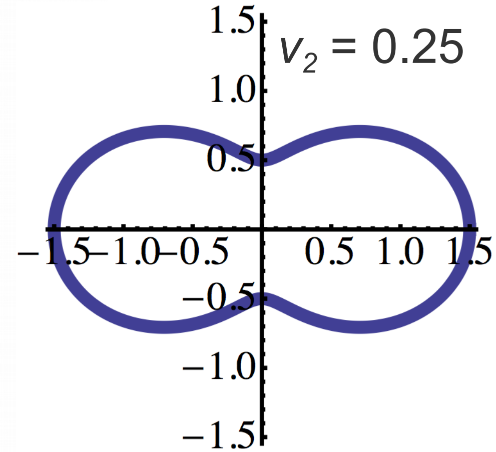

Elliptic Flow at the LHC Described by Nearly Ideal Hydrodynamics (with η/*s* = 0.20)

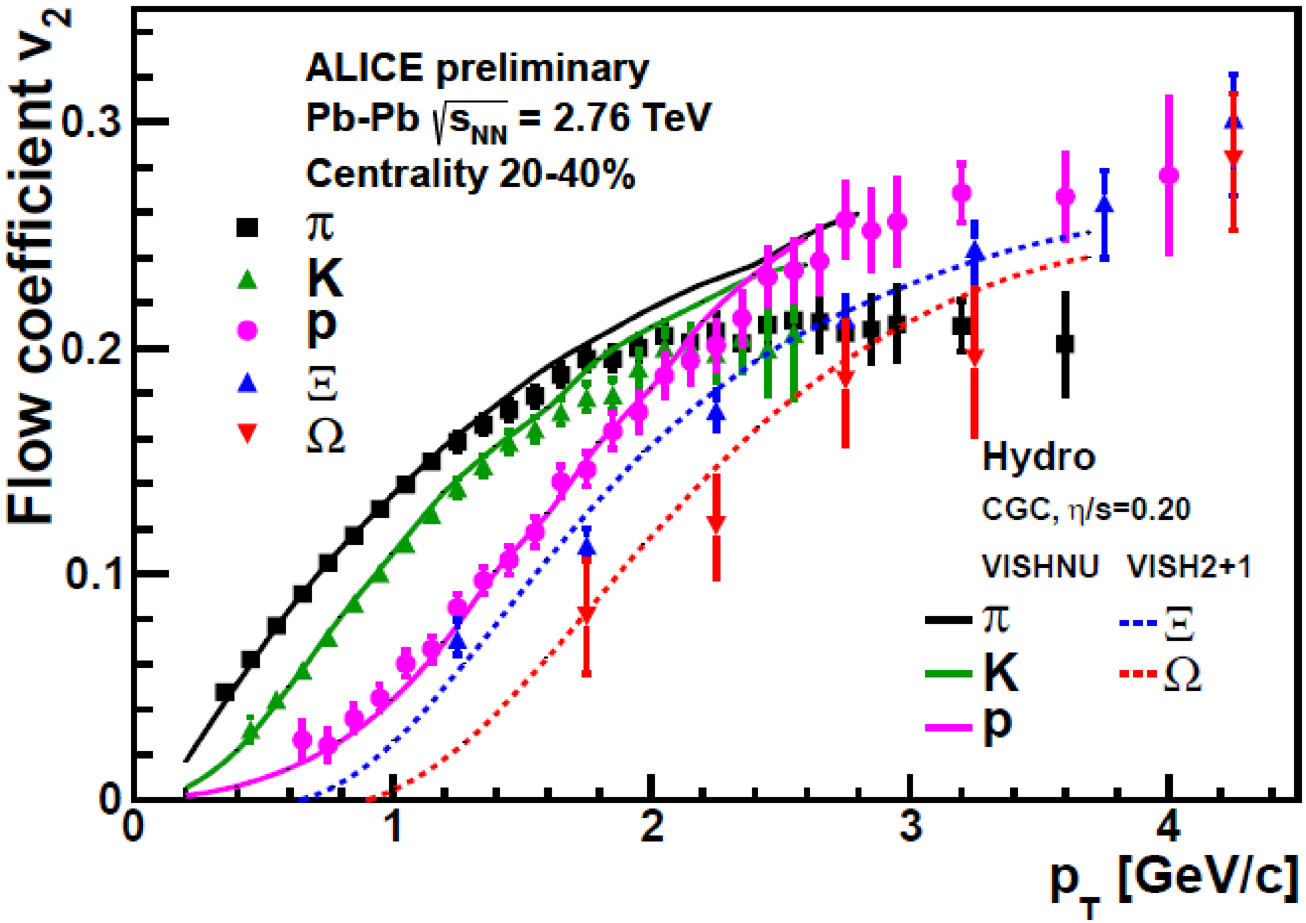

v_3 for Pions, Kaons, and Protons

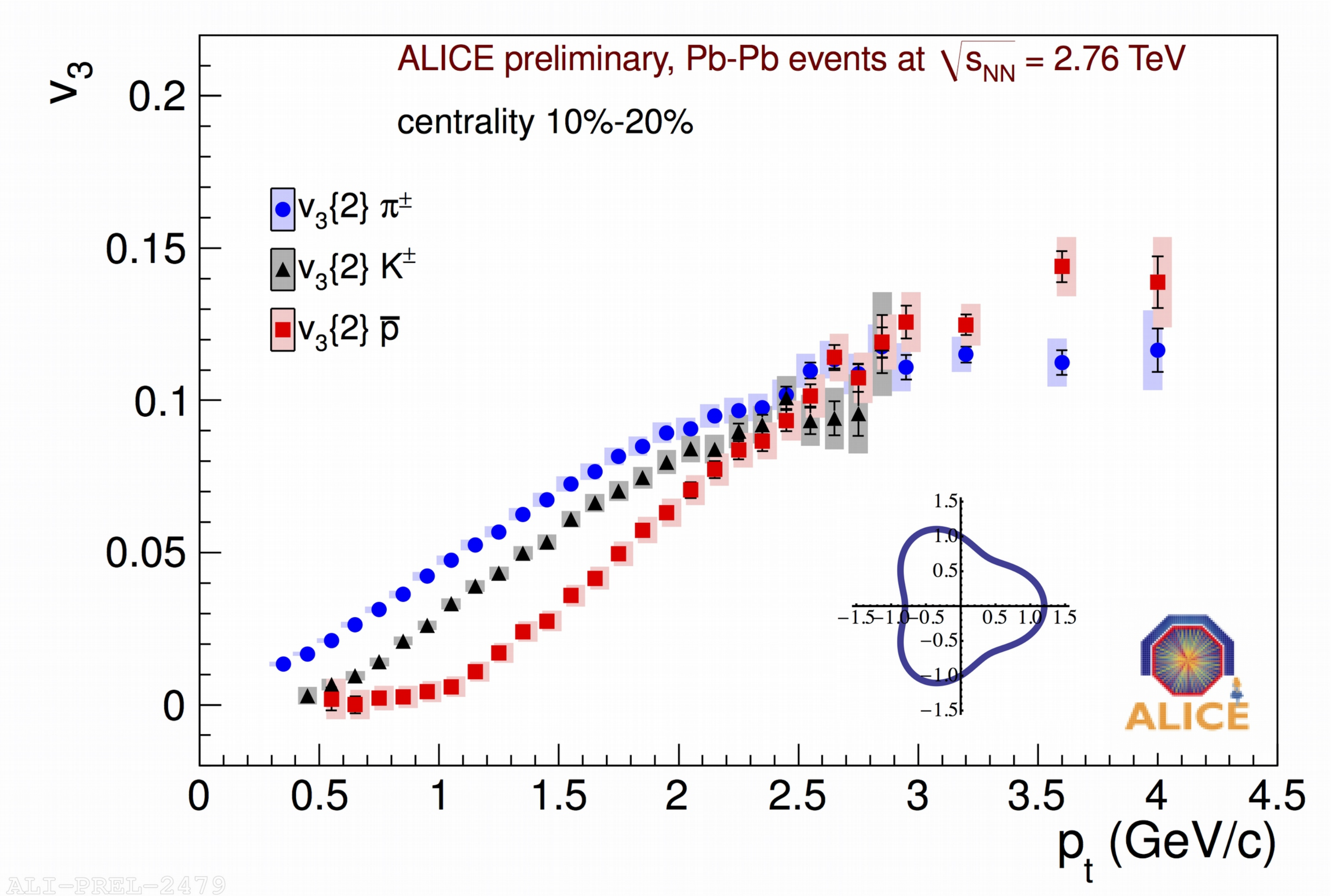

Sizable v_3. Mass splitting as expected from hydrodynamics.

Survival of Initial State Fluctuation: The Universe and Heavy Ion Collisions

U. Heinz

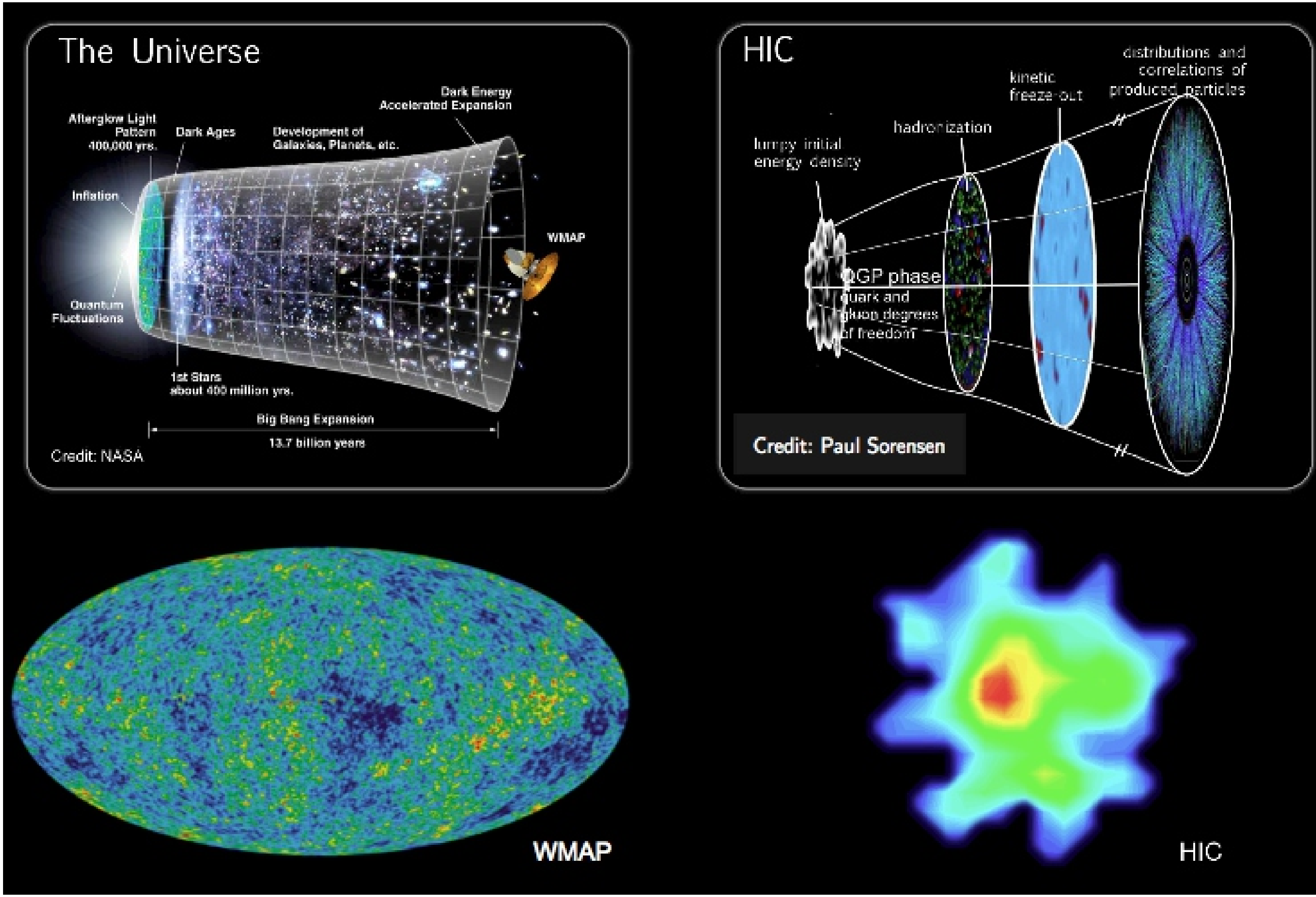

Centrality and p_T Dependence of v_n: Data vs. Event-by-Event Hydrodynamics

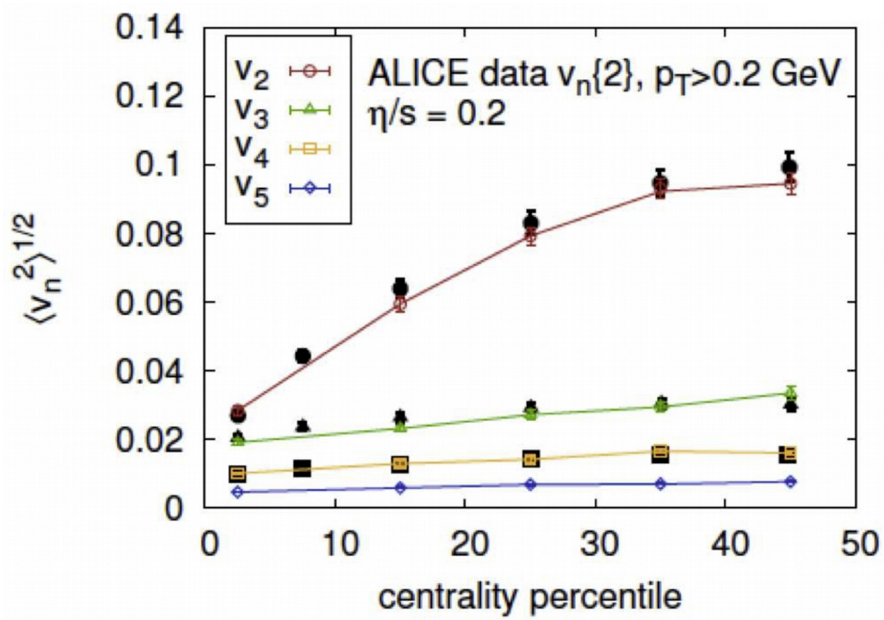

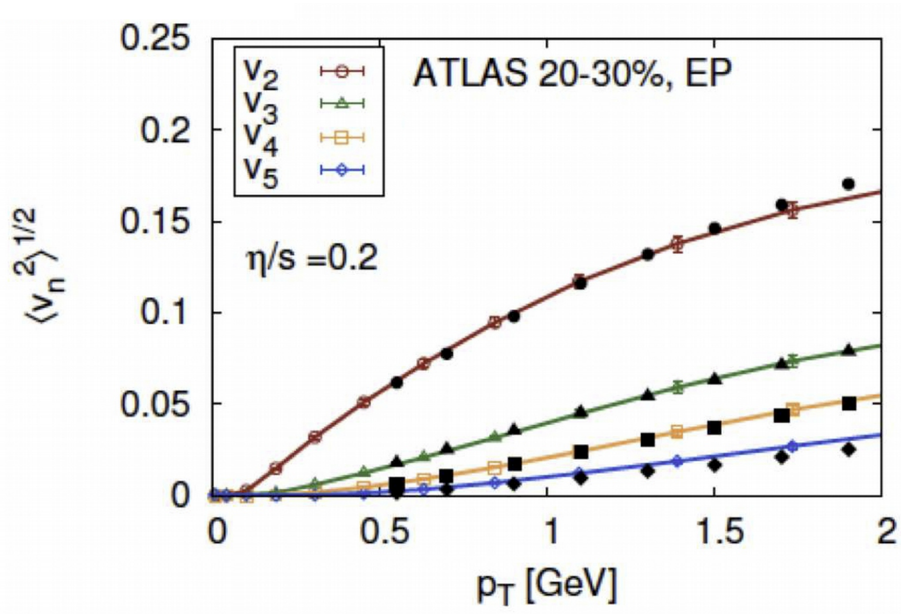

Current status (see e.g. arXiv:1301.2826):

$$(\eta/s)_{\mathrm{QGP}} \approx 0.2 = 2.5 \times \frac{1}{4\pi} \qquad (20\%\ \mathrm{stat.\ err.},\ 50\%\ \mathrm{syst.\ err.})$$

To What Extent Do Fluctuations of the Initial Energy Density Distribution Survive the Hydrodynamic Evolution?

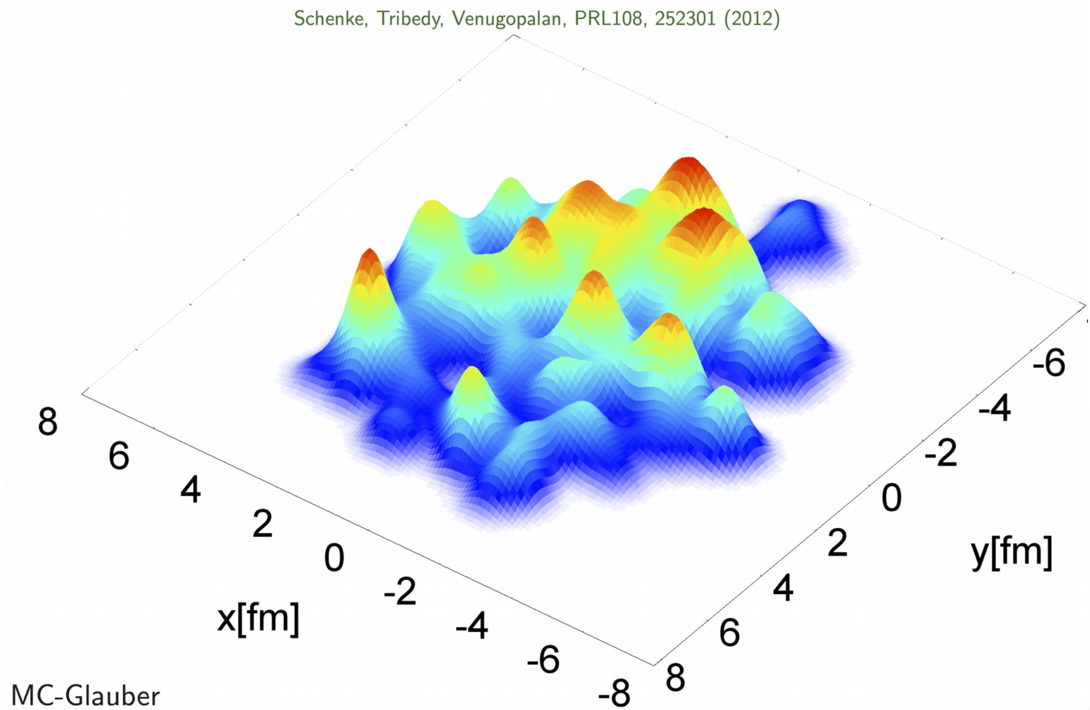

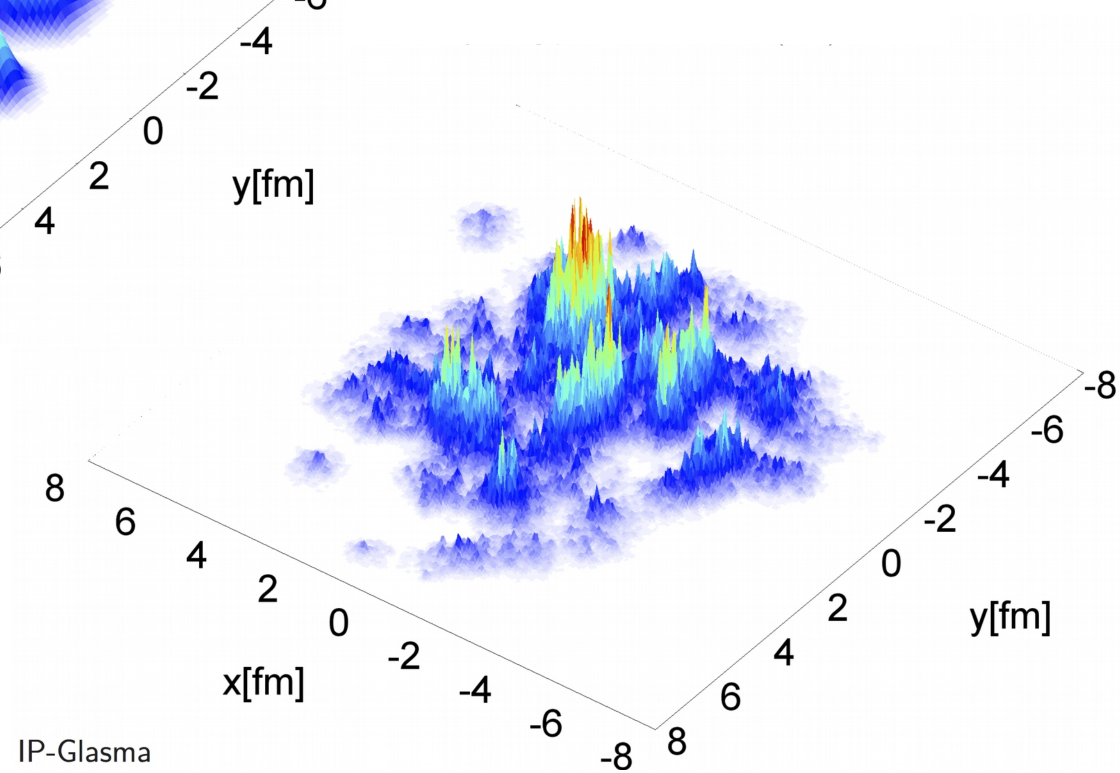

Can we determined the initial state from the measurement of v_n?

Viscosity Suppresses Higher Harmonics

B. Schenke et al.

Event-by-Event hydrodynamics

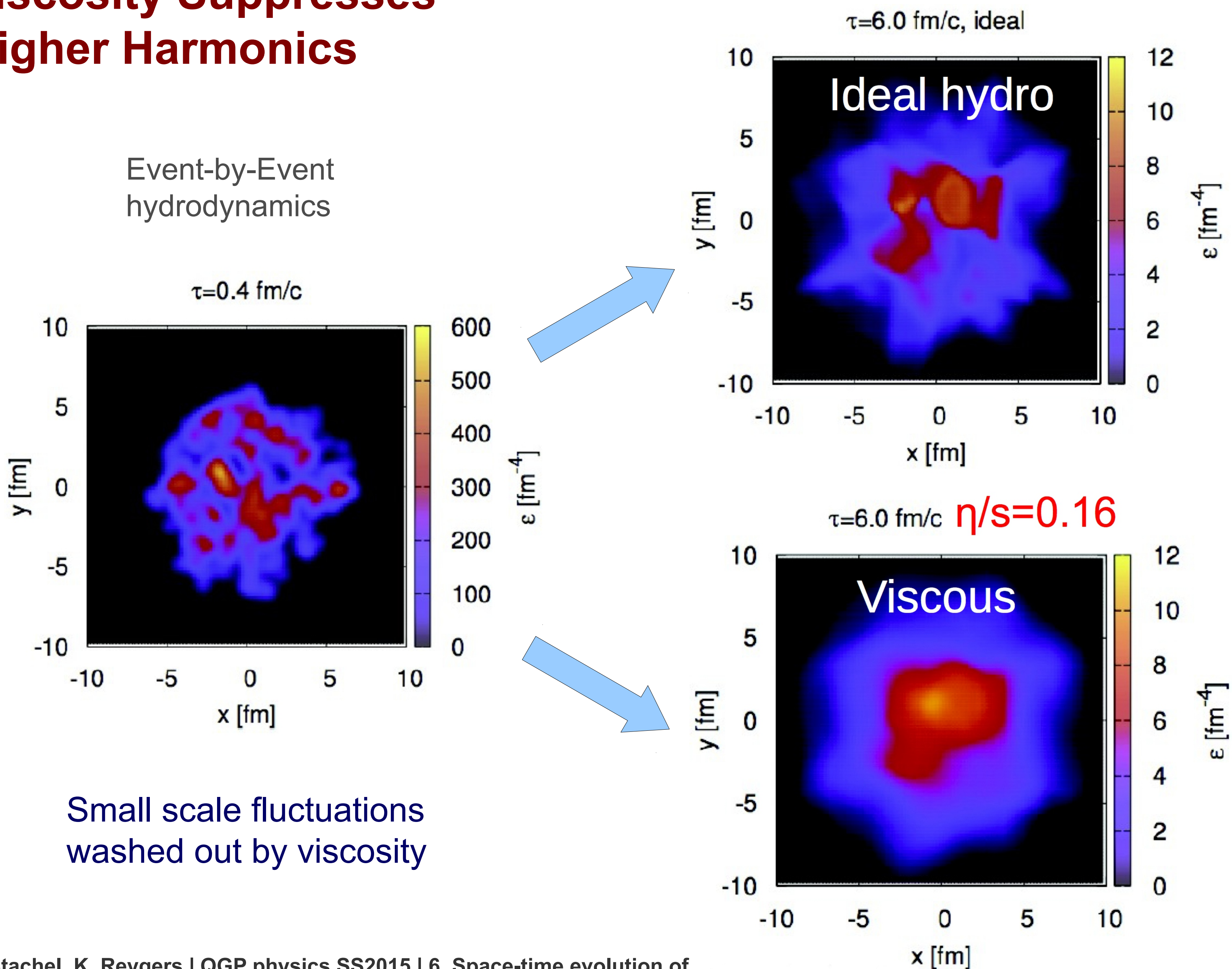

Small scale fluctuations washed out by viscosity

Viscosity Suppresses Higher Harmonics

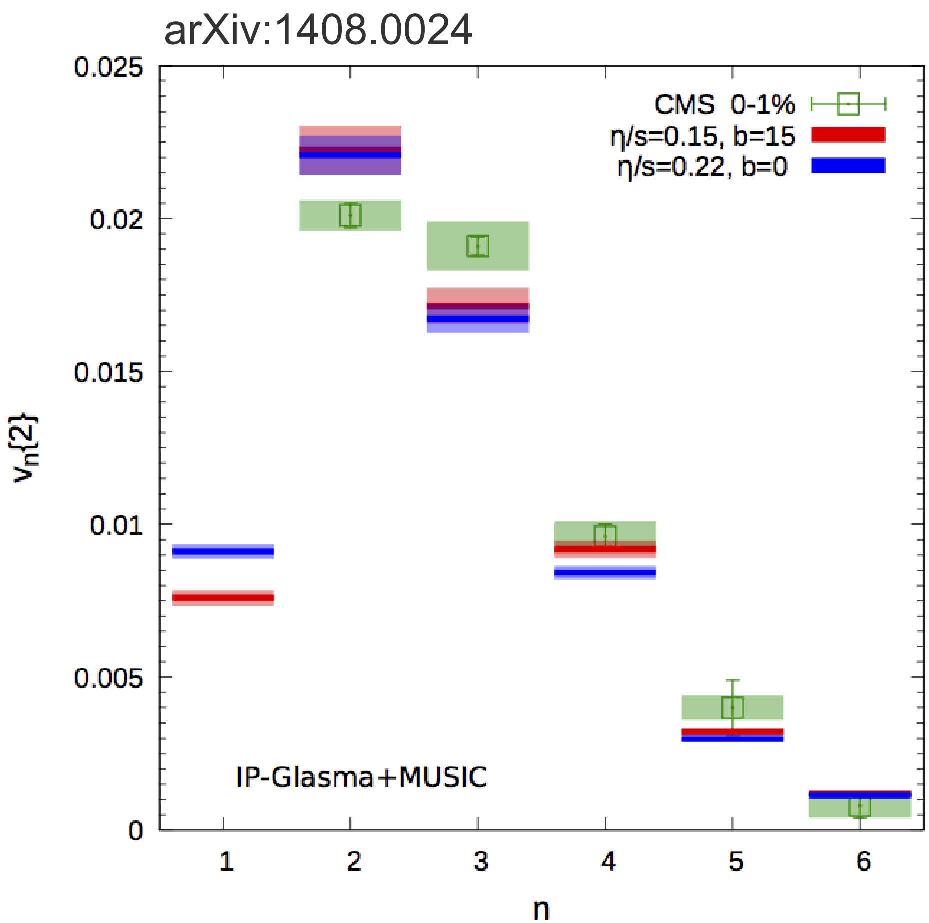

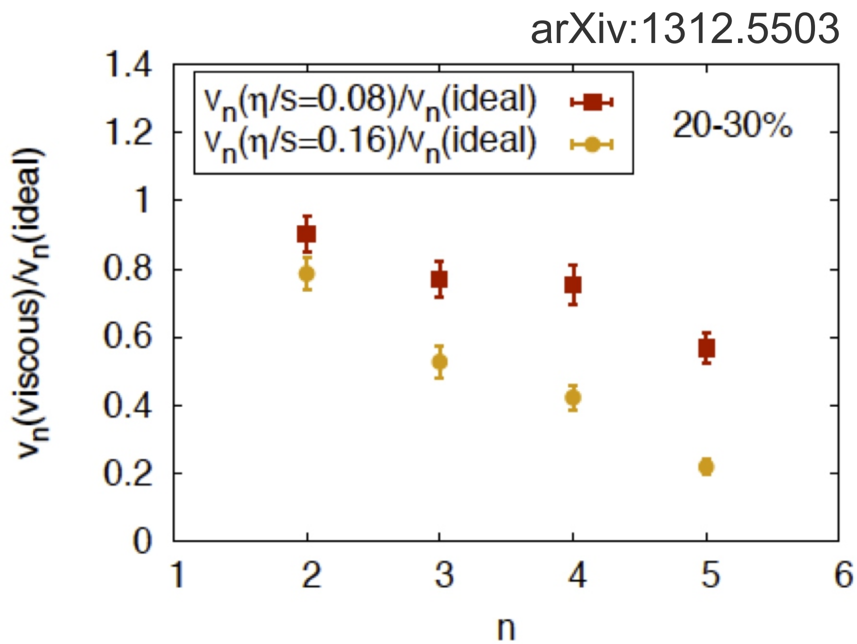

Higher harmonics provide additional constraint on η/s

Ultimate goal: Measure η/s and |initial wave function|^2

The Initial Motivation for p-Pb Collisions at the LHC

- Reference system in which effects of the initial nuclear wave function are present, but which too small to thermalize or to show collective effects (mean free path not smaller than system size)
- Study effects of gluon saturation at small Bjorken *x*

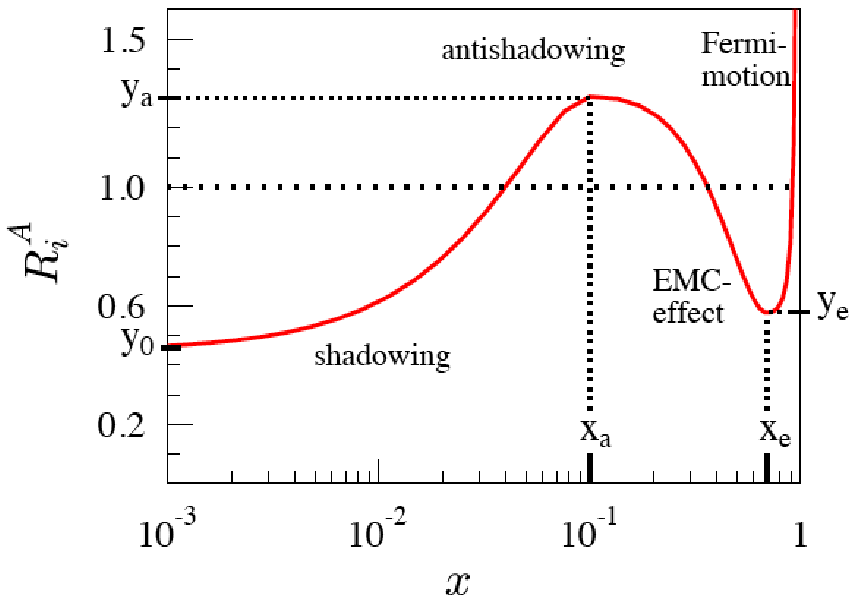

modification of parton distributions in nuclei

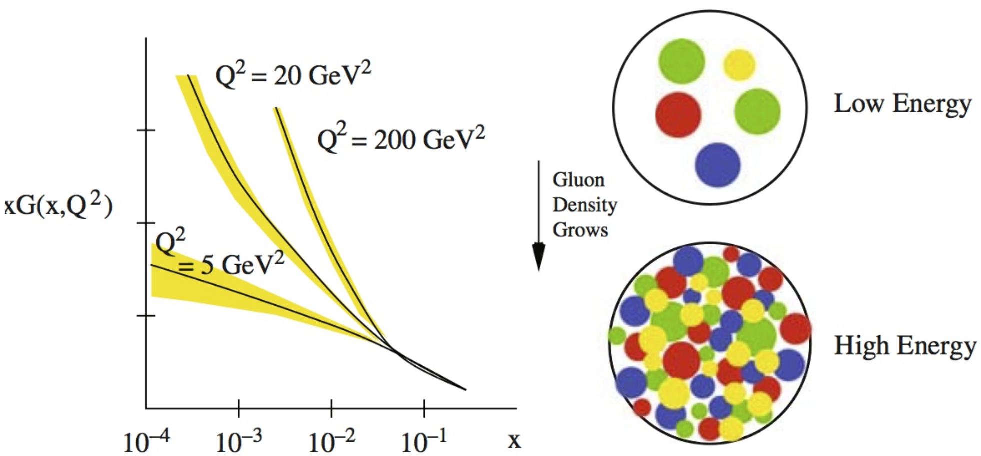

gluon saturation at small x

Blast-wave Fits work quite well in p-Pb with Average Flow Velocities up to β = 0.55 *c*

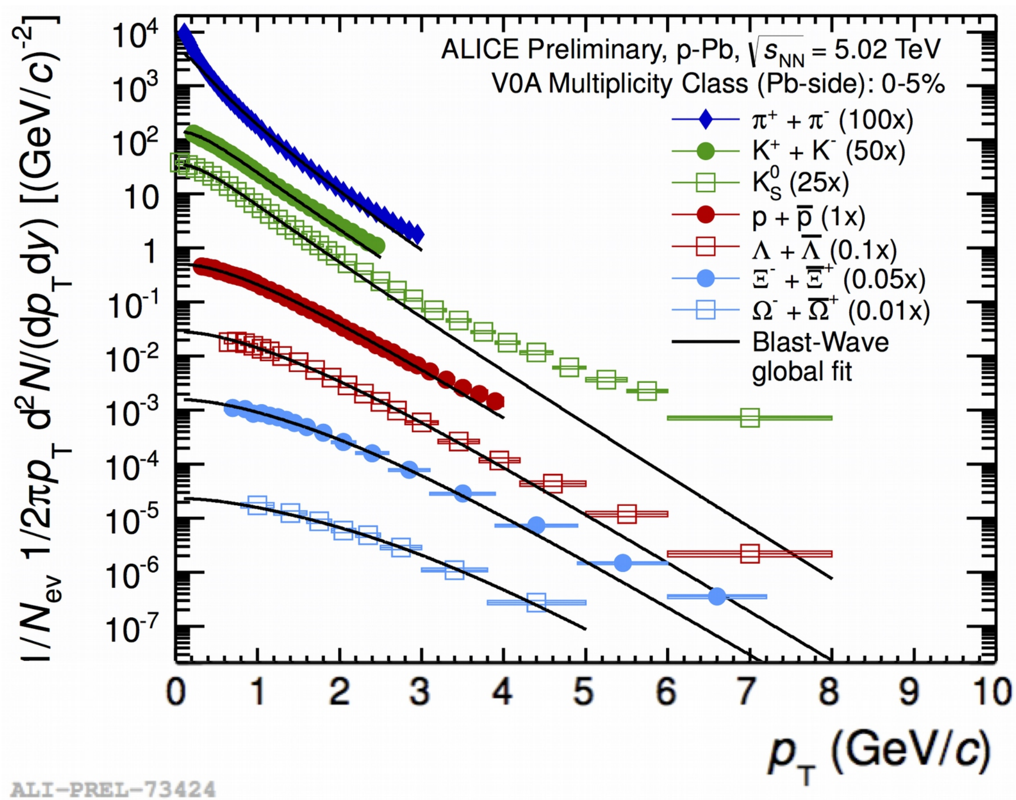

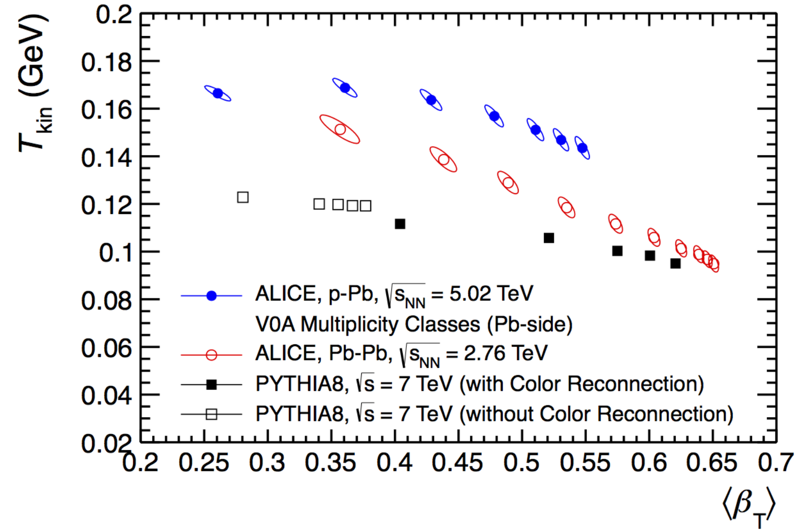

arXiv:1307.6796

Elliptic Flow is Large and Exhibits Mass Ordering

arXiv:1307.3237

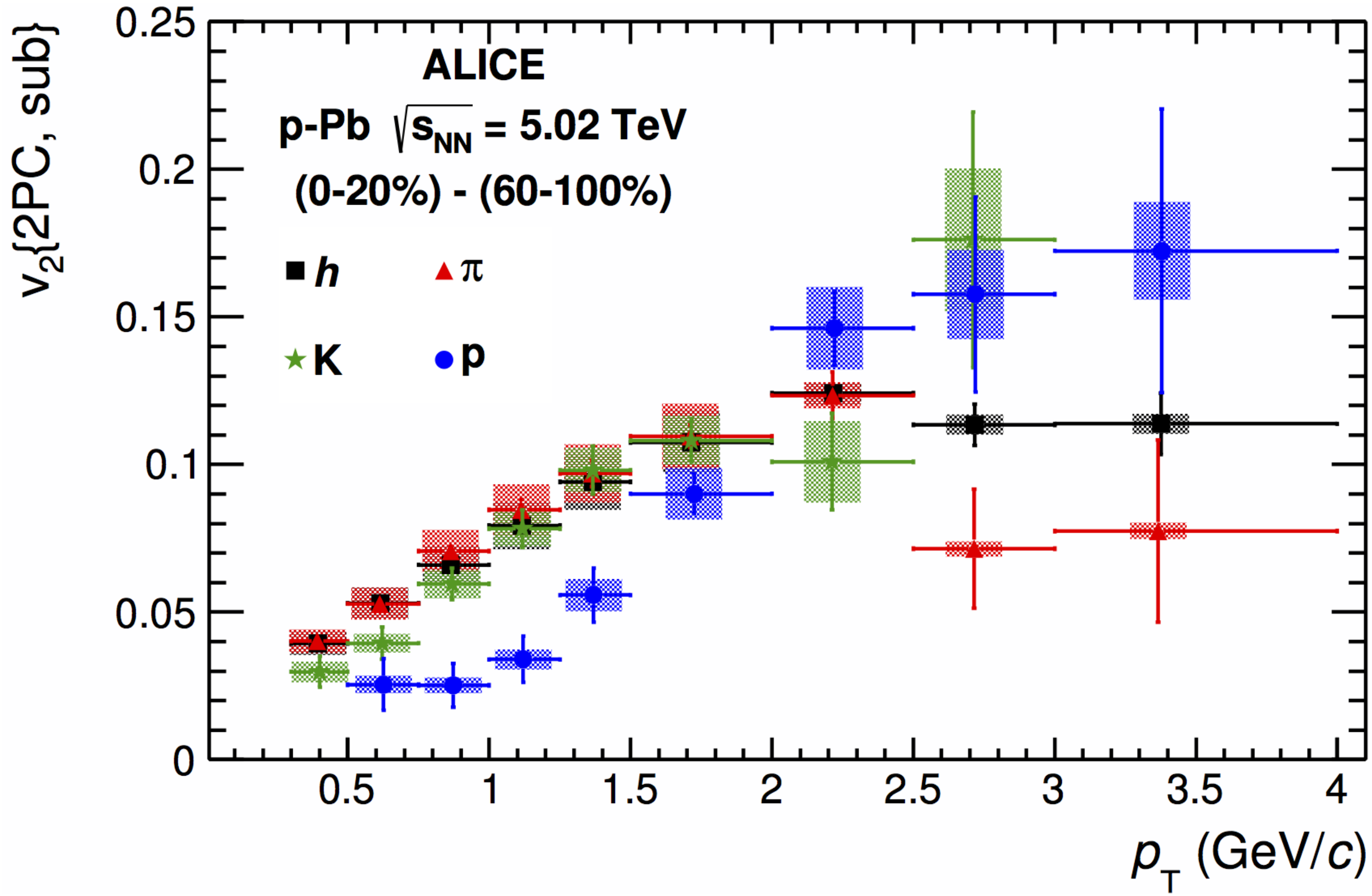

Comparison of v_2 in Pb-Pb and p-Pb for the same Track Multiplicity

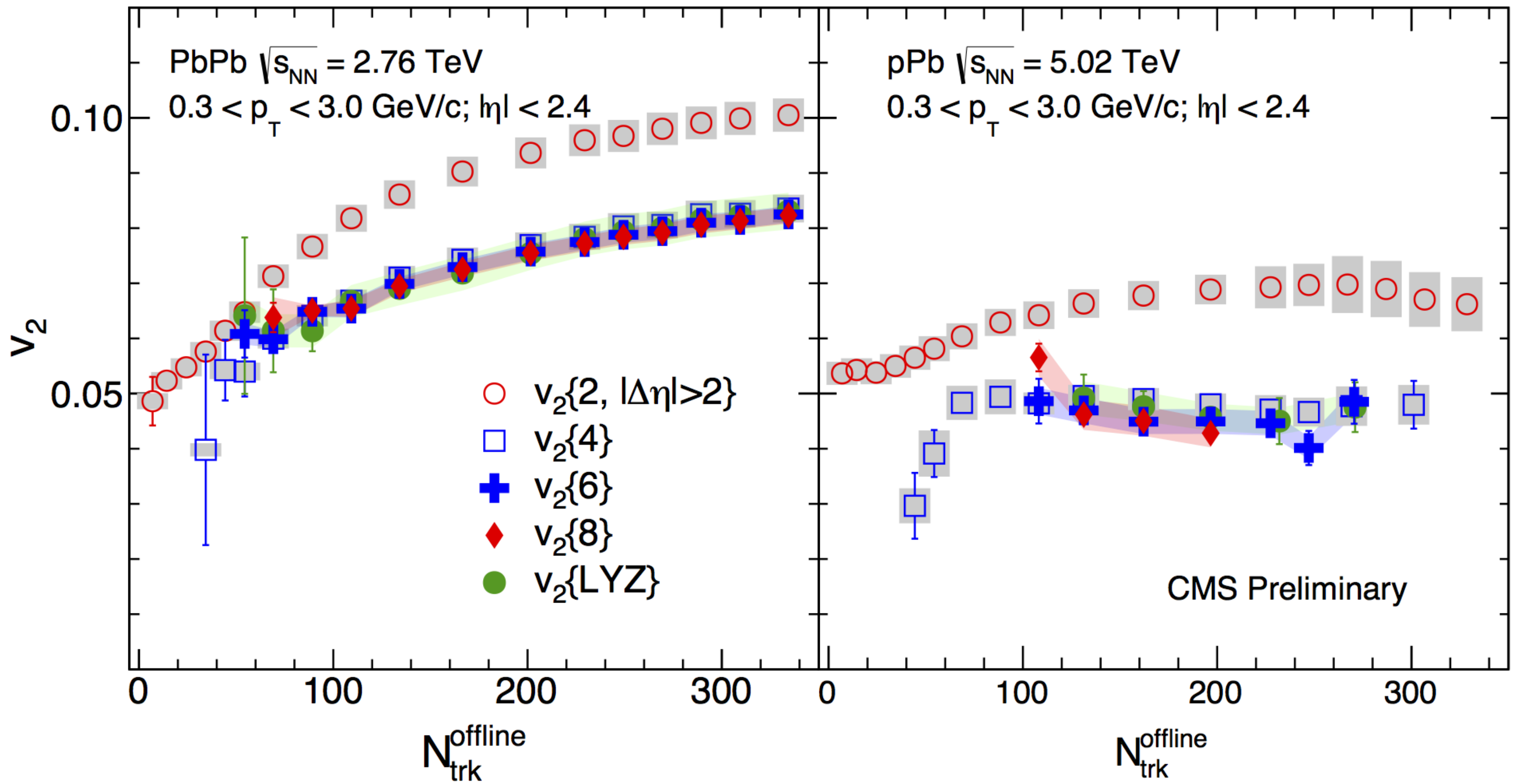

v_2 in p-Pb is a genuine multi-particle effect

An Interesting Observation at RHIC: Quark Number Scaling

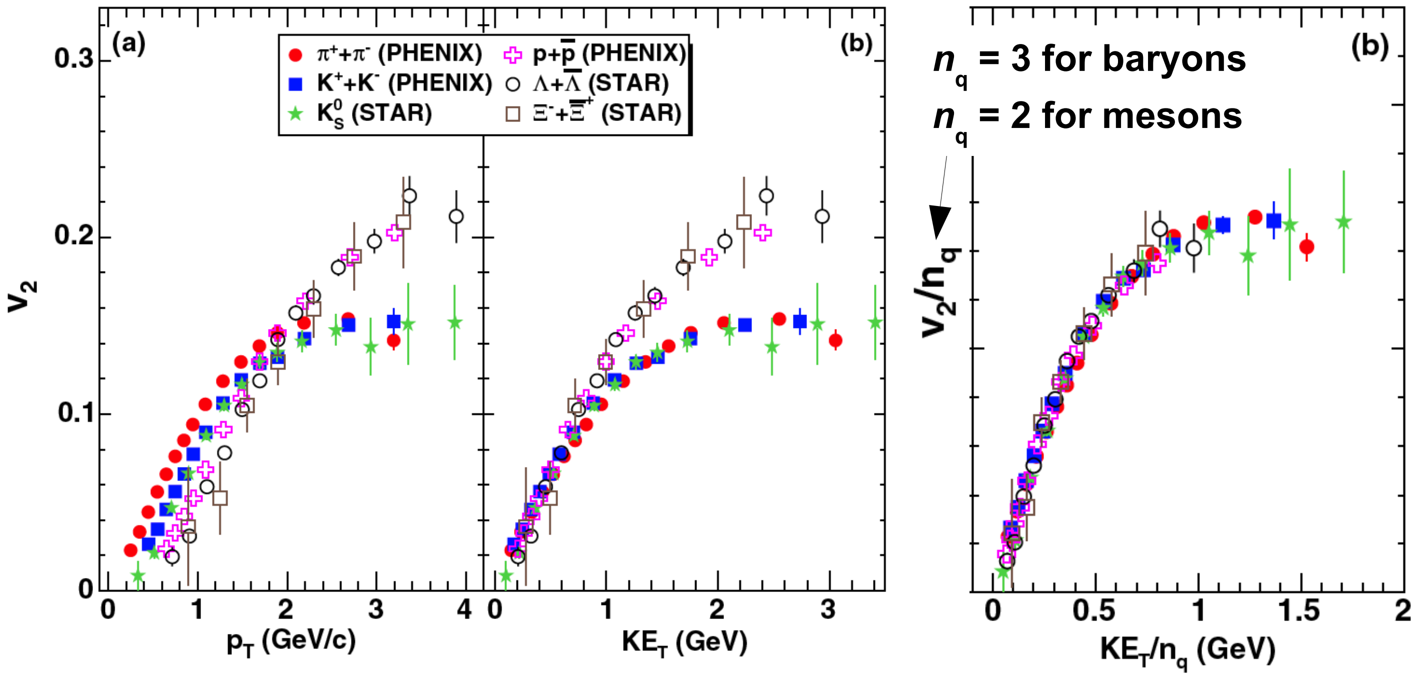

PHENIX, PRL, 98, 162301

Quark recombination:

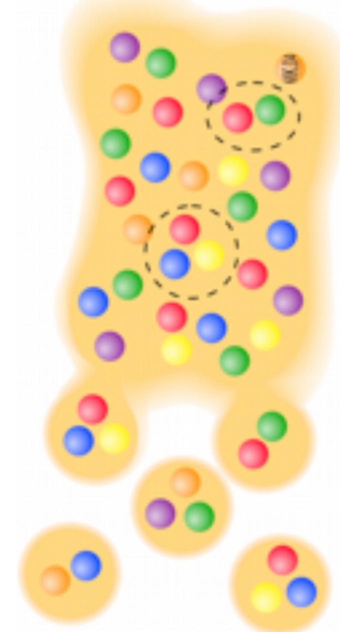

$$KE_T = \text{kin. energy in the transverse direction} = m_T - m_0$$

- Scaling of v2 with n_q suggests that the flowing medium at some point consists of constituent quarks (in line with recombination models)
- Is there a transition from massless u and d quarks to constituent quarks ($m_u \approx m_d \approx 300$ MeV)?

Heavy Quarks Apparently Take Part in the Flow

measured

Example for a semi-leptonic heavy quark decay: $D^0(c\bar{u}) \to K^-(s\bar{u}) + e^+ + \nu_e$

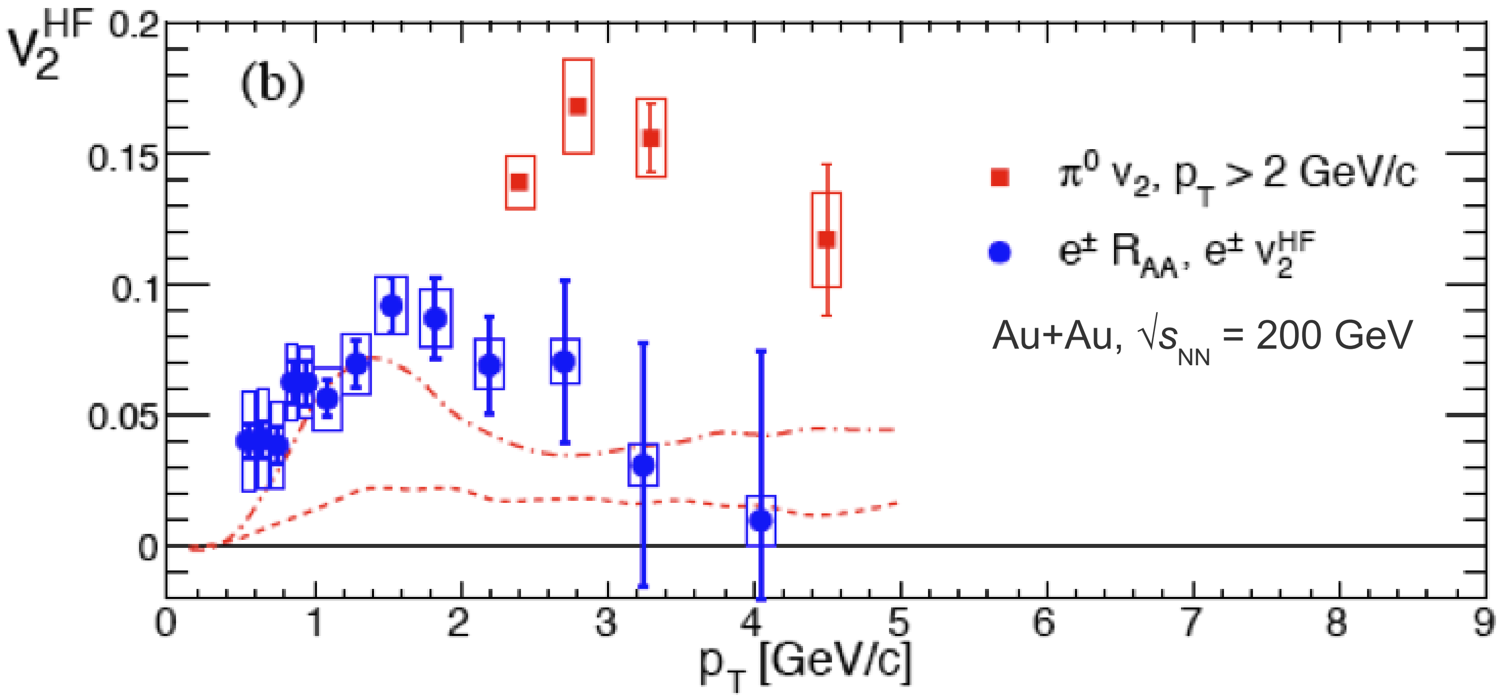

- Current masses: $m_u \approx m_d \approx 4$ MeV, $m_c \approx 1270$ MeV, $m_b \approx 4200$ MeV
- Even though $m_{\text{heavy, quark}} > 200 \cdot m_{\text{light,quark}}$ heavy and light quarks exhibit a similar flow strength

D Mesons seem to Flow also at the LHC

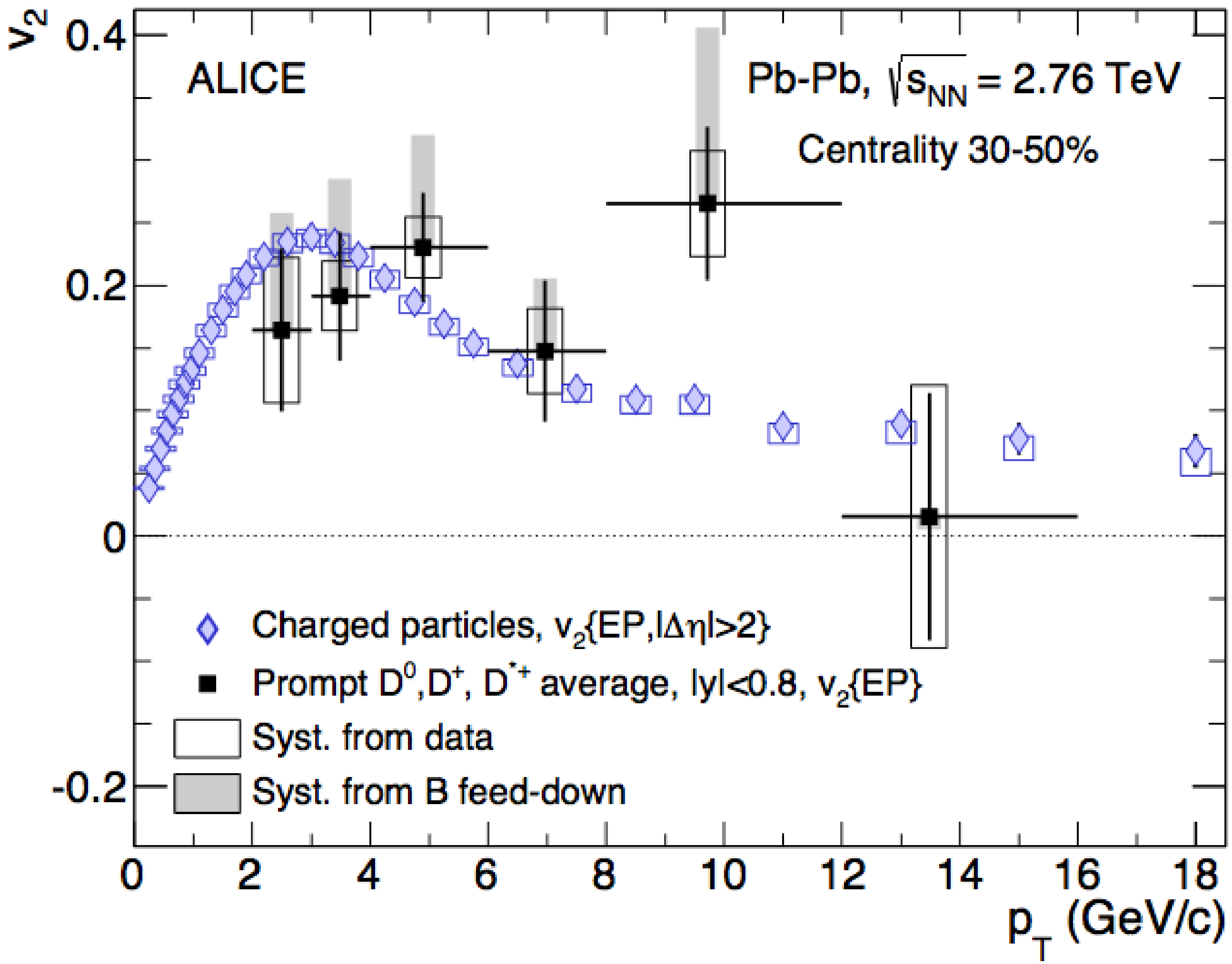

v_2 and Jet Quenching

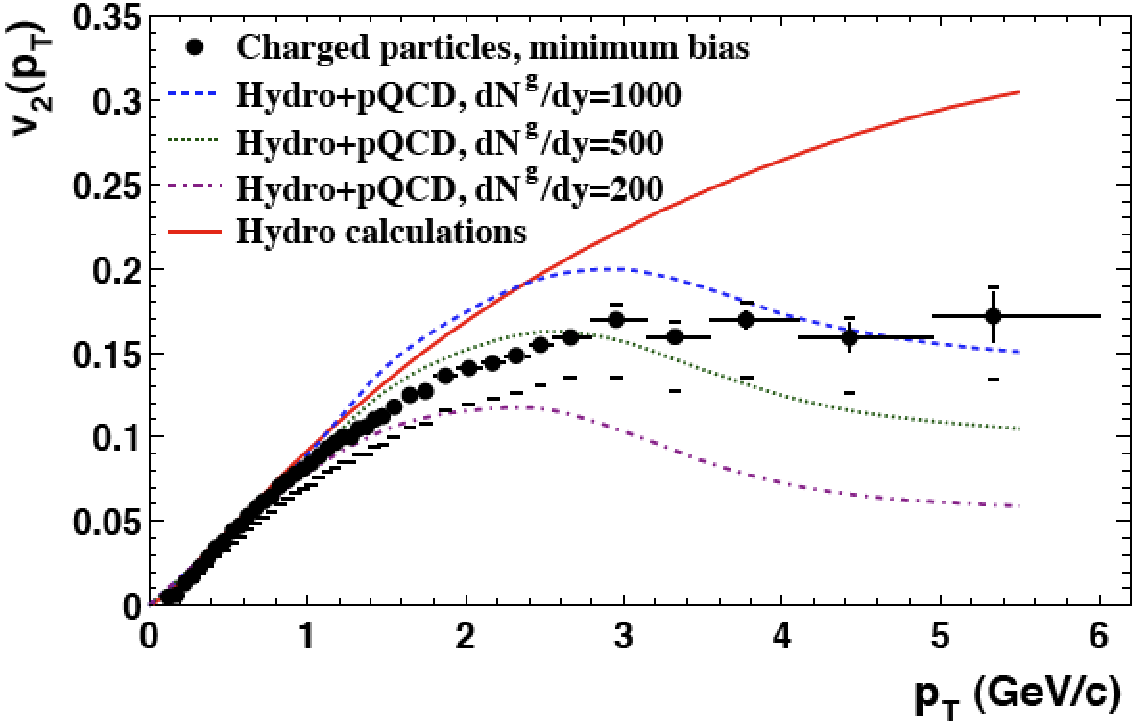

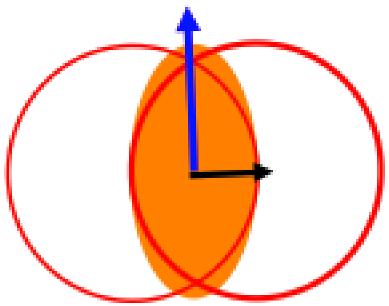

For p_T > 4-6 GeV/c particle production is dominated by jet fragmentation. Jets, i.e, energetic quark and gluons, are expected to lose energy in the QGP ("jet quenching"). The shorter path length for jets in the reaction plane compared to jets perpendicular to the reaction plane is expected to result in a positive v_2 at hight p_T.

v_2 and Jet Quenching

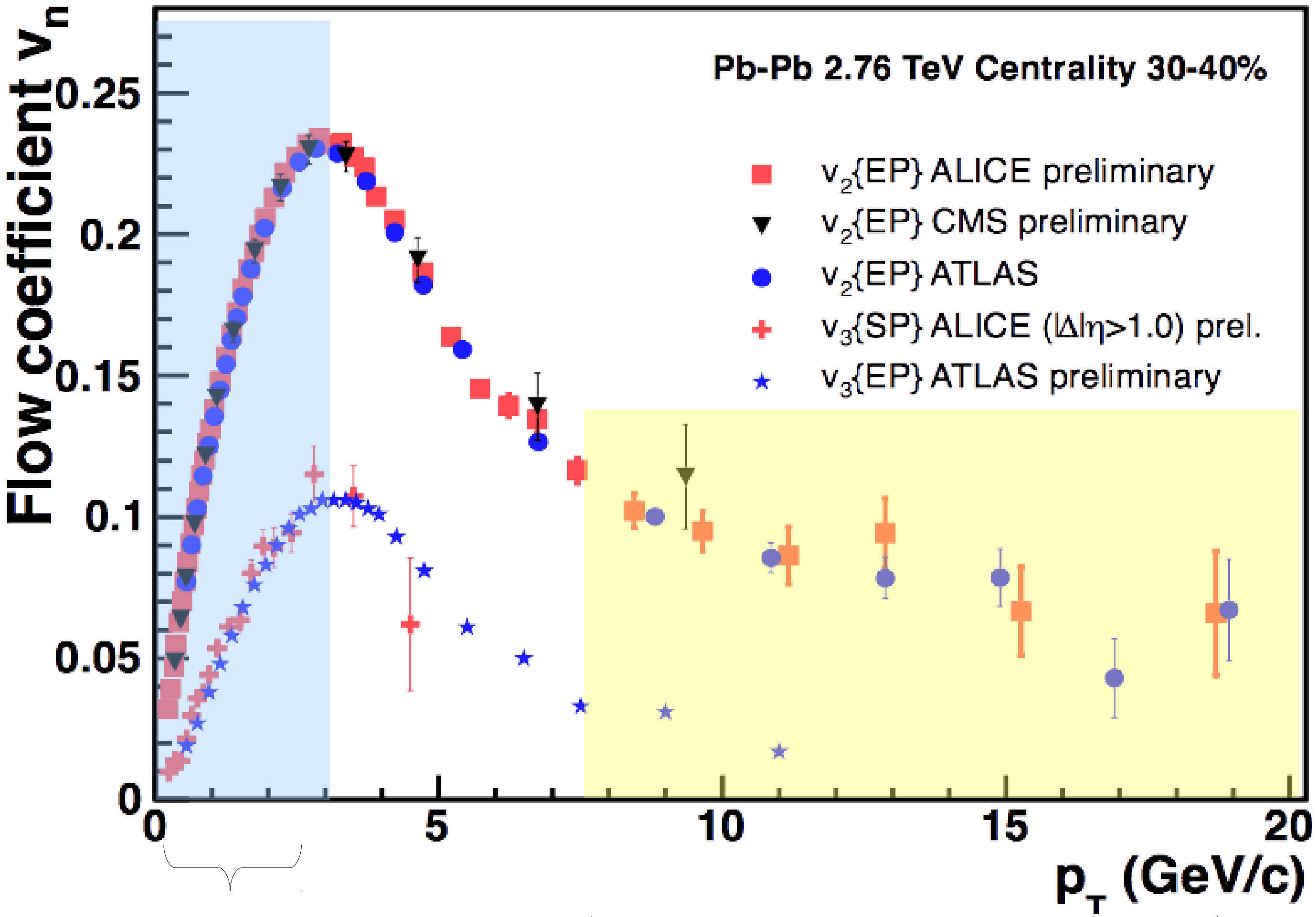

hydrodynamic regime
v_2 driven by pressure gradient

jet fragmentation regime
v_2 driven by energy loss

Points to Take Home

- QGP at RHIC and LHC is close to an ideal fluid (close to KSS bound)
- Elliptic flow coefficient v_2 and especially higher harmonics sensitive to viscosity of the QGP (viscosity reduces the v_n)
- Similar η/s for RHIC and LHC
- Upper limit from data/theory comparison (ca. 2013):

$$\eta/s \approx 0.2 = 2.5 \times \left.\frac{\eta}{s}\right|_{\mathrm{KSS}} = 2.5 \times \frac{1}{4\pi}$$

- p-Pb and pp collisions were considered reference systems without QGP formation
- However, many observables consistent with collective effects also in pp and p-Pb
  - QGP formation also in these systems?
  - Do these results challenge the flow observables as QGP signatures in A+A?
  - Or similar observations but different physics in p-Pb and Pb-Pb?